Electric Porsche Drivetrain Re-design

Final Report

Sponsored by

CAL POLY MOTOR CAR ASSOCIATION

Team E-Porsche

Taylor Carlson	tfcarso@calpoly.edu
Quinton Petty	qpetty@calpoly.edu
Spencer Treffry	streffry@calpoly.edu

Advisors

Dr. Schuster	pschuste@calpoly.edu
Dr. Ridgley	jridgely@calpoly.edu

Statement of Disclaimer

Since this project is a result of a class assignment, it has been graded and accepted as fulfillment of the course requirements. Acceptance does not imply technical accuracy or reliability. Any use of information in this report is done at the risk of the user. These risks may include catastrophic failure of the device or infringement of patent or copyright laws. California Polytechnic State University at San Luis Obispo and its staff cannot be held liable for any use or misuse of the project.

Table of Contents

Chapter 1. Introduction

Chapter 2. Background

Chapter 3. Design Development

Chapter 4. Final Design

Chapter 5. Product Realization & Test Fixture Design

Chapter 6. Design Verification

Appendix

List of Figures

Chapter 1. Introduction

Sponsor Background & Problem Definition

Cal Poly Motor Car Association is a student run club of car enthusiasts who received an electric 1977 Porsche 911 Targa S as a donation in 2011. It is the club's goal to return the Porsche to its former performance glory while retaining the existing electric motor. The long-term intentions are to generate funding for a lithium ion battery pack and streamline the drivetrain and reduce weight to better suit the motor. The problem is that the current stock transmission is not optimized for the motor's performance and includes many unnecessary components and weight that lead to power losses. A picture showing the current drivetrain configuration can be seen below in Figure 1.

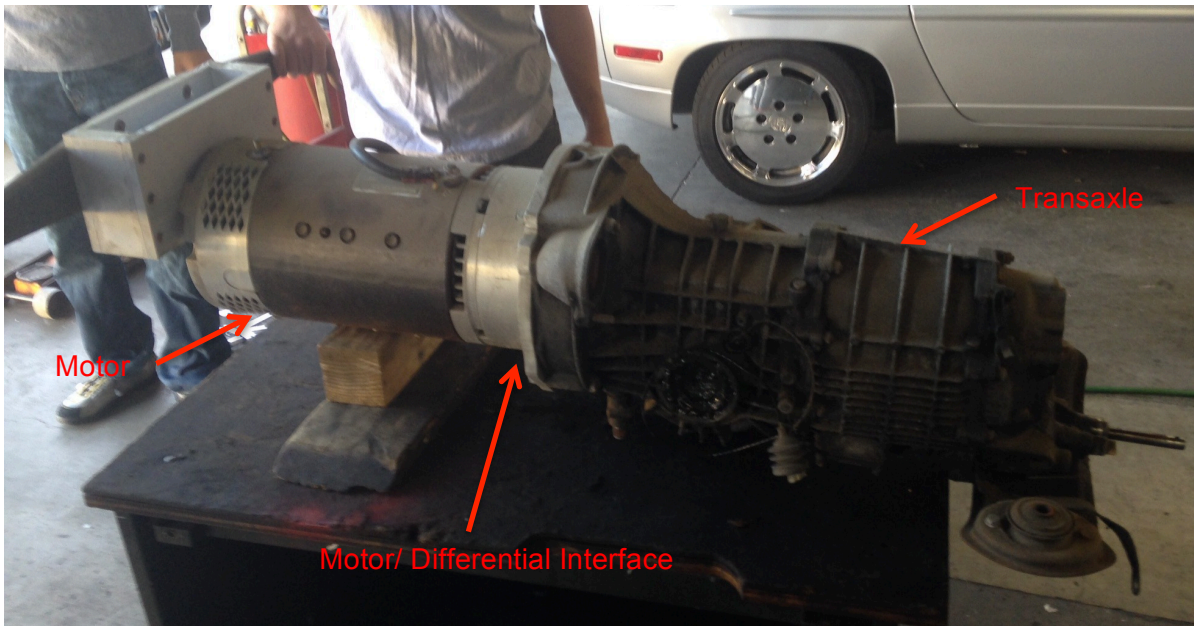

Figure 1: Original drivetrain configuration

Objective & Specification Development

The objective of our project was to redesign the drivetrain of the electric 1977 Porsche 911 Targa S with the goal of optimizing the drivetrain for motor efficiency and performance. Our focus was redesigning the interface between the electric motor and rear wheels to maximize the efficiency of power transmission from the motor to the ground. The project was completed under the supervision and guidance of Cal Poly Motor Car Association and overseen by Dr. Ridgley and Dr. Schuster as the faculty advisors.

We started with a list of customer requirements that included:

- safe to drive
- match factory driving specifications
- increased range
- efficiency
- adaptability
- ease of maintenance
- fun to drive
- aesthetics
- carbon neutral
- cost
- manufacturability

With this list of initial requirements we assigned values of relative importance to each of the parameters from the perspective of different target customers. This method allowed us to highlight the parameters that were the most meaningful to the majority of the market and to focus our attention on those. To come up with a metric to measure our design against the current vehicle setup, we decided to calculate the total mechanical loss in the system. By measuring the losses we would be able to get an efficiency value that will translate to our systems ability to efficiently transfer power and torque from the motor to the wheels.

Adaptability and ease of maintenance were also important parameters for us to address. Because it will likely be students working on and maintaining the vehicle, making our design safe and easy to maintain was very important. Additionally we wanted our design to be able to accommodate future upgrades to the vehicle i.e. new controller or higher voltage battery pack. By counting the total number of parts and fasteners, we will have an idea of how easy/difficult it will be to work on. Because we are looking to increase the range, cutting down on the overall vehicle weight, and/or making room for additional batteries would be valuable performance enhancements. By minimizing the size and weight of our system, we improved the range and efficiency of the vehicle as a whole. The compliance matrix on the following page summarizes our engineering specifications.

Spec. #	Parameter Description	Requirement or Target (units)	Tolerance	Risk	Compliance
1	Mechanical Losses	Less than current transmission (%)	Max	H	A, T, S, I
2	Peak Torque	176 (lb ft)	Y/N	M	T, I
3	Weight	Less than current transmission (lb)	Max	H	A, T, S
4	Volume	Less than current transmission (in^3)	Max	L	A, I
5	Cost	1900 ($)	Max	M	A, S
6	# of Parts	20	Max	M	A, S, I
7	# of Fasteners	30	Max	M	A, S, I
8	Maintenance	20,000 miles	Min	M	A, I

Table 1. Compliance matrix of engineering specifications.

Project Management

Throughout the course of the project, Spencer Treffry acted as the communications officer in charge of keeping in contact the sponsor and relaying information to the other group members. Quinton Petty was the treasurer, in charge of all the finances of the project, and Taylor Carlson was the secretary and responsible for keeping records of meetings. All other responsibilities were distributed among the team members evenly as they were identified. To organize the progress and completion of various subsystems of the project, we created a Gantt chart that can be found in Appendix VII of this report. The completion of the project required three main milestones: the Preliminary Design Report, the Final Design Report at the time of the Critical Design Review, and this, the Final Project Report that will be published and archived in the Cal Poly library.

Chapter 2. Background

Before doing any design of our system, we first needed to significant background research. We started by taking a close look at the components of the existing system to see what we had to work with and what could be reused for our project. This included removing the drivetrain of the Porsche to see what original components remained and what components had been made or replaces in the electric conversion. Additionally we looked into existing solutions to the problem to see if there was anything that had already been designed for this purpose. This gave us a more complete picture of our problem to base our own idea generation on.

Porsche 915 Transmission

The mechanism responsible for transmission of power from the motor to the wheels in the electric Porsche when it was donated was the stock 915 5-speed transmission. This transmission was built by Porsche to transmit power from a 2,687 cc Flat 6 engine capable of producing 165 h.p. and 176 lb-ft of torque, and remained in the car despite having replaced the engine with the electric motor. The transmission includes a Limited Slip Differential and weighs approximately 120 lbs. When the car is driven, the transmission is put into second gear using a mechanical cable pull clutch and is left there for the duration of the drive. According to Porsche's specifications, this gives the current car a 1.834:1 reduction ratio. Through experimentation, the Motor Car Association has found that this reduction works best out of the choices available: 1st Gear: 3.182:1, 2nd Gear: 1.834:1, 3rd Gear: 1.261:1, 4th Gear: 0.962:1, and 5th Gear: 0.759:1. With this configuration, the transmission acts as a fixed gear reduction, which is commonly used in other production electric vehicles.

Advanced DC Motor

The original Porsche Flat 6 engine had been replaced with an FB1-4001 Advanced DC Motor that was repurposed from a forklift. According to manufacturer's specifications this motor is capable to producing 100 h.p. peak if supplied with a 144 volt power source. Complete manufacturer specifications and motor curves can be found in Appendix I.

Existing Systems

- **Hybrid Synergy Drive**

A common DC motor included in a car that most people see daily on the road is part of the Hybrid Synergy Drive developed by Toyota. This transmission was developed to facilitate the combination of an Internal Combustion Engine (ICE) and two DC motors. The two DC motors act as both motors and generators to supplement and restore power delivered by the ICE. One of the motors is responsible for the acceleration of the car from a standstill and converts kinetic energy back to electric potential during regenerative braking. The other electric motor's primary purpose

is to control the system's continuously variable transmission (CVT). This electric motor is attached to a planetary gear set that is also connected to the engine and acts as a differential. Through this differential, the speed of the ICE and electric motor are summed to equal the wheel rotation speed. By monitoring the speed and torque of the drive shafts, the electric motor can be controlled to ensure the greatest efficiency of the motor and ICE combination. A visual explanation of the different driving modes of the Synergy drive can be found in Appendix VIII. Toyota's Hybrid Synergy drive has proven to be very efficient and one of the earliest successful applications of CVTs available in production cars today.

- **CVT**

There are many other types of CVTs that have been explored, all of which have some disadvantages. The goal of a CVT is to have an uninterrupted range of speed ratios to improve the efficiency or adjust torque and speed to be constantly at ideal conditions. Some of the simplest CVTs are friction based. One of the earliest designs is based on a wheel and disk. This "wheel and disk" CVT is comprised of a large disk rotating on a shaft at constant speed while a wheel on a perpendicular shaft is rolled through the disk's diameter. A wheel and disc CVT concept can be found in Appendix VIII. In this system there are a few sources of power loss that are common in most friction based CVTs. One source of power loss is from deformation of the individual components. To maintain constant contact between the wheel and disk, the wheel and disk must not deform or shed material. To minimize deformation the hardest available material with the highest coefficient of friction should be chosen. Another drawback to friction CVTs is their inability to transmit high torque. The static coefficient of friction is the major limiting factor in the application of friction CVTs.

Variable Diameter Pulley CVTs are a commonly known friction CVT that consists of two cones on each of two parallel rotating shafts and connected by a V-belt. The V-belt rests between the two cones on a single shaft and the surface contact between the cones and v-belt determines the speed ratio. The V-belt in this configuration needs to be constantly under tension to transmit power. With the change in position of the cones to vary the output speeds, the distance of the shafts needs to be adjusted to ensure proper belt tension. Appendix VIII includes an example of a cone CVT. This adjustment requires a few additional parts but this CVT has been use in many applications including snowmobiles and a few automobiles.

Toroidal CVTs are another attempt at friction based CVTs. Toroidal CVTs interface two parallel disks on colinear shafts with a pair of rotating wheels on a perpendicular axis to the disks. The wheels perpendicular to the driven shafts act as an interface between the driven shafts. The angle of these perpendicular wheels is adjusted which creates a larger radius on one driven disc (the motor) and a smaller radius on the other driven disc (the wheel). This difference in moment arms (radii) effectively changes the speed ratio of the two shafts. A concept example of this can be found in Appendix VIII. Many companies and academics have spent time studying and improving the full toroidal CVT as well as half toroidal CVTs which have appeared as some of the most efficient

CVTs available. A compact cone-shaped design was developed through research in the automotive industry and was used in a few production cars from companies including Nissan, Toyota and Audi.

- **Fixed Gear Reduction**

The most well known example of a fixed gear reduction in an electric vehicle is Tesla's line up of cars. Both the Roadster and Model S have a fixed gear reduction between the AC induction motor and the rear axle. While developing the Roadster, Tesla originally planned to have a two-speed gearbox to get higher performance out of the motor. However, after many delays the Roadster shipped with the gearbox locked in second gear with a promise of replacement when the gearbox was perfected. The Roadster ended up including a fixed gear reduction of 8.27:1. The Model S, developed with the lessons of the Roadster in mind shipped with a 9.73:1 reduction. This single gear reduction is a good fit for AC induction motors due to the motor's high efficiency and torque at high speeds. There have not been many applications of fixed gear reductions to DC motors due to their reaching higher peak efficiency at a much higher speed than AC induction motors. However, the efficiency of our DC motor is high over a large range of motor speeds, exemplified by the motor curves included in Appendix I.

Batteries

Ten 12V deep cycle batteries power the existing system. It is the club's goal to replace these batteries with a new lead acid pack and then eventually to lithium when the funds are available. Lead acid battery technology is the most widely used electrochemical system largely due to its cost per energy storage capacity. Within lead acid battery technologies there are several sub-categories including; flooded lead-acid batteries, valve-regulated lead –acid batteries with gel electrolyte immobilizer, and valve-regulated batteries with absorptive glass mat (AGM).

In flooded lead-acid batteries the positive and negative plates interact with the sulfuric acid electrolyte to cause the chemical reaction that is reversed during recharging. Valve-regulated lead acid batteries are closed cell batteries that don't use a liquid electrolyte. Instead they employ a gel or absorbed glass mat (AGM) to serve as the electrolyte. Hydrogen byproducts from charging create an internal pressure that requires a simple valve to regulate. These cells have the advantage of being safer due to the lack of fluid and self-regulating pressure, and are therefore often used in racing applications for safety in the event of a crash.

Nickel based battery technology include a nickel hydroxide cathode and either a metallic anode or a hydrogen storing anode. The cycle life and resistance to degradation of Nickel based batteries without a charge makes them a good candidate for standby or backup systems. Sodium batteries have high energy densities and are capable of operating in adverse conditions such as extreme high or low temperatures. They also have long life cycles making them very effective for energy grid storage. Their main advantage however is that they are fully recyclable because they are manufactured with non-toxic materials.

Lithium systems are currently the industry standard for portable systems due to their energy density. They provide the highest energy density of all rechargeable systems at room temperature operation. This characteristic alone makes them the obvious choice for an electric vehicle application. A lithium battery utilizes a lithium metal oxide cathode and an organic electrolyte to store energy but has the downside of being very high cost.

Electric Vehicle Codes and Standards

There are many organizations involved with standardizing the emerging market of electric vehicles. Of these many organizations, the Society of Automotive Engineers International (SAE) has the most complete library of standardized tests for electric vehicles. Feasible testing procedures for our team have been evaluated and are discussed in detail later in this report.

Chapter 3. Design Development

Design Development

The method of approach we chose to follow to achieve the sponsor's goals was that of a formal design process. This process began with the identification of the problem: a vehicle converted to an electric powertrain is still employing a transmission optimized for a combustion engine, not an electric motor. Our team was then formed in response to the expressed problem. The first order of business after team formation was to establish meeting frequency and times. It was decided our team would meet at a minimum twice a week regarding this project specifically to monitor the progress and completion of our goals. Next, a contract between our team members was completed to establish ground rules for decision-making, conflict resolution, and general team member responsibilities. A Gantt chart with tasks and deliverables relevant to the project was drafted to ensure we meet your goals for this project.

After a timeline was established, the next order of business was to further our understanding of the design problem. To do this we began extensively researching the problem and current solutions. This gave us a base of knowledge that allowed us to narrow down some of the customers' qualitative requirements into quantitative engineering specifications. We then completed the formal Project Proposal, which was reviewed by the sponsor to ensure we successfully identified the initial requirements. Recommendations from the sponsor were then applied to further our understanding of the design problem. This iterative process was continued throughout the project in order to learn more about the design problem and potential solutions.

After we gained a firm grasp of the design problem we began generating concepts of possible solutions. Our team used a few different idea generation methods to help bypass any mental barriers. We began our idea generation with what is called brain-writing. This is an exercise similar to brainstorming however instead of verbally announcing your ideas where they may be prematurely subjected to criticism, you simply write down your ideas for about five minutes. After five minutes, the group members exchange their list of ideas and then build on them for another ten minutes. This process continues until one receives their original list of ideas, which are now augmented, with the thoughts of the other group members. After discussing the ideas generated using the brain-writing method, our group used a brainstorming method involving triggers called the scamper method. Scamper is an acronym made of trigger words that helped eliminate mental barriers and allowed us to think of our problem in different ways. After exhausting these two methods of idea generation, our team moved on to evaluating our solutions.

We began our idea evaluation process with a Go-No Go assessment during which we gauged the feasibility of each solution using high-level analysis and a quick group discussion. If the solution passed a quick critique from the group, we kept the idea, and if the solution did not stand up to our critique, it was discarded. To narrow our list of ideas further, our team used what is known as a Pugh Matrix. A Pugh Matrix evaluates how well concepts fulfill the customer requirements relative to a datum concept. Each team member completed a Pugh Matrix that helped narrow down many of

our ideas. The Pugh Matrix allowed us to narrow down our list of concepts to two feasible solutions: a differential with a fixed gear ratio or two motors, each directly attached to one of the rear wheels. Our method to evaluate these final two ideas was to use a weighted decision matrix.

Similar to a Pugh Matrix, a weighted decision matrix evaluates concepts' ability to fulfill our customer requirements. However a weighted decision matrix assigns weights to each customer requirement to reflect the relative importance of each requirement. After completing this final matrix, our fixed gear differential concept proved to be the most promising solution.

Despite coming to this conclusion we chose to pursue both designs further and present both to our sponsors. The main reason the two motor solution did not emerge as our most promising design was the fact that it would cost more than our budget would allow. At the time we were in the process of finding more funding, so the two motor design remained in the running because of the much higher performance it could provide.

Leading Concepts

- **Fixed Gear Reduction**

Our top concept was a fixed gear reduction differential. This differential would be designed to maximize the motor's operation at an optimal operating speed. This optimal operating speed was determined based on the required performance and available power source. From the motor specifications in Appendix 1, it can be seen that the motor is most efficient when supplied with high current, which also leads to high torque. However, this performance and high motor efficiency cannot be sustained very long due to the low energy capacity of the current batteries. The Cal Poly Motorcar Association has had plans to replace the current lead-acid batteries with lithium-ion batteries and our design needed to accommodate this future change. When lithium-ion batteries are adopted, the car will be able to perform at a much higher current and operating speed. This was a large consideration when we design the optimal gear reduction.

Once the gear reduction ratio had been determined, the interface between the existing systems and the differential needed to be designed. By removing the current transmission, it opened up space in the rear engine for the installation of our differential gearbox. This gave us flexibility in the configuration of the differential beneath the car. When the current transmission and differential removed we evaluated the use of existing mounts for our differential. The rear drivetrain mounts were accessible but the front mounts were too far from where our gearbox would be located to be used.

Another aspect that we designed for was maintainability. Our design must be easily accessible and maintainable. The Porsche will be maintained by students at Cal Poly, which means that that the longest one person will maintain the car is four years. Our system should not require maintenance every 4 years but will require a student sometime in the future to perform maintenance once if needed. This leads to a requirement that our differential needs to be easily

maintainable and conform to standard automotive couplings so that a student with general automotive knowledge can perform any necessary maintenance.

Based on the Cal Poly Motorcar Association's plans we designed a drivetrain that will make large improvements over the existing system while preparing the system to fulfill the future goals of the car.

- **Two Motors with Electronic Differential**

Our second leading concept was to use two motors, each attached to one of the rear wheels. Since we would be introducing a new motor for this design, an additional motor controller will also be necessary to properly control the second motor. A microprocessor would act as the interface between the two motor controllers, effectively creating an electronic differential. The integration of a microprocessor would allow easy control of the torque applied to each wheel during times of varying weight distribution which will lead to much greater performance.

Important design requirements for this concept were to complete detailed stress and strain analysis of the shaft and interface piece between the motor and wheel shafts. Real time dynamic system analysis of wheel speed, weight distribution, and many other properties will also be necessary for the successful completion of this design. This would have required us to set up a control system and program a microprocessor to distribute torque to each wheel properly given certain dynamic conditions.

A significant setback to the feasibility of this design was the cost. The projected cost of approximately $4354 for this design greatly exceeds our modest budget of $2000.

Concept Selection

After presenting two concepts to our sponsors during the preliminary design review we were directed to focus our first concept; the single fixed gear reduction. It was chosen over the two motor design because no additional funding was secured to purchase a secondary motor. The chosen concept utilizes a stock differential from a 2000 Ford Ranger with a 4.10:1 ratio as the single fixed ratio gearbox between the motor and wheels. Designing and building a custom gearbox would have been preferred, however, its expense would be greater than our $2000 budget could accommodate. In addition to using a differential we got from a scrapyard, we repurposed parts from the original drivetrain to bring the cost of our system down. Using a differential in place of a custom gearbox allowed us to focus on the design of all of the new interfaces required to mate the Ford differential with the electric motor and the half-shafts of the Porsche.

Chapter 4. Final Design

Differential/Gear Ratio Selection

Before designing any components we needed to select the gear ratio at which we wanted to operate. After discussing desired performance with our sponsors, we looked at the performance curves of the motor provided by the manufacturer as seen in Appendix I. We decided on using 65 mph as our ideal operating point to keep the motor spinning at its highest efficiency throughout the majority of the expected speed range. Additionally, we wanted to maintain the low speed acceleration that has been a standard of Porsche performance throughout its history. At 3750 rpm the motor is operating at its most efficient speed. In order to drive at 65 mph at the desired rpm we need 874 rpm at the tires. Using equation (1) below we calculated a ratio of 4.3 to achieve the desired speed at 3750 motor rpm.

$$\frac{\omega_{motor}}{\omega_{axle}} = gear\ ratio \qquad (1)$$

We presented a range of potential ratios from 4.3:1 to 3.73:1 all producing desirable characteristics and searched for stock differentials within that range. We looked primarily at small truck differentials because they are designed to handle higher torque closer to those provided by our electric motor. After identifying a list of manufacturers and axle models that might have the ratio we were looking for, we called nearby scrap yards and found a rear axle assembly with a 4.10:1 ratio from a 2000 Ford Ranger. This ratio is achieved with a pinion gear having 10 teeth attached to an input shaft and a ring gear with 41 teeth attached to the open differential carrier. A picture and exploded view of the chosen axle assembly highlighting the ring and pinion can be seen in Figures 2 and 3 respectively below.

Figure 2: 2000 Ford Ranger rear axle purchased from San Luis Auto Salvage

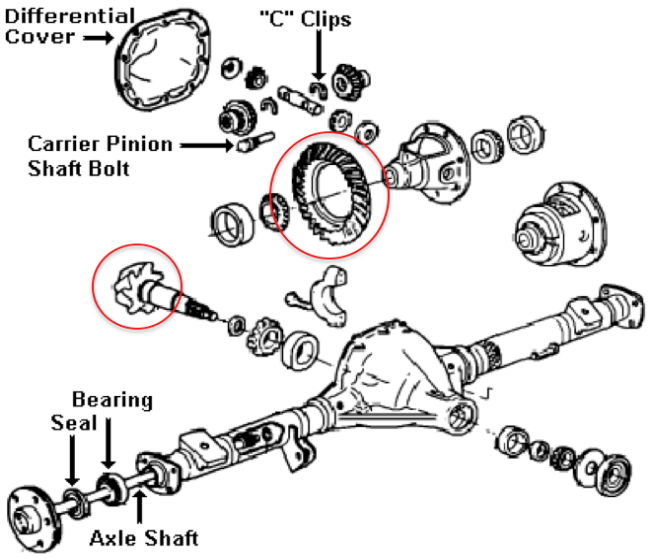

Figure 3: Location of ring and pinion gear in Ford Ranger rear axle assembly

This ratio will provide 914 rpm at the wheels at a motor speed of 3750 rpm resulting in peak efficiency of the motor at 68 mph. After selecting the differential, we were able to begin designing the various interfaces that would be required for installation. The three major interfaces are the motor differential shaft interface, half shaft interface, and front drivetrain mount.

Detailed Design

Components throughout this report will be referenced with respect to the vehicle orientation. For example, a component labeled as front will be located closest to the front of the car. Additionally, CV joint will be used in place of constant velocity joint for readability.

Detailed drawings of all components can be found at the end of this report in Appendix II. Additionally, all design calculations regarding system components can be found in Appendix III.

- **Aluminum Motor Interface**

The previous drivetrain configuration utilized two separate custom aluminum plates to interface the motor to the stock transaxle of the Porsche. The original configuration can be seen in Figure 4 on the following page.

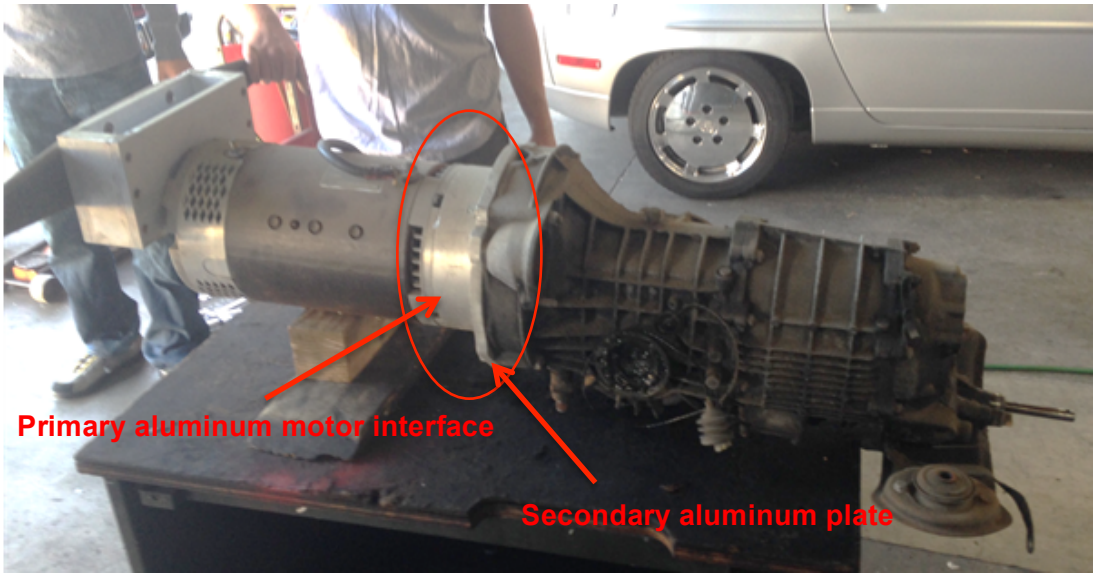

Figure 4: Original drivetrain configuration highlighting aluminum parts

To save on the cost of buying new aluminum stock we chose to reuse the primary aluminum motor interface into our design. The secondary aluminum plate was designed to interface with the original Porsche transaxle and would not serve any purpose in our design. The primary aluminum motor interface is already manufactured to fit the face of the motor and has pre-tapped 0.5" bolt holes that we utilized in our design. In our design, this part serves the purpose of spanning a portion of the gap between the motor and the differential. It also isolates the motor and differential shafts to maintain proper alignment and ensures they take only pure torsional load from the motor. Keeping the weight of the system off of the driveshaft assembly ensures longer bearing life and minimizes mechanical losses of the system.

The only modifications we would make to the primary aluminum motor interface would be to remove material from the inside diameter of the part and to add 0.125" countersinks around the tapped holes to allow a clearance fit for our aluminum spacers to nest in. Removing material from the inside diameter of the part would serve two purposes, allowing proper clearance for the differential flange to rotate freely and remove unnecessary material weight from the part. The countersinks allow the aluminum spacers to fit and better distribute the weight of the system over more surface area. It also takes some of the associated stresses off of the threaded rods that will tie the components together. A model of the modified part can be seen in Figures 5 on the following page.

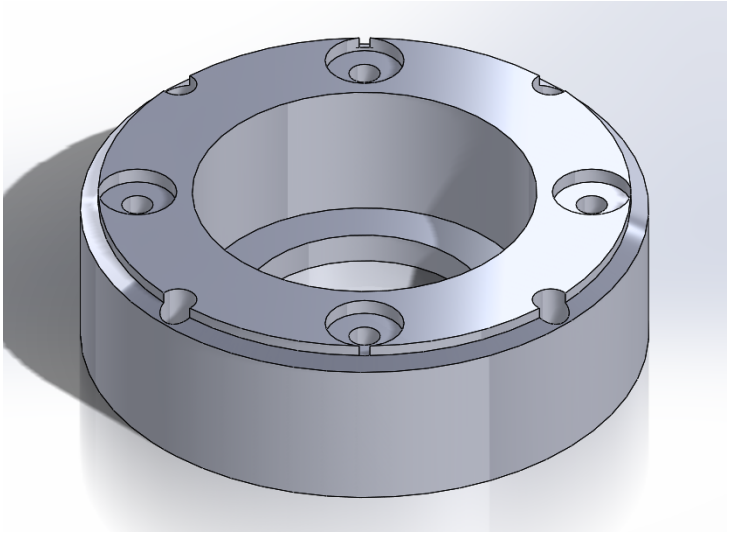

Figure 5: Modified aluminum interface

- **Motor Shaft Collar & Key**

The motor shaft interface is arguably the most important part in our system and includes two components, the key and the motor shaft collar. These two parts are responsible for transferring all of the torque from the motor shaft to the differential gearbox. The original 0.25" x 0.25" x 1.5" shaft key will be reused in our design to transfer the torque between the motor shaft and the motor shaft collar. We calculated the factor of safety against both shear and crushing to make sure we could reuse the shaft key in our assembly. We found the maximum force on the key by converting a peak torque value of 270 lb*ft to a force using equation (2) below.

$$F = T/r \qquad (2)$$

The force at the middle of the key was found to be 5760 lbs. By assuming a yield strength of 65 kpsi and using the distortion energy theory shown in equation (3) below, we found the shear strength of the key to be 37.51 kpsi.

$$S_{SY} = 0.577 * S_Y \qquad (3)$$

By solving for factor of safety in equations (4) & (5) below we found the factor of safety against crushing to be 2.12 and the factor of safety against shear to be 2.44. Knowing those values and considering our assumption of a torque value higher than the capabilities of our current motor, we feel very comfortable using the existing shaft key.

Crushing failure $$\frac{S_Y}{n} = \frac{F}{tl/2} \qquad (4)$$

Shear failure $$\frac{S_{SY}}{n} = \frac{F}{tl} \quad (5)$$

The original drivetrain included a motor shaft collar that was fixed to the motor shaft and then bolted to the clutch assembly of the Porsche transaxle. It was connected via the shaft key discussed above, a tapered lock collar and an outer mounting sleeve. A picture of the original collar can be seen below in Figure 6.

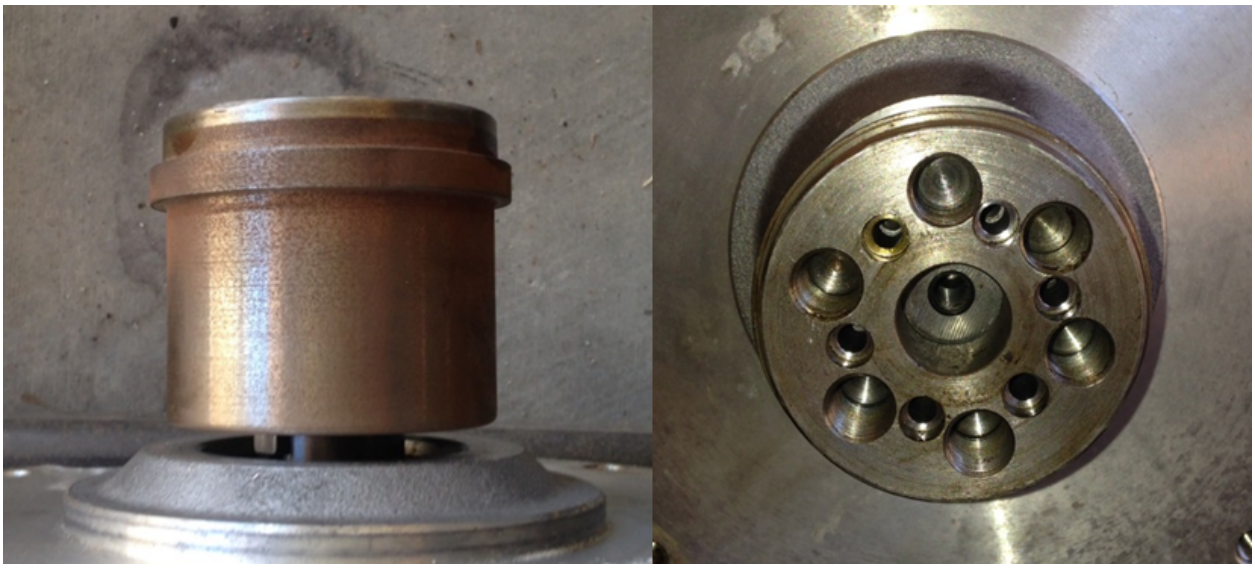

Figure 6: Old motor/differential shaft interface

We wanted to repurpose as many of the original drivetrain components as possible to keep the cost down, but after taking the drivetrain apart it became apparent using most of them would not be possible. As can be seen in Figure 6 above, the larger bolt holes responsible for connecting the motor shaft to the drivetrain are not evenly spaced around the circumference of the collar. This would have caused difficulties in the design of a part to properly interface with the original collar. Additionally this collar design requires bolts to be threaded towards the face of the motor. Initially this didn't seem like a problem however as we designed components moving away from the face of the motor, we continued to run into questions of how to assemble the drivetrain. To properly interface with the differential flange, we needed to bolt away from the face of the motor into the tapped holes of the flange. A picture of the differential flange can be seen in Figure 7 on the following page.

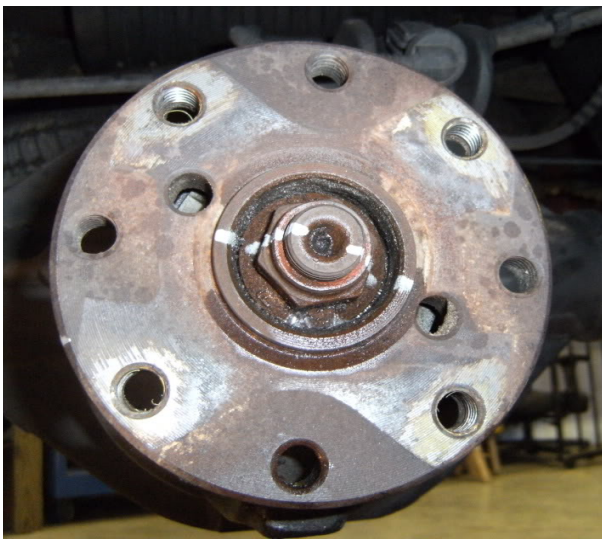

Figure 7: Ford differential flange

Effectively connecting these two components would have required an interface plate thick enough to first bolt to the motor shaft collar, clear the raised lip in the center of the flange, and then match bolt pattern of the flange to be bolted in the opposite direction. For this reason it was determined that trying to utilize the original collar would only add unnecessary complexity, hardware, and assembly time to our final design. A model of our new motor shaft collar can be seen below in Figure 8.

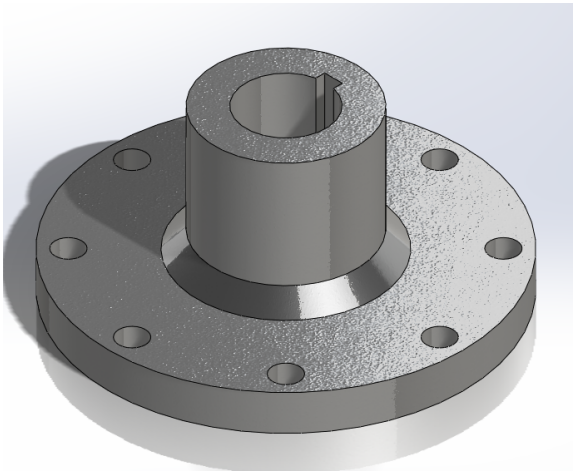

Figure 8: Motor/differential shaft interface

Key features of the new part include the hole to receive the motor shaft and the bolting flange. The hole needed to be cut large enough to allow a slight clearance fit around the 1.124" motor shaft, the key and the shaft collar keyway. This allows assembly without fasteners between the shaft and collar, which is necessary due to the fact that the interface will be hidden inside the aluminum motor interface. The flange of the new motor shaft collar also needs to line up with the existing interface of the Ford differential flange previously discussed. It will be connected via four 0.5" diameter bolts that will thread into the tapped holes of the differential flange.

Using equation (6) below for four bolts, we found the shear factor of safety of 6.3, where A_r is the minor diameter area and F is the force on the bolts due to the motors peak torque.

$$n_d = \frac{0.577 S_{ut} A_r}{F} \qquad (6)$$

The part would be manufactured out of 1 foot length of 5" 1018 steel round stock. We would turn down the outer diameters using the lathe and make the holes and key slot on the mill and drill press. This piece of stock would also be used to make both of the CV shaft interfaces discussed later in this report.

Modifications to minimize the dimensions of the differential flange were considered but using the stock interface has its own advantages. The flange and the input shaft of the differential are connected via a spline, which we would have needed to match with any part we designed. The flange is also attached to a seal that prevents the differential case from leaking oil. Trying to manufacture a part to seal that gap as well as interface with the shaft spline would require special tooling and be prone to manufacturing defects. Also by using the stock flange we can utilize the tapped holes that have already been manufactured. This means by drilling through holes in our flange we will be able to bolt our part directly to the differential without the need for a nut, reducing the total number of parts. A schematic highlighting the flange and seal assembly can be seen below in Figure 9 below.

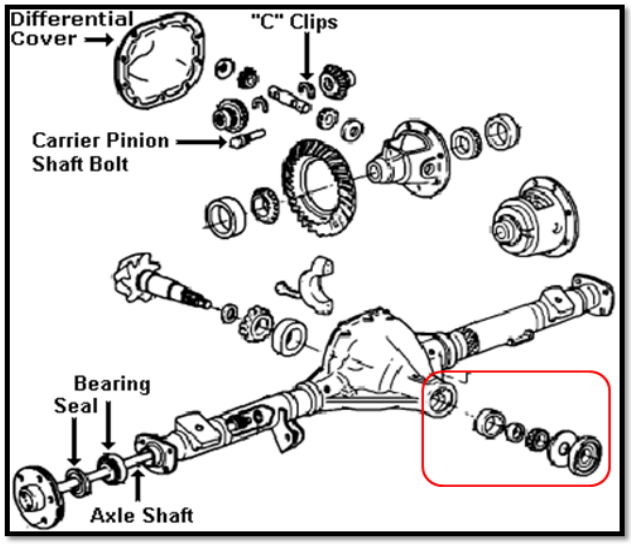

Figure 9: Differential flange and seal assembly

- **Motor-Differential Spacers**

The aluminum spacer will be machined out of 1.2" aluminum round bar with a 0.5" through hole bored out of the center. These spacers will nest into 0.125" countersunk holes in both the aluminum motor interface and in the front drivetrain mount to maintain proper alignment between the motor and differential shafts. They will also aid in distributing some of the load off of the bolts

that will hold the assembly together. A picture of the part and its location in the assembly can be seen below in Figure 10.

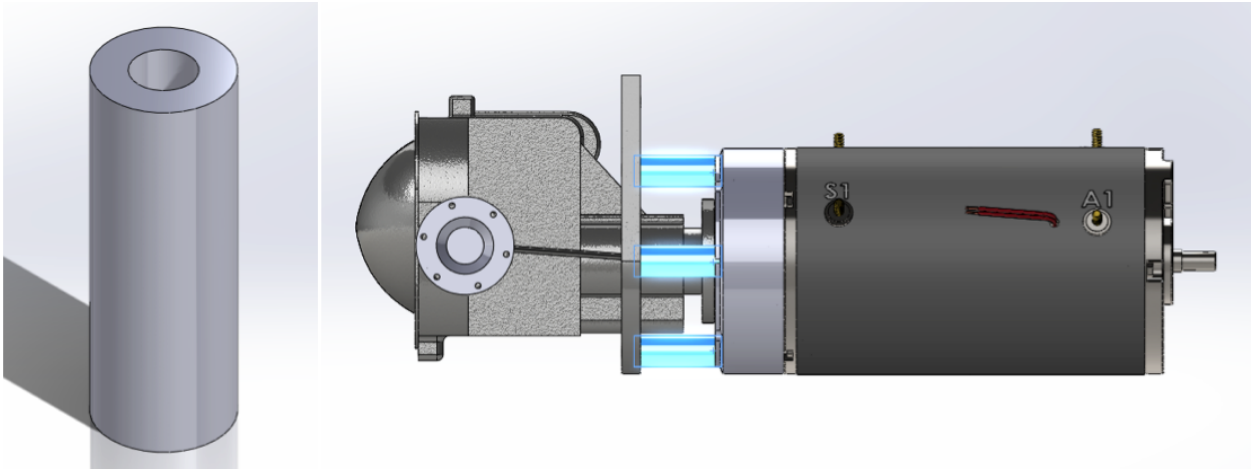

Figure 10: Spacer & location in assembly

- **Front Drivetrain Mount**

The front drivetrain mount is responsible for carrying the load of the front half of the drivetrain as well as providing a surface to mount the differential to the rest of the drivetrain. To create an interface at the differential to both mount to the motor interface and support the entire weight of the front of the system, we will be manufacturing a 0.375”flat steel plate with a hole matching the geometry of the differential to be welded to the differential case. The holes to mount to the motor will be countersunk to receive the other end of the aluminum spacers. A picture of the mounting plate can be seen in Figure 11 below.

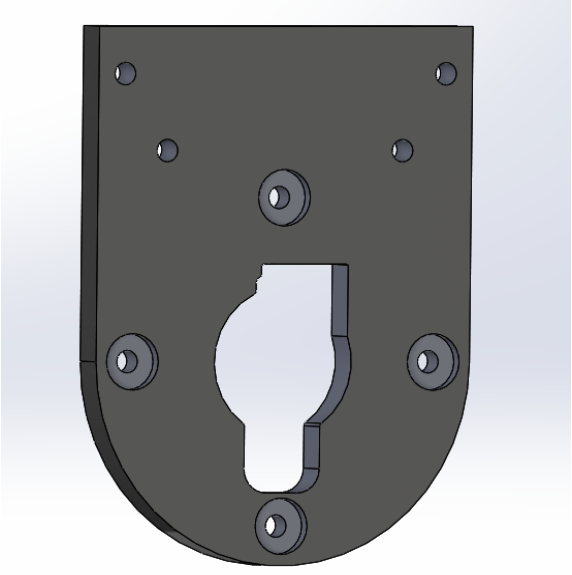

Figure 11: Front Drivetrain Mounting Plate

To make sure we weld the plate parallel to the face of the motor, it would be assembled and fixtured to maintain proper alignment while the plate was tack welded to the differential case. It would then be disassembled and the weld completed around both sides of the hole in the plate. Using a 0.375" plate gives us enough material to bore countersunk holes to receive the aluminum spacers and ensure there is enough material on either side to be welded effectively. To verify our weld would withstand any applied loads we modeled the assembly as if the differential were cantilevered off of the plate with a 2" weld along the top and bottom edges of one side. With these parameters we got a weld shear factor of safety of 2.88 and a fatigue factor of 2.37. Looking at this absolute worst case scenario and knowing the welds on the final design will continue around the entire outside edge of the hole on both sides of the plate we can be sure that the assembly will not fail along this joint. A picture showing the front drivetrain mounting plate location with respect to the assembly can be seen below in Figure 12.

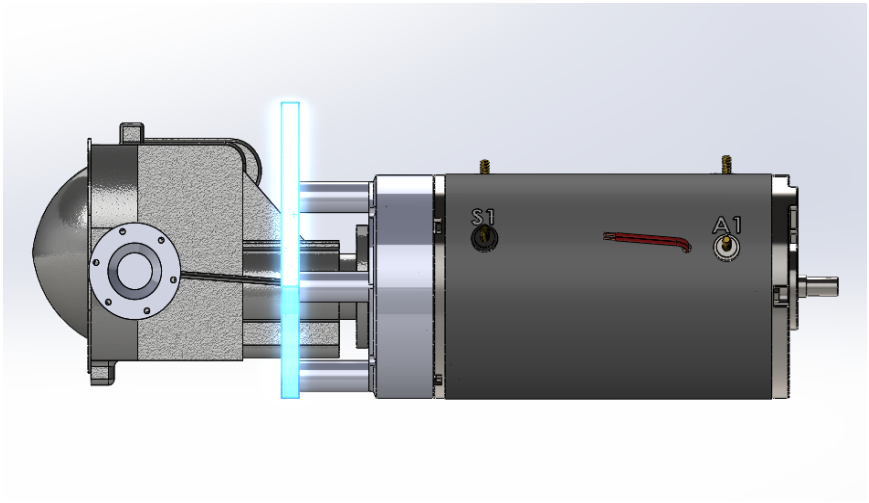

Figure 12: Assembly: Front Drivetrain Mount

- **Differential Modifications**

Once we purchased the 2000 Ford Ranger rear axle assembly from SLO Auto Salvage we began to deconstruct it in order to separate the differential case from the entire assembly. First, we researched how to remove the axle shafts from the assembly. First we removed the differential cover and carrier pin. Once the pin was removed the axle shafts were free to slide inward about 0.3 inches revealing the C-clips that lock the axle shafts in place. After removing the C-clips, the axle shafts could be pulled out of the axle housing. With the axle shafts removed we could see down into the axle housing to ensure we would not hit any bearings or other components when cutting through the axle housing. We could clearly see that the next bearing was inside the differential case so cutting anywhere along the housing would not be an issue. Next, we chose to cut the axle housing at the edge of the differential case using the horizontal band saw in the machine shop to remove the unnecessary material and isolate the differential case for use in our assembly. The outermost ends of the axle housings contained oil seals and bearings which we removed for inspection and dimensioning. Because we cut the axle housing at the intersection of the differential case, we cut off the portions of the housing that held the seal and bearing. An assembly view highlighting the bearing and seal can be seen on the following page in Figure 13.

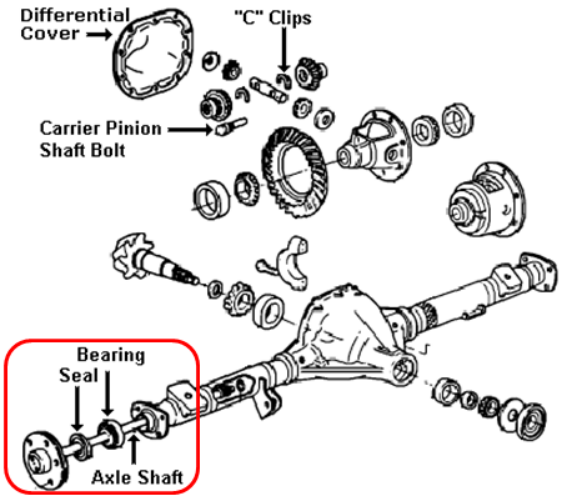

Figure 13: Axle shaft seal and bearing

Sealing the oil in the case and providing the additional bearing to counter any moments felt by the axle shafts are both things we knew we would have to include into our modified differential design. After removing and inspecting the outer bearings we found both sides to be in good shape. To save on the cost of new bearings, we chose to reuse these bearings in our modified differential design.

The original axle shafts will be cut to length using the horizontal band saw to fit inside the modified differential. Once the axles are cut to the proper length, an inch on the end of both shafts will be turned down on the lathe to a diameter of 1.002±0.001". This modified diameter section will then mate to the CV Half Shaft Interface using a press fit discussed in further detail in a later section.

In addition to case modifications we will also be making internal changes by replacing the open carrier with a limited slip carrier. Like the name suggests, this will turn our open differential into a limited slip differential. The primary advantage of installing a limited slip differential is to reduce power losses when a driven wheel loses traction. In an open differential, when one wheel loses traction a disproportionate amount of power is delivered to the slipping wheel. A limited slip differential limits the difference between the two axle's rotational speeds, ensuring more of the motors power reaches the ground. We selected the Powertrax L.S.D. that we will be ordering from Andy's Autosport.

After dimensioning the axle housing, we found the inner diameter of the axle housing increased over the length towards the center of the differential. This meant that the axle seals and bearings would not fit into the 2.5" inner diameter of the differential case. Manufacturing a spacer to make up the difference in diameter and welding it into place was determined to be too difficult so new axle oil seals that fit the diameter of the differential were selected. We picked Timken Timing cover seals from Autozone. The problem we encountered was that we could not find seals whose outer diameter would press fit into the 2.5" opening and whose inner diameter would seal nicely

around the diameter of the axle shafts. This same issue also applied to the bearings. For us to reuse the bearings we needed to both span the gap between the outer diameter of the bearing and the inside diameter of the differential case, and make up the distance between the inner bearing diameter and the outer diameter of the axle shafts. These differences in diameter were compensated for in the design of the bearing spacers and CV joint half shaft interfaces discussed below.

- **Bearing Spacers**

By cutting down the axle housing we removed one of the bearings that supported the axle shafts. To ensure we could handle any moments on the axle shafts we included a second bearing in our design. As stated previously, our problem was the new inside diameter of the housing was different than at the end of the axle housing. Additionally the differential case is not symmetric about the pinion shaft; meaning that to keep the CV interfaces symmetric about the vehicle centerline, we needed to locate the bearings at two different locations relative to the differential case. A top-down view highlighting this difference can be seen on the below in Figure 14.

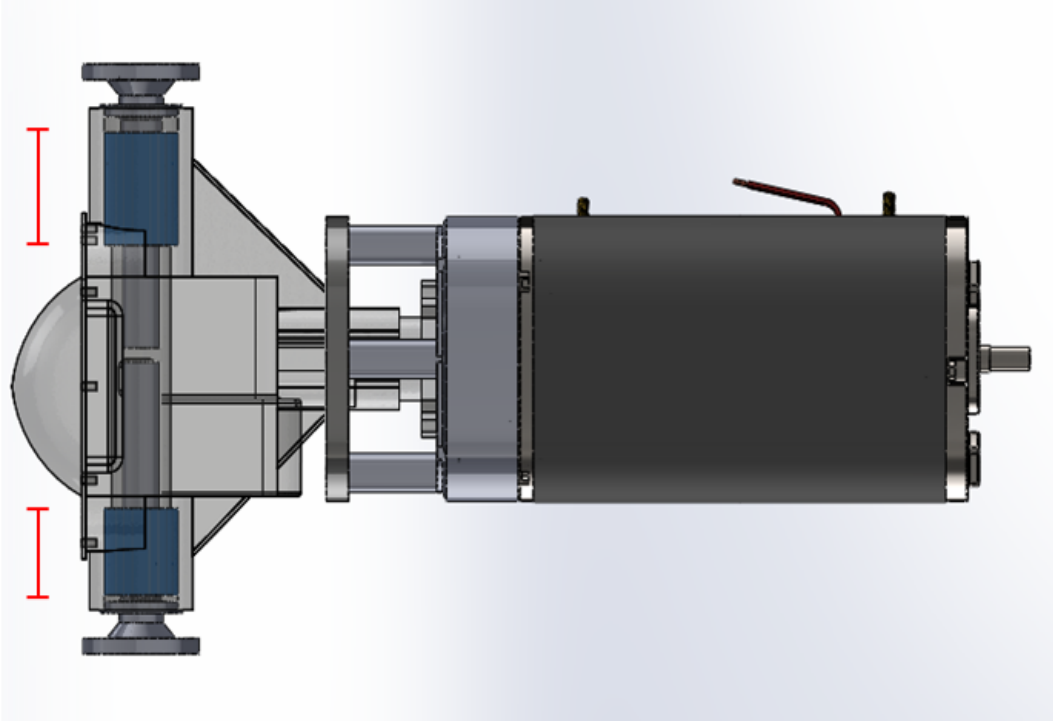

Figure 14: Bearing Spacer sizes & assembly

The spacers will have a 0.005 ± 0.003" clearance fit with the inner diameter of the housing and will butt up against a ridge inside the differential case. A picture showing where the spacer will stop in the differential case can be seen on the following page in Figure 15.

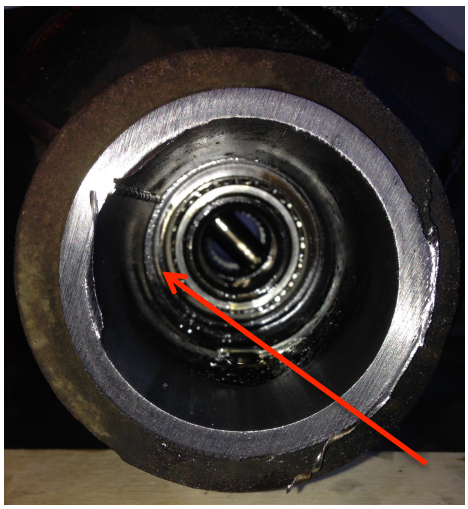

Figure 15: Interior of differential housing & bearing spacer stop

The bearing spacer will be manufactured from 2.5" outer diameter 6061 aluminum pipe that will be turned down by 0.002±0.001" on the lathe to fit inside the differential case. At the outside edge of the spacer, the inside diameter will be turned on the lathe to 2.252" to allow the bearing to be press fit into place. A picture showing a model of the part can be seen in Figure 16 below.

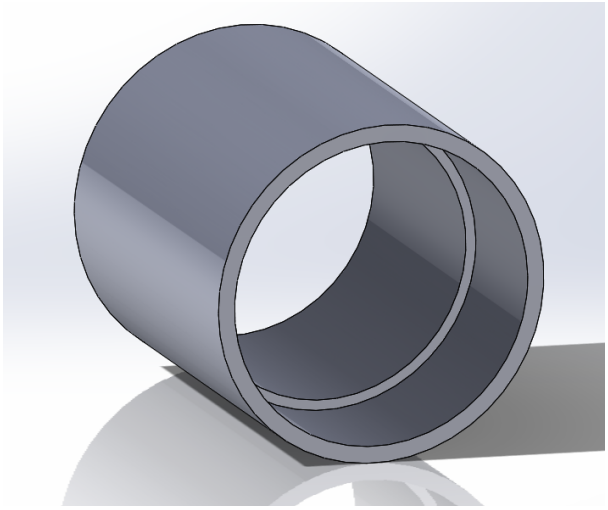

Figure 16: Bearing spacer

- **Constant Velocity Joint Half Shaft Interface**

The original Porsche rear axle assembly consisted of the transaxle and CV half shafts to transmit the torque from the motor to the rear wheels. However, the differential we selected was part of solid axle assembly that transmitted torque to the rear wheels directly through the axle shaft. In order to transmit the torque of the motor successfully, an interface that mates the Porsche's constant velocity half shafts to the axle shafts of the differential was necessary. A model of this interface can be seen on the following page in Figure 17.

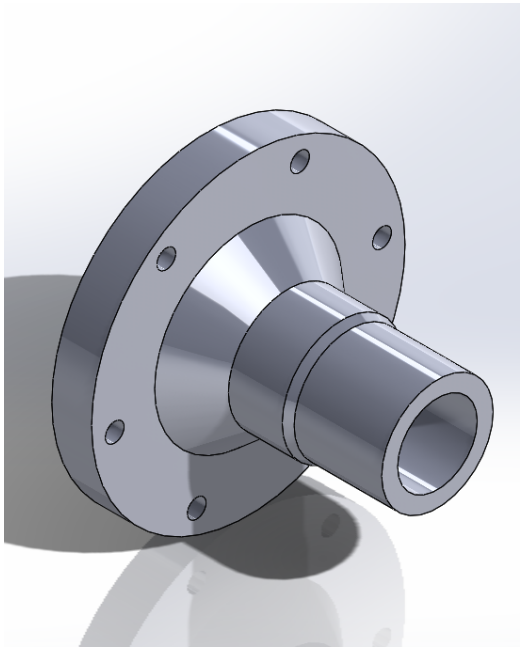

Figure 17: CV Half Shaft Interface

To secure the part to the modified axles of the differential, a 0.002" radial press fit would be used. The interference fit will support the entire torque of the motor (270 ft*lb) but because the power will be transferred through the differential before reaching this interface, it had to be designed keeping in mind the torque will be multiplied through the gear reduction. To ensure this joint won't fail we included a 0.25" weld around the entire circumference of the shaft. We calculated the factor of safety of this weld assuming twice of the peak motor output was applied directly to the weld without any consideration of the press fit and found the shear factor of safety to be 1.48.

This interface has been designed to serve more purposes than to exclusively transmit the torque from the axle shafts to the CV's. The outer surfaces of the part are also critical dimensions. The smaller outside diameter will serve as the rolling surface of the outer bearings. The first outer diameter of the half shaft interface will be 1.4" to fit the inside diameter of the original bearings from the Ford Ranger. The outer diameter of the interface part then steps up to 1.5" to match the inner diameter of the axle grease seals. The widths of both of these surfaces were designed to create enough space for the axle shafts to be pushed in and allow the C-clips to be removed for assembly and disassembly of the axles.

The threaded holes of the CV half shaft interface are sized and spaced to match the dimensions of the CV half shafts of the Porsche. These bolts were identified as an area of possible failure and were evaluated using equations (5) & (6) shown previously. Evaluating shear failure across these bolts gave us a factor of safety of 1.64 assuming no help from the press fit and twice the peak motor torque on a single joint. This being the lowest factor of safety in the system means that if failure is to occur anywhere, it should occur at these bolts before destroying anything else. This is an acceptable result for us because they are easily replaceable parts compared to other components in our system.

A grease well is also featured on this part that resembles the original grease well used in the Porsche transaxle. The inclusion of a grease well will allow more grease to be stored in the CV joint. The extra space in the joint will also allow for higher grease circulation while the joints are in operation to extend the life of the grease and the CV joints. A picture showing the grease well can be seen below in Figure 18.

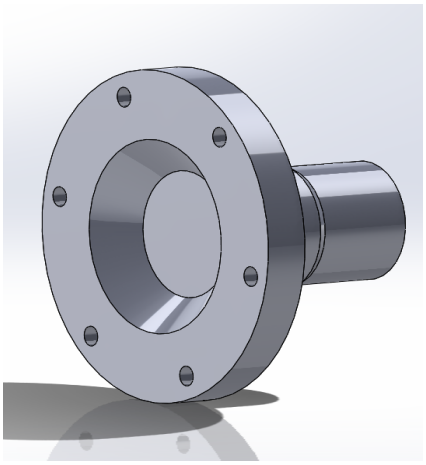

Figure 18: Grease well on CV Half Shaft Interface

These CV interface parts would be machined using the excess material from the 1-foot length of 5" round of AISI 1018 cold drawn steel used to create the motor/differential shaft interface. The outer surfaces and grease well would be manufactured using a lathe in one of the Cal Poly machine shops. The hole that will receive the axle shaft would be manufactured using a flat end mill and holes that mate with the CV half shaft bolts will be made using a drill press. The holes would then be threaded using a standard M6 metric tap.

- **Half Shaft Modifications**

The original transaxle of the Porsche has a width of 9". The modified Ford Ranger differential we will install in its place will be 16" wide. To accommodate this increased width we will need to decrease the lengths of the CV half shafts. This will be done by removing the middle 3.5" of both half shafts. The separated half shafts will then be press fit into a sleeve made from 1 .5" 1018 cold drawn steel round. The circumference of the interface will then be welded to increase the strength of the structure. The sleeve will be 0.25" thick and will be welded to the shafts with a 0.25" fillet weld. After completing the weld, the half shafts will be heat treated to increase their strength. We identified shear stress on the sleeve and sleeve weld to be the critical areas of interest and found the factor of safety for weld shear to be 1.52 while the factor of safety of sleeve shear was 1.81. In addition we performed deflection analysis on the sleeve and found it would only deflect 0.73° under full torque. This minimal deflection is acceptable due to the fact that our deflection equation does not take into account the distribution of the torque along the length of the sleeve since the sleeve will be press fit onto the CV shafts. With this torque distribution taken into account the expected deflection would be considerably less.

The half shaft sleeves will be manufactured out of a one-foot section of 1.5" 1018 cold drawn steel round. The inner diameter of the sleeve will be manufactured using a drill press with a 1.25" diameter bit. This inner diameter will allow a radial interference of 0.001" with the 1.252" diameter of the CV shafts. This press fit will alleviate a portion of the shear stress on the welds. To achieve this press fit, first the CV joints will be deconstructed so no damage of the joints will occur. Next, the sleeves will be thermally expanded using the oven at the shops on campus in preparation for the press fit. Finally, the two CV shafts will be press fit into the sleeve and allowed to cool. The joints will then be welded around their circumference to increase the joint strength.

- **Mounting**

Prior to our involvement in the electric Porsche conversion project, the electric motor was attached directly to the stock Porsche transmission and the rear motor mounting bar. Two bolts at the front of the transmission and two in the rear motor mounting bar attached the entire drivetrain to the body of the car allowing easy removal/installation. Figure 19 below shows the factory Porsche transmission's two bolts that vertically attach the transmission to the transmission mounts.

Figure 19: Front drivetrain mounts

The two rear bolts holding in this assembly seen in Figure 20 on the following page also attach vertically to the rear motor mounts.

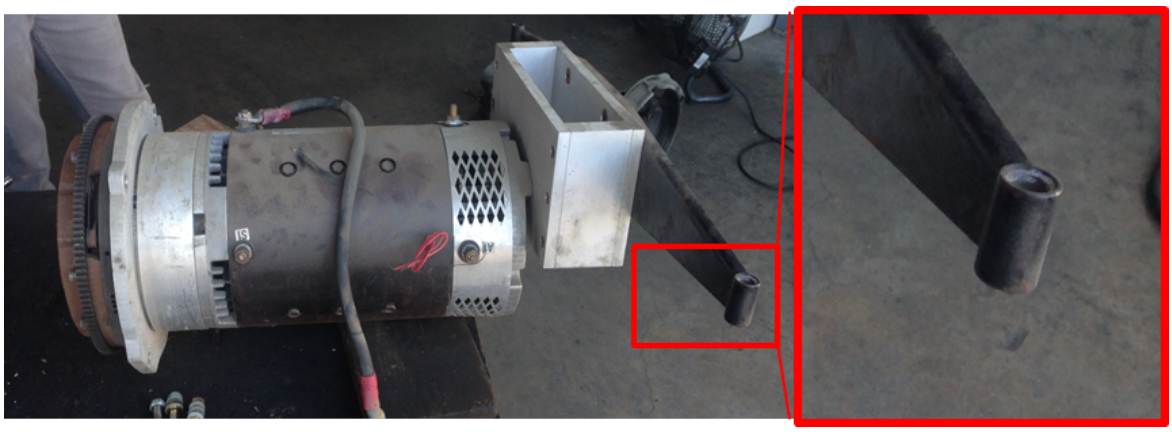

Figure 20: Rear drivetrain mounts

This allows access to all the drivetrain bolts when the car is placed on a lift. With the bolts removed, the engine and transmission drops down and out of the rear motor bay. Because of this removal/installation process, the interface between the motor and transmission can be looked at as a single rigid structure from a mounting standpoint. We have decided to maintain this single rigid structure in our design allowing us to take a similar approach in mounting our drivetrain system.

We have maintained the rear-mounting bar from the existing Porsche mounting system, however we have slightly modified the interface between the motor and the rear-mounting bar. This interface now consists of a single 0.5" aluminum plate replacing the previous aluminum block. For this part we will be able to repurpose one of aluminum plates that made up one side of the aluminum spacer block used in the original assembly. This will decrease our material costs and decrease manufacturing time because the top holes connecting the aluminum plate to the mounting bar have already been drilled. Analysis has been performed on the bolts required to hold our drivetrain in Appendix III and a minimum diameter of .008 inches is required, much smaller than the smallest bolt (0.375") currently used on the aluminum block. This will allow the reuse of the bolting hardware for the rear mounting system.

Another part that was reused is the existing motor mount on each side of the rear-mounting bar. These mounts were installed by Porsche and will be suitable to reduce vibration transmission to the drivetrain. The isolation of the drivetrain makes for a more comfortable ride and dampens impulse forces exerted by the Porsche's body. Isolation of the drivetrain was considered by the Porsche engineers and was a factor in the design of both our front drivetrain mount and rear mounting plate. The final configuration of the repurposed rear mounting plate can be seen in Figure 21 on the following page.

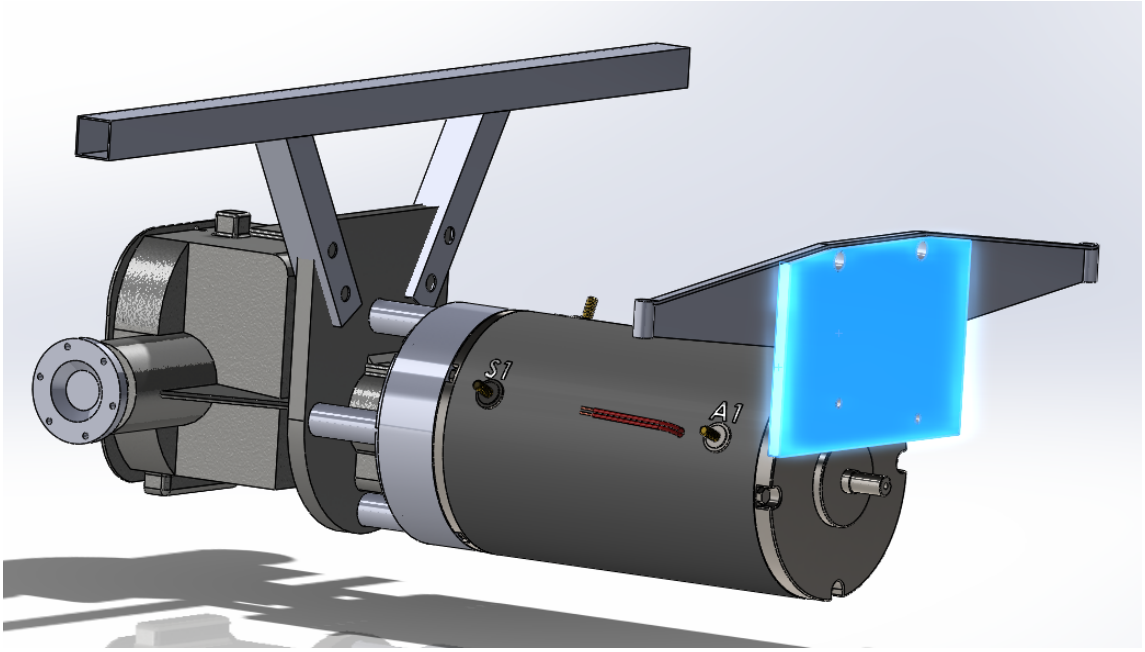

Figure 21: Rear drivetrain mounting plate

The front drivetrain mount unfortunately is not as similar or straightforward as the rear drivetrain mount design. The major factor that would require a different design than the existing solution was the shorter length of the drivetrain assembly. The differential is about twelve inches shorter than the length of the transmission. This requires either long support bars spanning the 12" gap to the original Porsche transmission mounts or a different mounting mechanism. Long support bars spanning the distance from the differential to the transmission mounts will need to be rigid in many directions and require a high second moment of area in the vertical direction to support the weight of the drivetrain as a cantilevered beam. This design would require an excessive amount of material and would significantly increase the cost of the system. After exploring a few options, we found that a design suspending the system from above would be the most structurally sound for the least amount of cost and material.

Figure 22 on the next page shows our front mounting system. The rear mounting system worked well for the factory installed internal combustion engine as well as the initial electric conversion. This rear mount was the inspiration for the front suspension design. The design incorporates a horizontal bar spanning the engine bay with two welded vertical supports at opposing 35° angles attaching the front differential mounting plate to the horizontal bar.

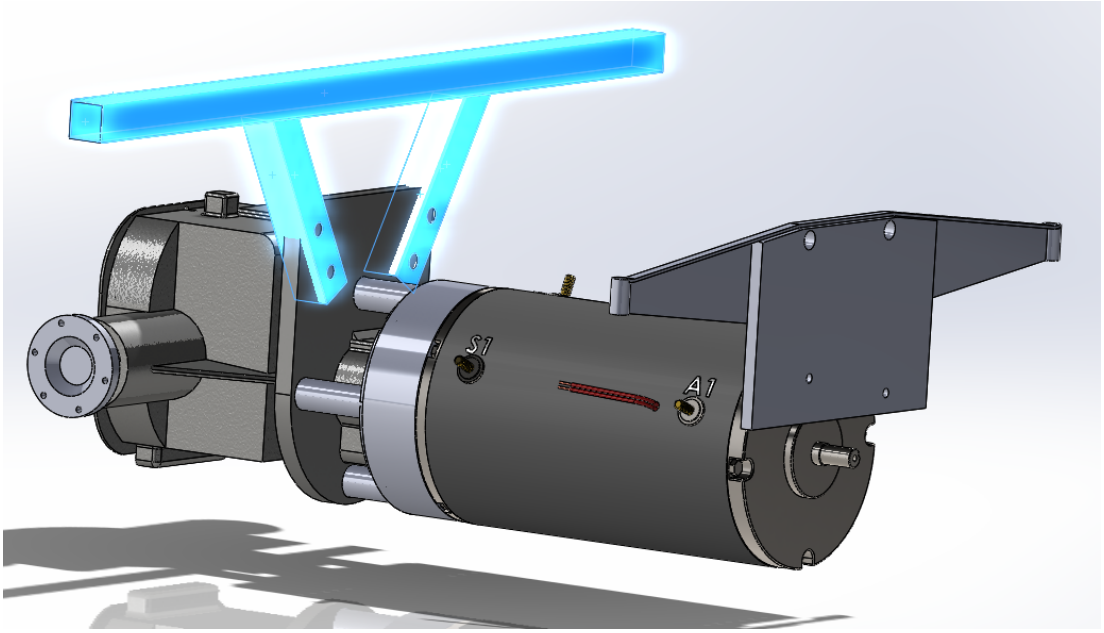

Figure 22: Front drivetrain mount

The vertical bars are welded onto the horizontal support bar and are bolted to the front differential mounting plate. The bars will be made of structural tubing to cut down on weight and the cross-sectional dimensions of the vertical bars were chosen to allow for a vertical cut in the bottom of each bar to straddle the mounting plate. Specifically square tubing was chosen to increase the second moment of area of the cross section of the pipe for maximum structural rigidity in bending. The 0.75" inch thickness of the mounting plate requires the mounting bars to have an opening of at least 1" inch to fit over the mounting plate and have sufficient geometry to withstand the bending moments that can be supplied by the lateral movement of the drivetrain in the axis of the car's movement. 1.5" steel structural tubing was chosen to make the vertical bars identical to the horizontal suspension bar. This similarity in tubing will allow the vertical and horizontal bars to be joined with a 0.125" weld and analyzed as a large rigid body.

A 39" long horizontal suspension bar will be welded to the inside body of the Porsche's engine bay with four 0.1875" fillet welds, 2.5" in length on each edge that the bar contacts the engine bay. This weld size has been chosen to withstand the maximum torque the motor can deliver amplified through the mount as well as the maximum deceleration force exerted on the bar during a crash. According to the National Highway Traffic Safety Administration, a typical crash results in around 10g of deceleration and that is the standard that we have held our welds to. At 10g of acceleration the welds of the horizontal suspension bar will still hold with a factor of safety of 1.49 without considering the rear mounting bar sharing some of the load. Although this is not a high factor of safety, this is a factor of safety when the car has been in a collision and there is very likely large damage done to the rest of the car. If the weld were to fail, for example in a more severe collision, the lack of deflection of the front steel structures would pivot the drivetrain and force the rear of the motor into the ground before the drivetrain would travel significantly in the direction of the front of the car.

One caveat, as introduced from the rear mounting system, was the isolation of the drivetrain from the body of the Porsche. This design would not allow the drivetrain to be attached through a rubber motor mount so another solution was necessary. Our solution was to use a polyurethane bushing at each attachment point of the drivetrain and the front motor mount. This bushing would preserve the drivetrain isolation and fill empty space in the attachment points of the mounting bar to the front drivetrain mounting plate as seen in Figure 23 below.

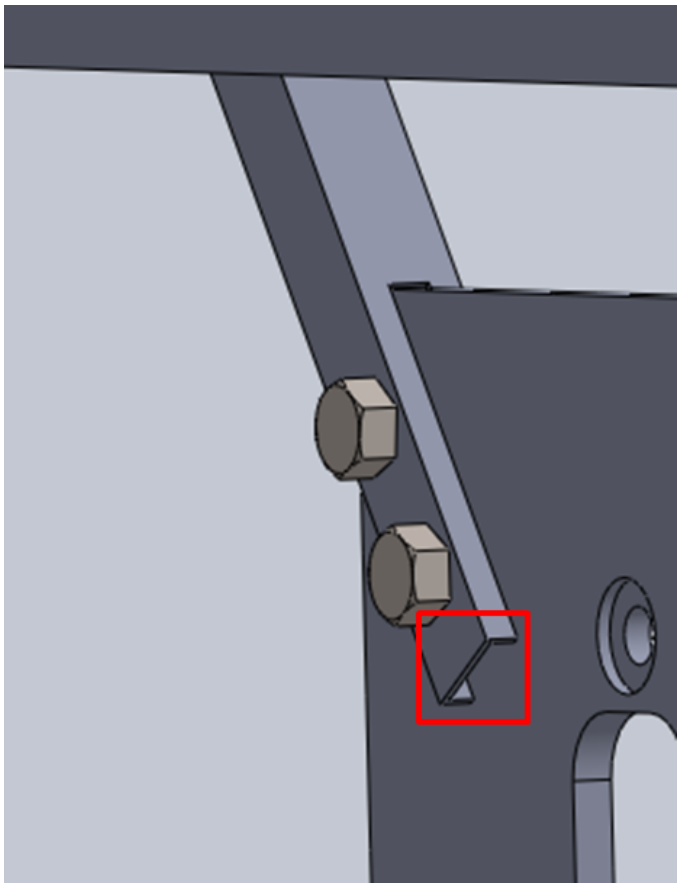

Figure 23: Bushing gap

A Prothane 19-921 Bushing was chosen to fit in each of the boltholes. The inside diameter of the bushing is 0.375" to accommodate the 0.375" bolts that will secure the interface between the vertical bars and the front differential mount plate. The bushing will fill the 0.2475" gap seen above and replace the function of the rubber transmission mount previously attaching the front of the drivetrain to the Porsche.

Assembly

We wanted the assembly of the new drivetrain to be as close to the original as possible. The entire original drivetrain is held into the frame of the car by four mounting bolts. To do any disassembly of drivetrain components you must first remove the entire drivetrain as one unit and

then disassemble it on a bench. Our drivetrain design will operate under the same procedure. Detailed step-by-step installation instructions are provided below:

Drivetrain Assembly

1. Bolt the motor shaft collar to the differential flange using the 0.5" standard coarse thread bolts tightened to 44 lb*ft with a torque wrench.
2. Bolt the aluminum motor interface to the face of the motor using the four existing bolts.
3. Screw threaded rods into the tapped holes in the aluminum motor interface until they stop.
4. Put aluminum spacers over the threaded rods and push them into the countersunk holes of the aluminum motor interface.
5. Turn motor shaft manually to put key slot facing upward and put key into the key slot.
6. Align threaded rods with the holes in the front drivetrain mounting plate and bring motor assembly and differential gearbox together making sure to align the motor collar key slot with the orientation of the key on the motor shaft.
7. Press assembly together to make sure aluminum spacers are fully set into their respective countersinks.
8. Install a 0.5" lock washer and nut on each of the exposed ends of threaded rod.
9. Use floor jack to lift assembly into relative position.
10. Install bushings and bolts into the front drivetrain mount.
11. Install bolts on rear drivetrain mount.
12. Align half shaft CV joints with the CV interface flange of the differential and bolt together using M6 bolts.
13. Repeat step 12 for other CV joint.

Additional Analysis

The CV coupling was identified as a possible point of failure under peak loading conditions and was therefore a good candidate for further analysis using finite element models. Finite element modeling of the CV coupling was performed to determine the max Von Mises stress in the part as well as to compare the max deflections with those found in preliminary hand calculations.

The interface includes a flange with 6 symmetrically spaced bolts and a 0.002 inch press fit between the axle shaft and the coupling. Complete details of the parts involved are discussed further in the summary section below. The goal of the model was to confirm that no failure would occur across this interface. Additionally, we wanted to see where the peak stresses would be in the system to show where it would fail if a load exceeding the peak abilities of the motor was applied.

Summary

The system was modeled with linear quadratic elements and meshed using a seed size of 0.025 inches. A convergence study was performed to ensure there was mesh convergence in the model. The convergence study plot can be found in Figure 31 of the Mesh Development &

Convergence section. Three different models were created. A 2D axisymmetric model of the system, a full 3D model of the press fit stresses and deformations, and a separate model of the bolt shear. The axisymmetric model was used to model the torque transmission from the gearbox, down the shaft, through the interference fit, to the coupling. The interference fit was defined with small sliding and contact pressure data. The pressure created by the interference fit was found to be 24751.8 psi with a coefficient of friction of 0.6.

FE analysis yielded radial deformation of the coupling due to the press fit to be 0.000916 inches. Peak Von Mises stresses in the part were found to occur in the wall of the coupling through the plane defined by the end of the input shaft with a value of 97330 psi. A plot of the deformed axisymmetric FE model can be seen below in Figure 24.

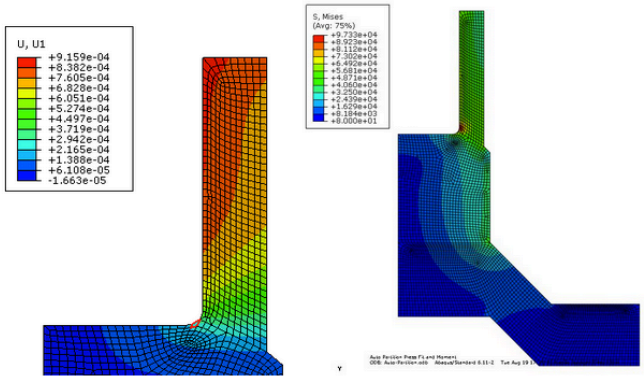

Figure 24. Axel shaft CV Joint coupling.

Bolt shear was modeled separately and when compared to stresses in the coupling was determined to be negligible. If anything in the system were to fail it will be the coupling at the point of the stress concentration in Figure 24, through the plane defined by the bottom of the axle shaft.

Model Development

To make sure our model produced accurate results we broke the problem into multiple models to highlight individual interactions so we could compare and validate the results of the full 3D model. Additionally, from our initial hand calculations we used a peak torque value of 1107 ft*lbs applied across the bolts which is two times the peak torque of the motor multiplied through the gearbox and applied entirely to one side. Calculating the shear factor of safety under these conditions we get a value of 1.64. Even in the worst-case scenario where the rear wheels are off the ground spinning under full power and are dropped on the ground, the system would not feel loads of this magnitude. Because we have a factor of safety under these conditions, with no consideration for the frictional forces between the part faces due to bolt preload, we assumed that failure across the bolts to be negligible. This allowed us to remove one of the components of the model and to set our Encastre boundary conditions on the face of the coupling when applying torques to the model. Also, because the stresses associated with the bearing and oil seal are so small in comparison to the stresses associated with the press fit we chose not to include them in the model.

With these two assumptions in mind we were able to model the press fit and applied torque using deformable solid axisymmetric elements. The basic model layout can be seen below in Figure 25.

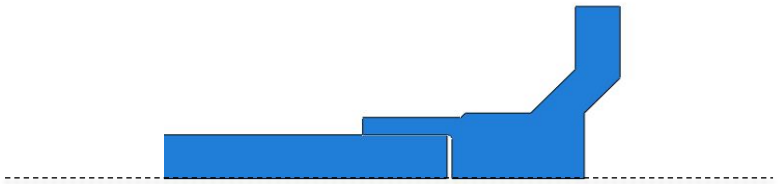

Figure 25. Axisymmetric configuration of shaft and coupling.

- Coupling

To model the coupling we used a variety of different techniques to try to validate our results. Initially we took the CAD model from Solidworks and saved the part as a ".stat" file. This file type allows conversion from Solidworks part to Abaqus. After struggling to partition the part and mesh it using the bottom-up method, we built a part with simplified geometry as seen in Figure 26 below. The cross section of the surface containing the press fit, bearing, and oil seal surfaces were changed to be consistent along the parts length to make meshing easier.

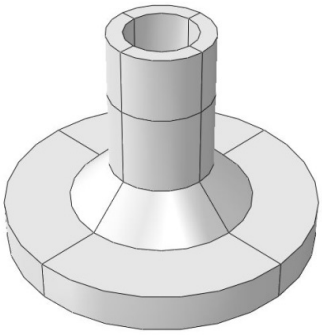

Figure 26. 3D render of the simplified coupling geometry.

For the axisymmetric model, the coupling was modeled with complete part geometry as seen in Figure 27 on the following page. We expected to see the most accurate results in this model because it is a closer representation of the actual parts geometry.

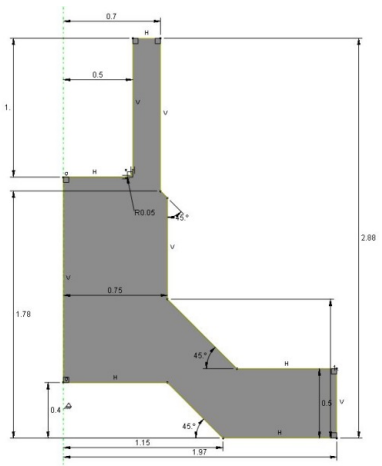

Figure 27. Sketch dimensions of axisymmetric coupling model.

- Bolt preload

In order to simplify the complete model of the system, a separate model was analyzed to show the effects of the bolt preload and shear. Two steel plates with thickness of 0.5 inches were modeled as being held together with a bolt. The model configuration can be seen below in Figure 28. The bottom plate, which acted as the CV joint face was held stationary with an Encastre boundary condition along the entire bottom surface. The bolt was partitioned at the center to allow the bolt preload to be applied, pulling the two plates together. Contact interactions were defined between the bottom of the bolt head and the surface of the plate, between the two plates, and between the bolt and the interior of the hole. After analyzing this configuration, the force on each bolt was found to be 1307.7 lb. We converted that force to a pressure of the surface area of one side of the top plate and applied a shearing pressure of 871 psi to the part. This pressure is equal in magnitude of that provided by a full-braking condition. The results this analysis can be seen in Figure 33 in the results section.

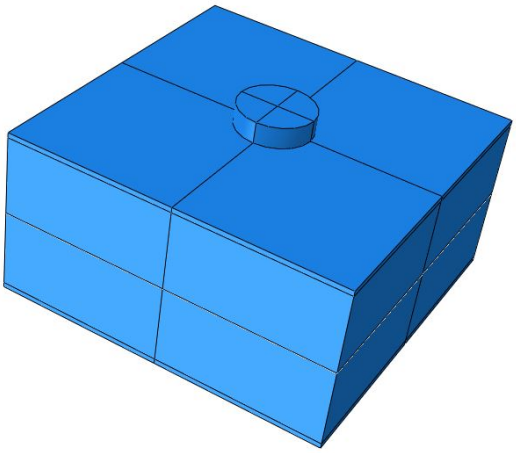

Figure 28. Bolt shear model configuration.

- Press fit and Applied Torque

As stated previously, without the presence of the bolt-holes, the coupling-shaft interface can be modeled with a 2D axisymmetric elements. The cross sections of the coupling and shaft were drawn in Abaqus and aligned so that the shaft overlapped the coupling by 0.002 inches.

After the model was positioned correctly, boundary conditions and loads had to be applied. The nodes along the bottom surface of the coupling were constrained in all directions. A contact interaction was then created between the interior surface of the coupling and the outside surface of the shaft using the surface pressure data preferences in Abaqus. The coupling was chosen as the master surface and the shaft as the slave. The coefficient of friction between the steel faces was chosen to be 0.6 and the pressure between the two surfaces was calculated to be 24751.8 psi. The interaction was specified to have small sliding and surface-to-surface contact. This contact interaction, in conjunction with the positioning of the shaft, provided the press fit stresses shown in the results section in Figure 13. The press fit was also modeled using a full 3D analysis using our simplified geometry. Results from the 3D model can be seen in Figure 35 of the results section.

After the press fit was established, we wanted to apply a torque to the shaft. To accomplish this we needed to create a reference node on the top surface of the shaft on the axis of symmetry. This reference node was tied with a coupling constraint to all of the nodes along the top surface of the shaft. The applied torque was then assigned to the reference point. The results of this analysis can be seen in Figure 34.

Mesh Development & Convergence

When we began working with our 2D axisymmetric model, we were unsure how to partition it to create the best mesh. After some research, we came across the auto-partition face tool in Abaqus. We used this tool to break up our cross section into smaller pieces, which allowed Abaqus to generate a more uniform mesh. This partitioning is shown below in Figure 29.

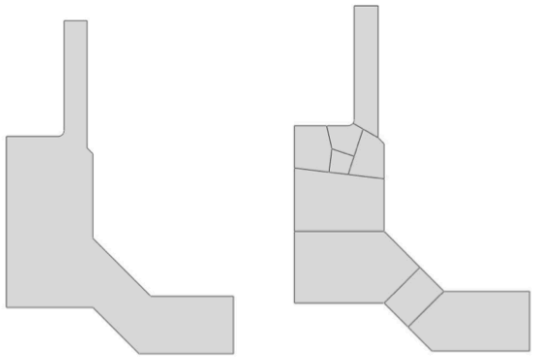

Figure 29. Cross-section of coupling before and after partitioning.

After properly partitioning the part, we performed a convergence study to find the ideal seed size with which to mesh our part. Linear quad elements were used throughout the model. We chose to perform this convergence study on the Von Mises Stress felt by an element in the upper left hand corner of the part seen in Figure 30 below.

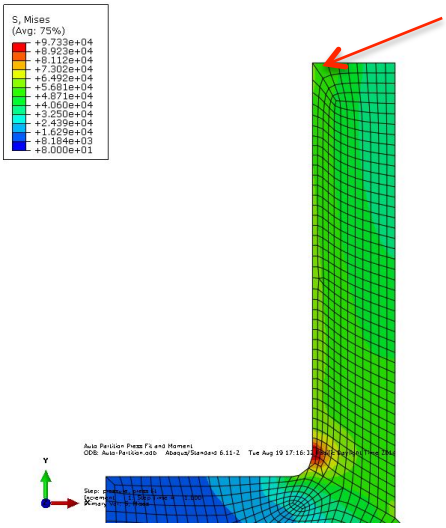

Figure 30. Element selected for convergence study highlighted with arrow.

We chose this location because it is a critical area of interest, but is also far away from the stress concentration and discontinuities seen in the corner of the part. We ran five trials with seed sizes from 0.1 to 0.01 inches. When the seed size changed from 0.025 inches to 0.01 inches, the value of the Von Mises stress in the element of interest changed by only 1.9%. The convergence plot can be seen below in Figure 31.

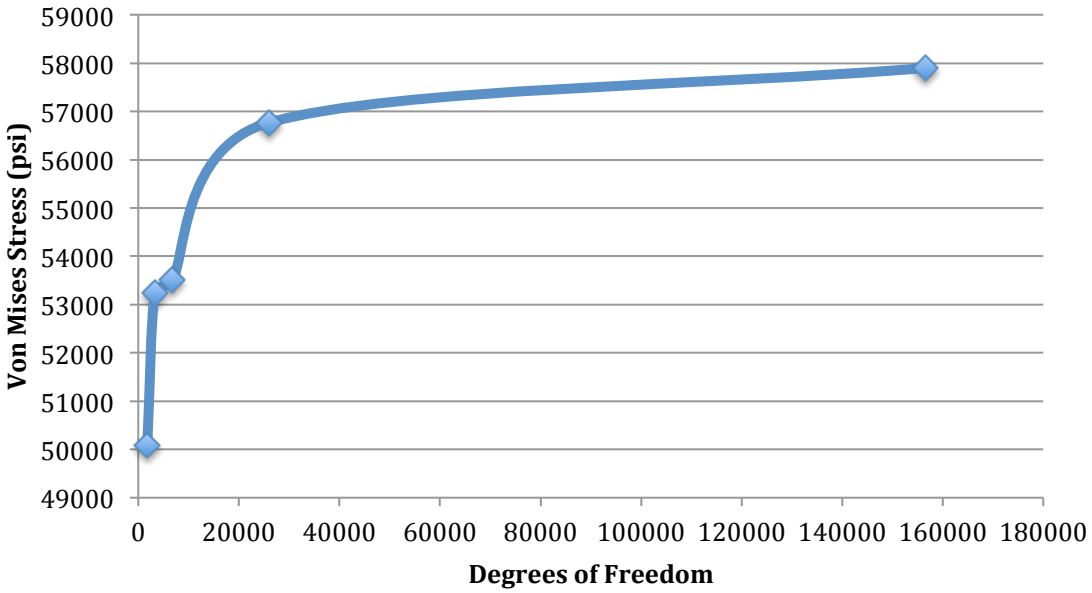

Figure 31. Convergence study on max Von Mises stress.

When running the analysis, we were presented with a warning saying that we had 11 elements that were distorted. Upon further analysis, we found that there was only one element in the area of interest that was distorted. This element is shown highlighted in red in Figure 32 below.

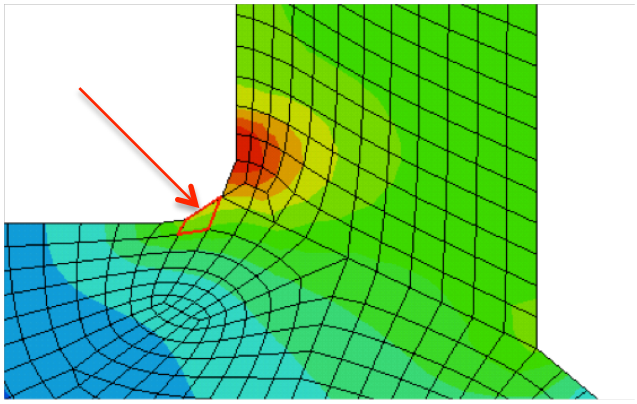

Figure 32. Distorted element highlighted in red.

Having many distorted elements can make it nearly impossible to get a converging mesh and also makes the local results less accurate. Because there was only one localized case, and the mesh in surrounding area is good, the effects of this one element were neglected.

The shaft was meshed using the same seed size and element type as the coupling. Because the geometry of the shaft is simple, we could assume that if the mesh of the coupling converged, then the mesh of the shaft would converge also. The final mesh converged at seed sizes of 0.025 inches. This made the coupling mesh with 8249 elements and 25978 degrees of freedom.

Results & Discussion

When analyzing the bolt shear model, we found that when the preload was applied to the bolt, the stresses from the preload greatly outweighed stresses from the shear force. To ensure that we were getting proper results from our contact interaction we ran the model again without the preload activated. The results of these tests are shown below in Figure 33. It can be seen in the figure on the right that the loads on the bolt are symmetric from the bolt being sheared by the two plates.

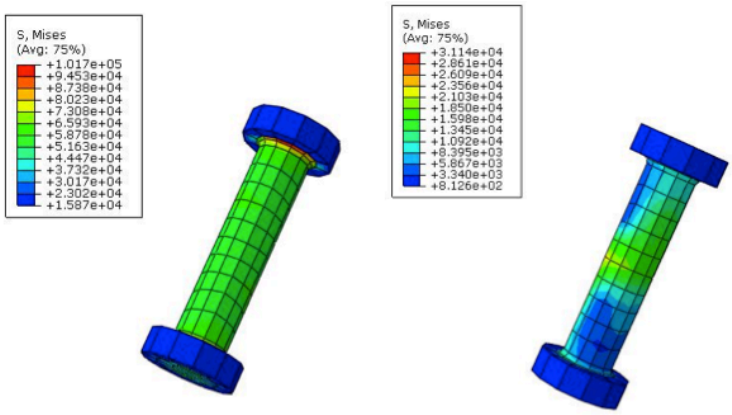

Figure 33. Stresses in bolt with preload and applied shear (left), bolt with only applied shear (right).

The stress in the body of the bolt where we are concerned about shearing is about 50,000 psi. The largest stress felt in the bolt occurs right at the interface between the bolt body and the bolt head, with a Von Mises stress of 1.02×10^5 psi. However, these stresses are not of concern when compared to the ultimate strength of the bolts of 176,900 psi.

In order to verify the axisymmetric model, a quick comparison was made between the model and hand calculations regarding the radial deformation of the coupling. As can be seen on the left of Figure 34 below, the model predicts radial deformations of 9.916×10^{-4} inches, which is very close to the value provided from the hand calculations of 1.166×10^{-3} inches. These results served to verify that our model was outputting correct data. After verifying the radial deflection, we looked at the stresses throughout the part shown on the right of Figure 34. It can be seen that the press fit and applied torque only affect the part locally, and that further away from this location the effects are minimal.

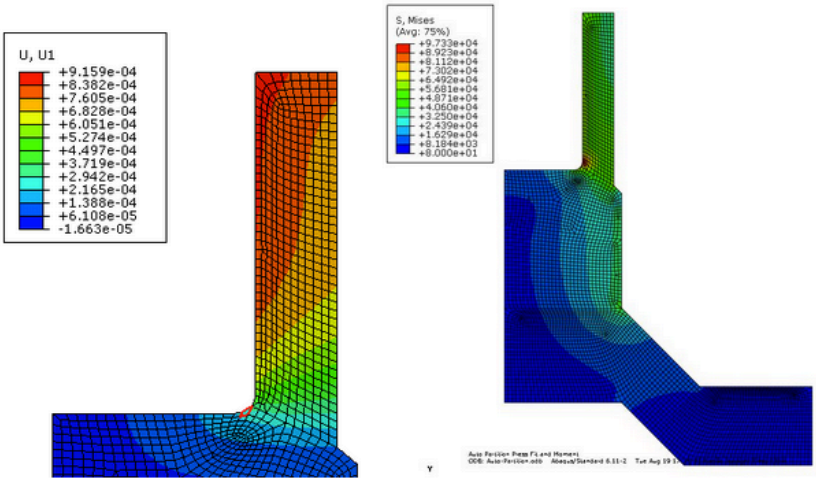

Figure 34. Results of axisymmetric model.

It can be seen from Figure 34, on the previous page, that the stresses throughout much of the area of interest are right around the ultimate strength of 63,800 psi (the element on which the convergence study was taken had a stress value of 56,768 psi). There also exists a significant stress concentration in the corner of the part with a stress value reaching as high as 97,330 psi. Values of this magnitude are not surprising however, because of the high torque applied in the model. Under normal loading conditions, the part will never feel stresses of this magnitude. However, this stress concentration is still valuable because it highlights the area where the part would likely fail if something catastrophic were to occur. These results could justify doing some real life testing on the part when it is created. Strain gauges could be placed at this location on the part under static loading conditions to obtain more experimental results. Hopefully these results could be used to further verify this finite element model.

For the full 3D model, the press fit was modeled as a pressure on the inside surface of the coupling and the torque was applied through the shaft with tie constraints. The results from this analysis can be seen below in Figure 35. It can be seen that the maximum stresses in this model are even greater than those provided by the axisymmetric model. This is justifiable because in the axisymmetric model the stress is shared between the expansion of the coupling and the compression of the shaft. In this model, the whole pressure is applied to expanding the coupling, causing even greater levels of stress.

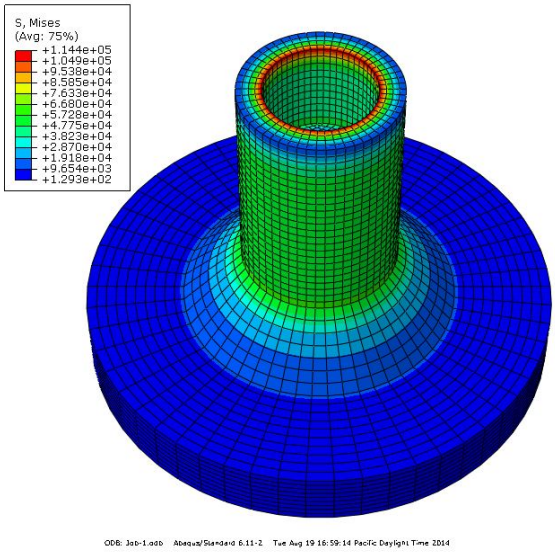

Figure 35. Stress results of 3D model.

As discussed previously we tried modeling the entire system in 3D with all of the interactions and geometry with no success. Meshing the 3D model of the coupling turned into a much more difficult problem than we had anticipated and we spent hours trying to partition the part in a way that would allow us to get a good mesh. Because of the geometry of the part, Abaqus would not automatically mesh the part and required the use of the bottom-up meshing technique. Bottom-up meshing requires the user to partition the part into many smaller regions and mesh each region independently. To do this effectively, we partitioned the part at each change in cross

section along the axis of symmetry. This left us with cross sections of simpler geometry that was easier to seed and mesh.

After meshing the entire assembly, a query was run to look for mesh gaps and intersections. This exposed issues between each of the various sections where there were gaps in the mesh. Fixing this problem requires associating the mesh with specific part geometry and/or editing and merging nodes between bottom-up cells. We were successful in merging some of the nodes to close gaps but were still unsuccessful in getting a satisfactory mesh that could converge at all. The other option to solve our problem was to mesh the part using Tet elements. This is not a desirable choice for the accuracy of the results and even after meshing the part with Tet elements we continued to encounter problems that prevented us from getting any results. At that point we decided to move to the more simplified models of individual interactions discussed above before trying to come back to the full 3D system model.

Conclusion

Finite element modeling of an axle coupling was performed to determine the max Von Mises stress in the part as well as to compare the max deflections with those found in preliminary hand calculations. The system was modeled with linear quadratic elements and meshed using a seed size of 0.025 inches. To simplify the analysis three different models were created. A 2D axisymmetric model of the system, a full 3D model of the press fit stresses and deformations, and a separate model of the bolt shear. Convergence studies were performed to ensure there was mesh convergence in the model.

The interference fit was defined with small sliding and contact pressure data. The pressure created by the interference fit was found to be 24751.8 psi with a coefficient of friction of 0.6. The bolt pre-load was applied by using the bolt load options applied to the center of the bolt model.

FE analysis yielded radial deformation of the coupling due to the press fit to be 0.000916 inches. Peak Von Mises stresses in the part were found to occur in the wall of the coupling through the plane defined by the end of the input shaft with a value of 97330 psi. Bolt shear was found to be negligible compared with the stress due the preload and both values are below the ultimate strength of the bolts. If anything in the system fails it will be the coupling at the point of the stress concentration in Figure 24, through the plane defined by the bottom of the axle shaft.

Chapter 5. Product Realization & Test Fixture Design

Sponsor Redirection

After summer break, our team met with the new Cal Poly Motor Car Association President, Michael Saggese, to discuss the manufacturing and testing plan. Mr. Saggese informed us of additional funds the club received to be used on the Porsche remodel. He also informed us of his desire to pursue our concept that included the two electric AC motors with an electronic differential. These shifting club goals limited the utility of our project. In particular, the club's goal of replacing the Advanced DC motor, whose characteristics our design is optimized for, would drastically limit the usefulness of manufacturing our entire design using the club's money. For this reason we adjusted our approach to the manufacturing and testing of our project to be most useful to the club moving forward. We focused our efforts and resources on rigorously testing the current transmission as well as our differential in order to limit the club's cost for our project. We canceled the integration of our proposed differential into the Porsche due to considerable structural modifications including welds to the Porsche's frame. This would limit the future plans of the club to replace the motor as well as use funds the club will need to complete a more comprehensive rebuild of the Porsche.

Test Fixture Design

Typically, a dynamometer would be used to test the mechanical losses of the Porsche transmission and our system. However, since we were unable to locate a power source capable of supporting our Advanced DC motor, a dynamometer would not have been useful for our testing. Since our mechanical loss test is only concerned with the change in shaft rotational speed, we decided to design and build our own test fixture with tachometers. The tachometers were made out of an infrared led emitter and receiver that detected a change in brightness as a set portion of the shaft broke the beam between emitter and receiver. The test fixture consisted of a wooden frame made to secure both the transmission and differential. We clamped the front transmission mounts using threaded rod with nuts and washers to secure the transmission. We then wrapped a ratcheting tie down around the rear (input) of the transmission for added safety. Once the wooden fixture for the transmission was completed, we modified the fixture so it could temporarily support the differential during testing. The bearing mounts for the output shafts of both drivetrains were the last parts of the wooden fixture to be manufactured by cutting a slot in a piece of wood for the shafts to pass through. Then we made slots perpendicular to the previous for the bearings to be pressed into.

The next stage of manufacturing consisted of modifications to the differential half shafts and stock steel round used as the half shafts of the transmission. First we cut all four shafts to a manageable length for testing. Then we turned down the end of each shaft from 1.25 inches to 1 inch in order to slide weights onto the end of the shaft that act as additional inertial load during testing. The stock steel round was turned down quickly; however, the hardened steel shafts we used for the differential testing fixture were incredibly difficult to machine. We had many

discussions with nearly every Cal Poly shop technician in order to diagnose our inability to any significant amount of material from the hardened steel shafts. One of our first ideas was to replace the carbide cutting tools but the shop techs stood by the shop's cutting tools. Instead, many of the shop techs believed the age and low quality of the lathe was to blame and advised us to continue turning down the shafts at a painfully slow rate. After exhausting the suggestions from the shop technicians, we decided to purchase new carbide cutting tools. Once we attached the new carbide cutting tool to one of the shop lathes, the hardened steel shaft was quickly turned down. After this frustrating experience was behind us, we moved onto the motor shaft interface.

The motor interface transferred the torque of the motor to the input of the drivetrains. We first cut a piece of the steel round to be used for the motor interface. We then drilled a clearance hole in the steel round for the half-inch motor shaft and aligned a set-screw with the flat section of the motor shaft. A hole on the other side of the shaft interface was drilled and tapped in order to attach the steel plate interface using a bolt, locker, and lock washer. Next, we cut square pieces of sheet steel to be used as mating interfaces between the output of the transmission and the half shafts as well as the interfaces between the motor and the inputs of the two drivetrains. Once the steel squares were cut, we drilled clearance holes in the center of the square in order to secure the plates to their respective shafts using a bolt, washer, and lock washer. After, we drilled the circular pattern of holes needed to mate the plate to its respective surface, i.e. the CV circular hole pattern or the transmission input circular hole pattern. Finally we were able to attach and secure the interface plates to one another. For the CV half shaft interfaces, we simply bolted the respective steel mate plate to the half shaft with the original bolts used to attach the Porsche's CV coupling. For the transmission and differential input interfaces, we used threaded rod, nuts, washers, and lock washers to clamp the steel mate plates to their respective input shaft.

Chapter 6. Design Verification

Testing Method

We have devised a series of tests that will determine the added efficiency of our new drivetrain over the existing internal combustion engine transmission. The tests will determine the electric motor's power transmission to the differential and the stock Porsche transmission individually. The power transmission will be determined by measuring the electrical power draw of the motor as the motor brings the output of the drivetrain options up to a specified speed. Each drivetrain option will have a measured weight on each output shaft to simulate a load that would be seen when installed in the Porsche. Identical tests will be repeated on both the transmission and the replacement differential after initial baseline testing is completed.

Both the transmission and the replacement differential will be secured in a custom jig that will allow an electric motor to power the drivetrain options in a safe and consistent manner. The jig ensures that the electric motor used for testing is attached directly to the input shaft of the drivetrain option and the output shafts are supported identically. There is a large difference in geometry between the transmission and differential and this difference has been accounted for with inserts made to secure the much smaller differential in the same location as well as locate the input shafts identically as the mounted transmission. This consistency between mounting the differential and transmission will ensure that all sensors acquiring data during the test will have reliable readings for each drivetrain option tested in the jig.

Three tachometers and an ammeter are required to ensure that we can collect all the necessary data to determine the power transmission. Each of the three tachometers consist of an infrared emitter and an infrared detector. There will be a tachometer on the input shaft and each output shaft of the drivetrain option in the custom testing jig. There will also be a non-invasive current sensor to measure the current draw of the electric motor. The Hall-Effect current sensor wraps around one of the power input lines of the motor to safely measure the incoming current. All of these sensors will be attached to an Arduino Uno that will measure each sensor at the same time interval. This data acquisition setup will allow measurement of all the important aspects on the same time scale making the comparison between the data for the differential and transmission as accurate as possible.

The first baseline testing will include running the motor up to its maximum speed while measuring current draw and motor shaft output speed. This will provide an unloaded measurement of how quickly the motor can reach its maximum speed. The data from this baseline test will also show the resolution, reliability and steadiness of each of sensor's outputs.

The actual test for each of the drive train options will consist of multiple speed increases from a low speed to a higher speed. The tests will be categorized by the voltage supplied to the motor at the lower speed and the higher speed. The first test will begin with the motor at 0V and increased immediately to 120V. This will be the most extreme test that can be completed with our

supplied electric motor. The next test will start the motor at 40V and increase the voltage immediately to 120V. For the final test the motor will begin at 80V and increased immediately to 120V. Each of these tests will be repeated 3 times to ensure the most accurate data was acquired. Once all nine tests are run on the internal combustion engine transmission, each will be repeated on the differential after the jig is converted. After the all test are completed, there will be nine sets of data for each of the drivetrain options.

Power transmission from the electric motor will be calculated from the rotational speed of the shafts in relation to time. The known mass inertias on the output shaft, the change in rotational speed and the change in time will allow the power to be calculated though:

$$P = I * \frac{\Delta\omega^2}{2\Delta t}$$

Due to consistency between the rotating inertia and the data acquisition between the drivetrain option tests, it is not absolutely necessary to measure the rotating inertia to prove that one option is more efficient than the other. The more efficient option can be calculated simply by finding the greater quantity $\frac{\omega_2-\omega_1}{t_2-t_1}$ for the transmission and differential.

The completion of these tests with only four sensors will show which of the transmission and differential is most efficient in power transmission from a power source to the wheels. Our test will be conducted with the minimum amount of materials and therefore the minimum cost so the club will maintain as much capital as possible for future improvements to the Cal Poly Electric Porsche.

Testing Procedure

1. Setup jig inside a room near the door.
2. Attach one tachometer to the electric motor's output shaft and the current sensor to the motor's power cord.
3. Run the wires for the sensors out through the door and attach to an Arduino that is connected to a computer.
4. Run the power cord out through the door and attach to a variac.
5. Ensure that all bolts are correctly tightened and all moving parts are anchored correctly.
6. With the door closed and everyone out of the room, increase the variac quickly from 0V to 120V while recording data from the sensors.
7. Repeat step 6 twice to get baseline data.
8. Install the transmission into the jig and attach to the electric motor.
9. Attach 2 5-lb weights on each of the output shafts.
10. Install the 2 additional tachometers on each of the output shafts of the transmission and hook up the tachometers up to the Arduino.
11. Ensure that all bolts are correctly tightened and all moving parts are anchored correctly.

12. With the door closed and everyone out of the room, increase the variac quickly from 0V to 120V while recording data from the sensors.
13. Repeat step 12 twice.
14. Then with the same setup, start the variac at 40V and increase the variac quickly to 120V while recording data from the sensors.
15. Repeat step 14 twice.
16. Then with the same setup, start the variac at 80V and increase the variac quickly to 120V while recording data from the sensors.
17. Repeat step 16 twice.
18. Repeat steps 11 through 17 with 1 5-lb weight on each of the output shafts.
19. Remove the transmission from the jig.
20. Install the differential and attach the electric motor to the differential.
21. Attach 2 5-lb weights on each of the output shafts.
22. Make sure the tachometers are installed on the input shaft and both output shafts of the differential.
23. Ensure that all bolts are correctly tightened and all moving parts are anchored correctly.
24. With the door closed and everyone out of the room, increase the variac quickly from 0V to 120V while recording data from the sensors.
25. Repeat step 24 twice.
26. Then with the same setup, start the variac at 40V and increase the variac quickly to 120V while recording data from the sensors.
27. Repeat step 26 twice.
28. Then with the same setup, start the variac at 80V and increase the variac quickly to 120V while recording data from the sensors.
29. Repeat step 28 twice.
30. Repeat steps 23 through 29 with 1 5-lb weight on each of the output shafts.
31. There should be 18 sets of data for the transmission, 18 sets of data for the differential and 3 sets of data for just the electric motor.

Results

While performing the testing procedure, we learned of the actual capabilities of our electric motor. Our 3 HP electric motor was able to turn both the transmission and the differential, however the additional weights we planned to simulate a load were too much inertial for the electric motor to rotate. This meant that we were only able to performance test the differential and transmission without any additional load besides the output shaft's inertia. This decreased the number of tests actually completed but still produced results that were meaningful and described the performance characteristics of our design. We ended up with 3 complete sets of data for each drivetrain option. We obtained three complete runs: 0-120V, 80-120V and 100-120V, for the transmission that described the mechanical losses of the transmission through the slope of the input shaft rotation vs. time. We were only able to get data for the differential from 100-120V because of the startup torque required. The higher gear ratio tuned to the larger electric motor and desired by our sponsor was

not easily overcome by the small electric motor available for our testing. This limited the data available to be analyzed to only one range, however multiple runs within this range produced consistent data on the same scale as the transmission.

After analyzing the data from all test runs, the most descriptive data reflecting the mechanical losses in both the differential and transmission were the input shaft rotational speed. The input shaft speed increased from a low steady state speed as the voltage increased up until the shaft was rotating at a higher steady state speed. The input shaft speed was plotted vs the data point number to find the rotational acceleration during the rotational speed change. We plotted the natural log of rotational speed to linearize the data and then were able to apply a linear fit line to approximate the slope. We used the number of the data point instead of a time scale because of the very slight time difference that was possible between the measured data points. We used the Arduino to collect and send data points to a computer and the time delay in communication between the computer and Arduino before sending the next data point was not always constant. However, this slight inconsistency does not affect our data because of sampling rate was much faster than the rotational speeds that were measured as seen by the steps in the below graphs. All data sets of the transmission can be seen in Figure 36 below summarized into one graph.

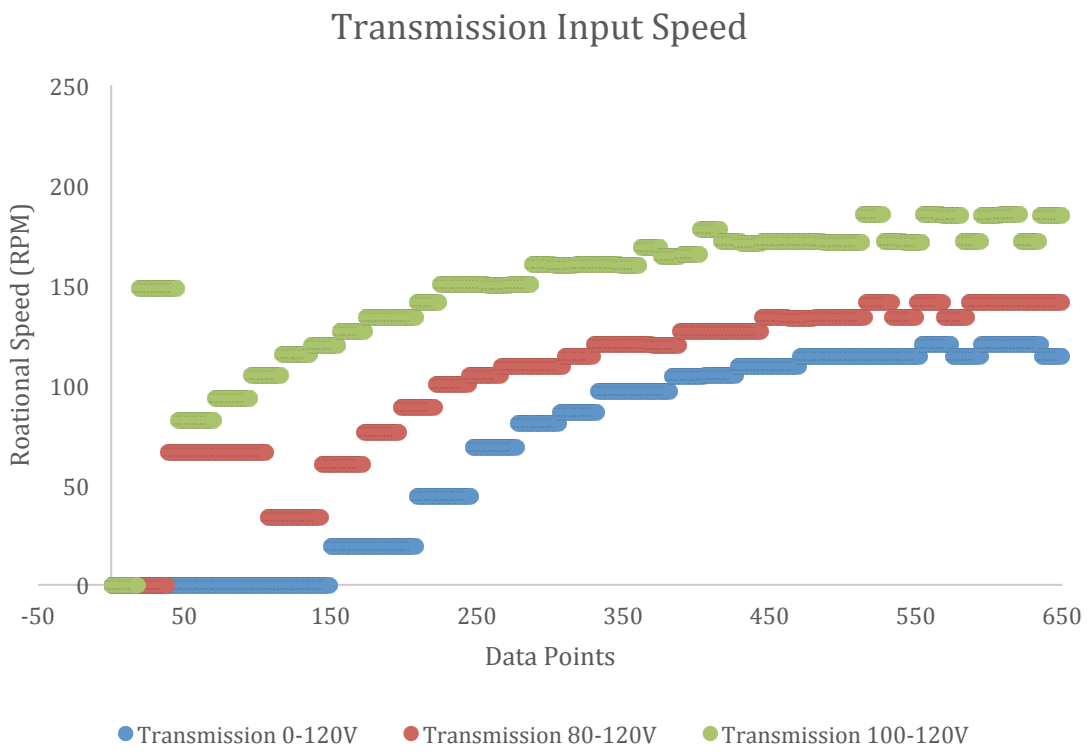

Figure 36: Transmission Input Speed Graph.

All differential data sets can be seen below in Figure 37 summarized into one graph.

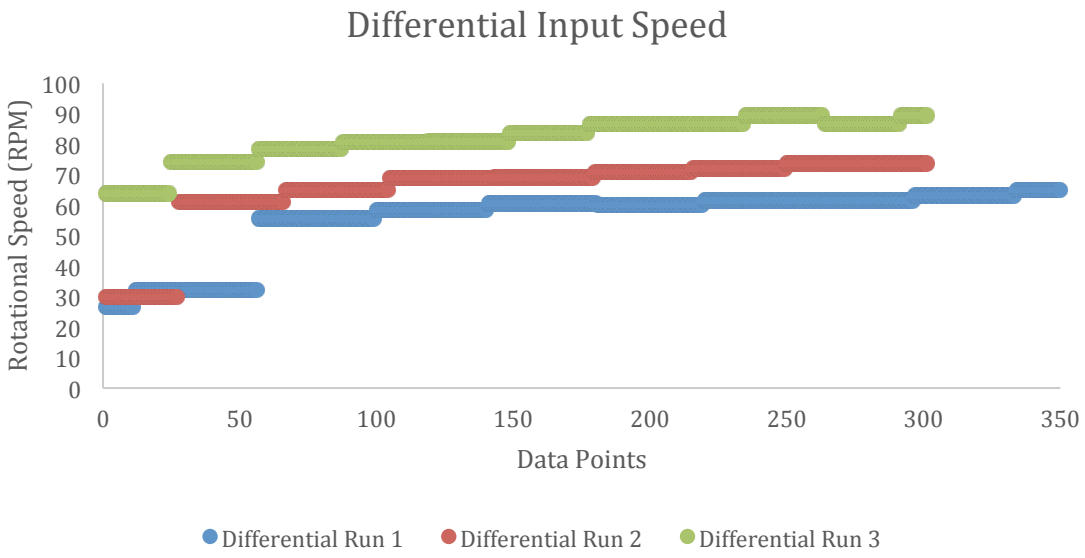

Figure 37: Differential Input Speed Graph.

Each of the graphs above have been limited to the acceleration range of interest. The transmission speed graph shows the different starting speeds and how each levels off at a constant speed. The differential graph shows all the runs from 100-120V and follow the same graphical shape. The graphs above can be quantified through the slopes comparing transmission and differential acceleration at 100-120V. Figures 38 and 39 below show this slope calculation.

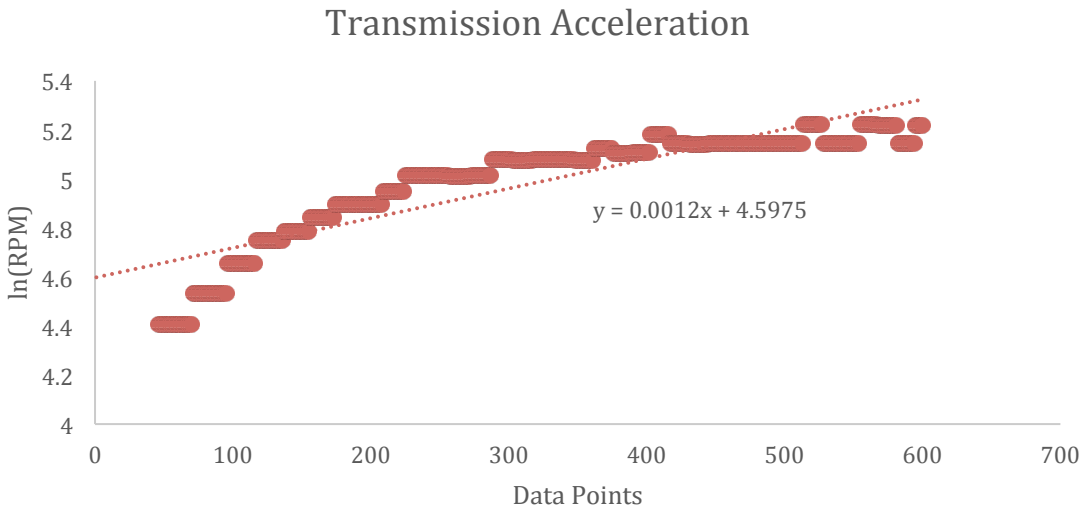

Figure 38: Transmission Acceleration Graph.

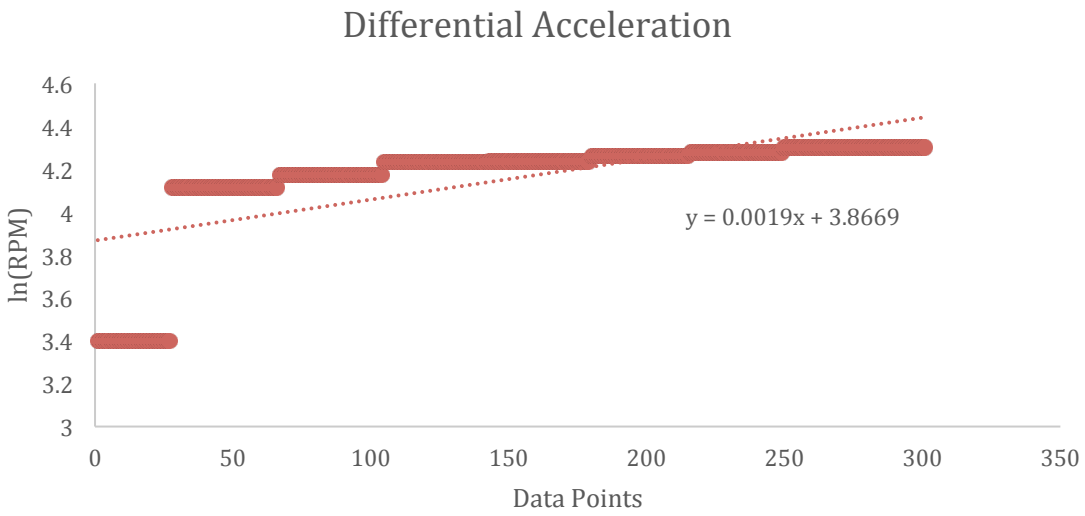

Figure 39: Differential Acceleration Graph.

The differential's acceleration has a slope of 0.0019 and the transmission's acceleration has a slope of 0.0012. This translates to a 58.3% better acceleration of the differential than the transmission. The transmission acceleration graph was clipped more aggressively to obtain the highest rate of acceleration. Even with the more aggressive clipping the differential has a larger slope and therefore accelerates faster to the desired speed. With every other variable in the system constant, the higher average acceleration shown through the slope shows that there are less mechanical losses in the differential than the transmission.

Chapter 7. Future Project Management

Moving forward, Cal Poly Motor Car Association has a few options to pursue. To get the Porsche to drive again, the club could reinstall the original transmission. If the club were to pursue this option the current battery pack would need to be refurbished or replaced entirely in order to provide adequate power to the Advanced DC motor. This option is not our recommended direction for the project.

As discussed earlier, the club could still choose to implement our differential design. However, this option would greatly limit the long-term possibilities of the car and therefore is also not our recommendation for the projects future.

The best option for the future of the E-Porsche would be the design, manufacturing, and implementation of the two electric motor concept we originally pitched to the club. To do this correctly we believe a new club with the focus of the Porsches restoration as the primary focus. Securing funding for future improvements will be much easier once a dedicated club is formed with a more dedicated focus and plan for the future of the vehicle. Organizing a club around the car would also allow the project to more efficiently carry over to future students while maintaining consistent design objectives. Having a multidisciplinary team would also allow a more thorough bottom up redesign of all of the cars systems resulting in a much more cohesive final design.

Chapter 7. Conclusion

Our project has had a profound impact on the current state of the Cal Poly Motorcar Association's electric Porsche. Prior to our project, the Porsche had only undergone aesthetic improvements but now the club is looking toward major drivetrain improvements. We were able to determine a few plausible paths the club could pursue during the beginning of this project to get the Porsche back to it's original, if not better, driving performance. The club chose to have us pursue a system improvement that would utilize the existing motor by replacing the transmission with a differential gearbox. We were able to design the system over the next quarter and show that the design was possible but that it might not be the best option for the best performance of the car. Our testing proved that our design would be an improvement over the original drivetrain but we also realized that by implementing our design, the future of the car's drivetrain would be limited. After thorough exploration of using the existing motor and differential as well as speaking with club leadership about the future aspirations of the Porsche, the club has decided the Porsche will have 2 independent motors on the rear wheels after seeking some additional funding. We believe that the club has made the correct informed decision for the future of the Porsche that was made possible by the results of our senior project.

Appendix I

FBI-4001A

Advanced D.C. Motors, Inc.

ELECTRIC VEHICLE APPLICATIONS

CONVERSION OR ORIGINAL EQUIPMENT

- 12 THROUGH 25 HORSEPOWER AT 72 THROUGH 144 VOLTS ONE HOUR RATING

"The Engineering Service People"

- MOTOR DIAMETERS
  6.7" - 8.0" - 9.1"
  U.L. APPROVED

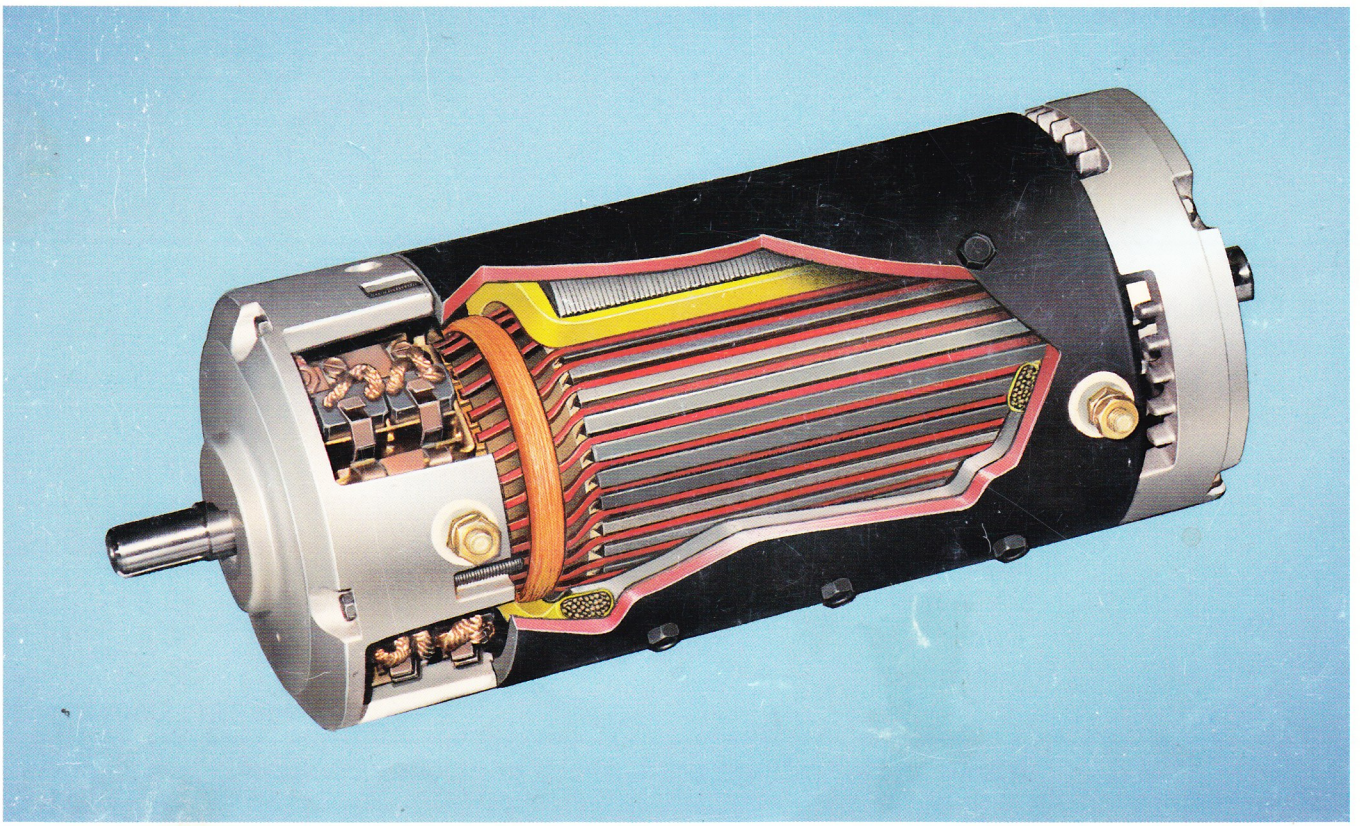

6268 EAST MOLLOY ROAD • EAST SYRACUSE, NEW YORK 13057
Telephone (315) 434-9303 Fax (315) 432-9290

ELECTRIC VEHICLE APPLICATION GUIDE

S-2 THERMAL TESTS PER DIN & ISO STANDARDS
TEST VOLTAGE 96 VOLTS - .03I
120 VOLTS - .03I
144 VOLTS - .03I

	Time - On	Volts	Amps	RPM	H.P.	KW
L91-4003	5 minutes	87	280	3650	26.4	20.00
6.7" Dia. Motor	1 hour	91	150	4950	15.0	11.40
Weight 82 lbs.	Continuous	92	130	5100	13.6	10.25
38 kg					**Peak HP. Developed 62**	
	5 minutes	112	260	4650	31.0	23.40
	1 hour	115	135	6200	17.9	13.50
	Continuous	116	122	6500	16.0	12.00
					Peak H.P. Developed 72	
203-06-4001	5 minutes	86	322	3600	31.5	23.80
8" Dia. Motor	1 hour	90	190	4800	20.6	15.50
Weight 107 lbs.	Continuous	91	178	5000	19.0	14.40
49 kg					**Peak H.P. Developed 68**	
	5 minutes	111	300	4650	37.0	28.00
	1 hour	114	180	6200	24.0	18.00
	Continuous	115	165	6500	21.7	16.30
					Peak H.P. Developed 83	
FB1-4001	5 minutes	88	360	3300	35.0	26.50
9.1" Dia. Motor	1 hour	89	210	3600	23.0	17.30
Weight 143 lbs.	Continuous	90	190	3900	20.0	15.00
65 kg					**Peak H.P. Developed 70**	
	5 minutes	109	340	3520	43.0	32.50
	1 hour	114	205	4800	27.5	20.80
	Continuous	115	182	5200	25.2	19.00
					Peak H.P. Developed 85	
	5 minutes	134	320	4200	48.8	36.80
	1 hour	138	185	5700	30.4	22.90
	Continuous	139	170	6000	28.5	21.50
					Peak H.P. Developed 100	

Above motor ratings are without controller in circuit.

Updated Data
Revised Data 12-10-92

Advanced D.C. Motors, Inc.

219 Lamson Street, Syracuse, New York 13206
(315) 434-9303 Fax (315) 432-9290

ELECTRIC VEHICLE MOTORS
GENERAL OPERATION INFORMATION

1) ALL ADVANCED DC MOTORS ARE 100% LOAD TESTED AND PRE-RUN FOR 15 MINUTES. THE MOTORS AE SHIPPED TO THE CUSTOMER IN PERFECT CONDITION. EVERY PRECAUTION IS TAKEN TO DELIVER THE MOTOR IN THE SAME CONDITION.

   WHEN THE MOTOR IS RECEIVED, IT SHOULD BE INSPECTED FOR :

   1) DAMAGED TERMINAL STUDS
   2) BROKEN OR CRACKED CASTINGS
   3) DAMAGED BRUSH CONNECTIONS
   4) PHYSICAL DAMAGE THAT MAY HAVE BEEN CAUSED BY IMPROPER HANDLING.

   ANY DAMAGE MUST BE IMMEDIATELY REPORTED TO THE CARRIER.

2) IN THE EVENT THE MOTOR IS STORED FOR A LONGER PERIOD OF TIME THE FOLLOWING SHOULD APPLY:

   A) MOTORS SHOULD BE STORED IN A CLEAN, DRY, WELL VENTILATED AREA THAT DOES NOT HAVE ANY EXCESSIVE OR WIDE VARIATIONS IN TEMPERATURES.

   B) IF POSSIBLE MOTOR SHOULD BE OPERATED PERIODICALLY AT NO LOAD - LOWER VOLTAGE TO COAT THE BEARINGS WITH LUBRICANT TO RETARD OXIDATION AND CORROSION.

3) BATTERY OPERATION OF DC MOTORS

   BATTERIES HAVE AN INTERNAL RESISTANCE TO THE FLOW OF CURRENT WHICH REDUCES THE OUTPUT VOLTAGE AS CURRENT IS INCREASED. IN THE CASE OF A ELECTRIC VEHCILE ALL CONDUCTORS SUCH AS WIRE, SWITCH CONTACTS, AND TERMINAL CONNECTIONS HAVE RESISTANCE TO FLOW OF CURRENT WHICH REDUCES THE APPLIED VOLTAGE.

   BECAUSE OF THESE REDUCED VOLTAGE (VOLTAGE DROP) THE MOTOR WILL ALWAYS "SEE" LESS VOLTAGE AT ITS TERMINALS THAN MEASURED AT THE BATTERY TERMINAL.

   EXAMPLE

   BATTERY TERMINAL VOLTAGE 75 VOLT

   MOTOR TERMINAL VOLTAGE
   AT 100 AMP CURRENT DRAW 72 VOLT

4) INSULATION RATING

THERE ARE SEVERAL CLASSES OF INSULATION RATINGS WHICH MOTORS WILL RUN AND PRODUCE LONG AND TROUBLE FREE OPERATION.

INSULATION CLASS	INTERNAL MOTOR	TEMPERATURE LIMIT
A	105° C	221° F
B	130° C	266° F
F	155° C	311° F
H	180° C	356° F
C	220° C	428° F

5) MOTOR TYPES

WOUND FIELD MOTORS CAN BE DIVIDED INTO THREE CATEGORIES BY FIELD TYPE.

A) SHUNT MOTOR
MOTOR HAS FIELD SHUNTED ACROSS THE ARMATURE. SEE FIGURE BELOW

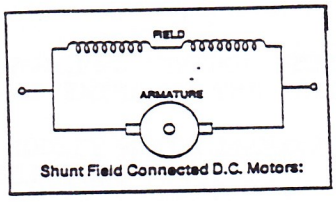

B) SERIES OR SERIES-PARALLEL MOTOR

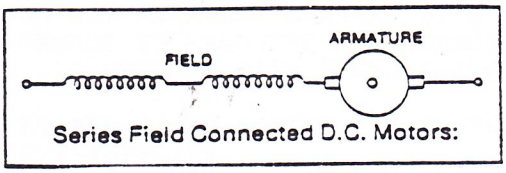

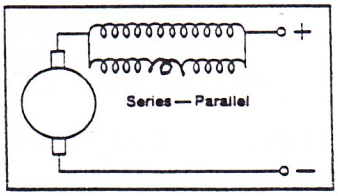

FIELD COILS ARE IN SERIES OR SERIES PARALLEL WITH THE ARMATURE.

C) COMPOUND WOUND MOTOR

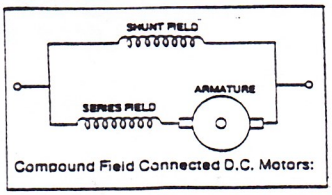

THE COMPOUND WOUND MOTOR HAS A COMBINATION OF BOTH SHUNT AND SERIES FIELD COILS.

MOTOR OPERATION
STEPS TO FOLLOW

A) VERIFY MOTOR AGAINST PART ORDERED

B) CHECK VEHICLE TRANSMISSION AND CONFIRM MOTORS FORWARD ROTATION IS AS SPECIFIED ON MOTOR DRAWING.

C) MAKE ALL CONNECTIONS AS SPECIFIED ON MOTOR PRINT. ASSURE THAT ALL CONNECTIONS ARE TIGHT - 100 TO 120 IN/LBS.

D) DO NOT OPERATE MOTOR AT FULL VOLTAGE. FOR NO LOAD OPERATION 12 VOLTS AT THE MOTOR TERMINAL IS SUFFICIENT. DANGER - FULL MOTOR VOLTAGE MAY DESTROY ARMATURE WINDING.

E) VERIFY ALL ELECTRICAL CONNECTION PRIOR TO BATTERY HOOK-UP. MAKE SURE HAND TOOLS ARE AWAY FROM MOTOR TERMINALS AND NO TOOLS OR OTHER SMALL OBJECTS HAVE FALLEN INTO MOTOR.

F) PROTECT MOTOR AGAINST GROUND DEBRIS, WATER AND OTHER FOREIGN MATERIALS ENTERING THE MOTOR.

G) NEVER ALTER OR MODIFY MOTOR ENCLOSURE WITHOUT CONSULTING WITH YOUR DISTRIBUTOR.

H) NEVER OPERATE OR ACCELERATE MOTOR WHEN INSTALLED IN VEHICLES NEUTRAL GEAR POSITION. DANGER - DAMAGE TO ARMATURE MAY OCCUR.

I) DO NOT EXCHANGE BRUSHES WITH DIFFERENT GRADES.
DAMAGE TO ARMATURE AND COMMUTATOR MAY RESULT.
ONLY REPLACE WITH BRUSHES SUPPLIED BY YOUR DEALER.

J) AT ALL TIMES FOLLOW THE INSTRUCTIONS OF YOUR CONVERSION KIT SUPPLIER.

K) IF MOTOR PROBLEMS ARE NOTICED OR IF ASSISTANCE REGARDING PROPER MOTOR OPERATION IS REQUIRED PLEASE CONTACT YOUR AUTORIZED DISTRIBUTOR FROM WHICH YOU PURCHASED YOUR ADVANCED DC MOTOR.

AT NO TIME - DO NOT ATTEMPT TO DISASSEMBLE THE MOTOR.
WARRANTY WILL BE VOID.

Advanced D.C. Motors, Inc.

6268 East Molloy Road, East Syracuse, NY 13057
(315) 434-9303 Fax (315) 432-9290

ADVANCED D.C. MOTORS, INC.
LIMITED - NON TRANSFERABLE
COMMERCIAL WARRANTY POLICY
ELECTRIC ON-ROAD VEHICLE APPLICATIONS

ADVANCED D.C. MOTORS, INC. WARRANTS EACH OF IT'S MOTORS TO BE FREE OF DEFECTS, RELATED TO WORKMANSHIP OR MATERIAL, FOR A PERIOD OF (2) YEARS FROM DATE OF SALE OF THE VEHICLE OR FOR THE FIRST TWENTY-FOUR THOUSAND MILES OF VEHICLE USE, WHICHEVER COMES FIRST, PROVIDED:

1) *THE MOTOR HAS RECEIVED NORMAL USE AND SERVICE,*

2) *ADVANCED D.C. MOTORS, INC. HAS APPROVED THE APPLICATION OF THE MOTOR,*

3) *THE MOTOR HAS NOT BEEN DISMANTLED, REPAIRED OR ALTERED FOR APPLICATION WITHOUT THE PRIOR CONSENT OF ADVANCED D.C. MOTORS, INC.,*

4) *THAT FAILURE OF THE MOTOR WAS NOT THE RESULT OF IMPROPER INSTALLATION, VEHICLE ACCIDENT OR MISUSE.*

IT WILL BE THE RESPONSIBILITY OF THE VEHICLE MANUFACTURER OR CONVERTER TO VALIDATE THE DATE OF SALE OF VEHICLE AND THE VEHICLE MILEAGE AT TIME MANUFACTURE OR CONVERSION.

THIS WARRANTY DOES NOT COVER ANY DAMAGE TO THE VEHICLE, ANY COMPENSATION FOR LOSS OF TIME OR INCONVENIENCE AND DOES NOT PROVIDE FOR ANY LIABILITY FOR INCIDENTAL OR CONSEQUENTIAL DAMAGE ARISING FROM THE USE OF THE PRODUCT BY THE BUYER, ITS ASSIGNEES, CUSTOMERS, AGENTS OR EMPLOYEES.

ADVANCED D.C. MOTORS, INC. WILL PROVIDE WARRANTY DISPOSITION:

1) BY MUTUAL EVALUATION OF PRODUCT PRESENTED FOR WARRANTY AT CUSTOMER'S FACILITY

(OR)

2) BY EVALUATION OF PRODUCT AFTER RETURN TO ADVANCED D.C. MOTORS, INC. SYRACUSE, NEW YORK

PROVIDED THAT ALL NECESSARY DOCUMENTATION REQUIRED BY THE "WARRANTY CLAIM" PROCEDURE HAD BEEN COMPLETED AND SUBMITTED FOR EACH UNIT; ADVANCED D.C. MOTORS, INC. WILL REPLACE THE MOTOR AT NO CHARGE.

Revised 4-13-94

RECLOCKING THE COMMUTATOR / BRUSH RIGGING FOR CLOCKWISE ROTATION

Almost without exception, Advanced DC Motors manufactures their motors to rotate in the C.C.W. direction as viewed from the DRIVE END of the motor. This is done for compatibility with the most commonly used types of transmissions and drivelines available. When the direction of rotation is known for a particular application, it is possible to lead the brushes into the direction of rotation slightly in order to gain a few efficiency points. While this lead angle is very small (about 10-13 degrees), the amount of lead angle is critical for good commutation. Unless otherwise noted, all Advanced DC motors have a slight lead angle in the C.C.W. direction. Conversely, if an application requires rotation in the C.W. direction as viewed from the DRIVE END of the motor, the lead angle will have to be restored in the C.W. direction for proper commutation. Failure to restore the prescribed lead angle will result in inefficient operation and premature brush and commutator wear. The following procedure describes how to set up a motor for C.W. operation.

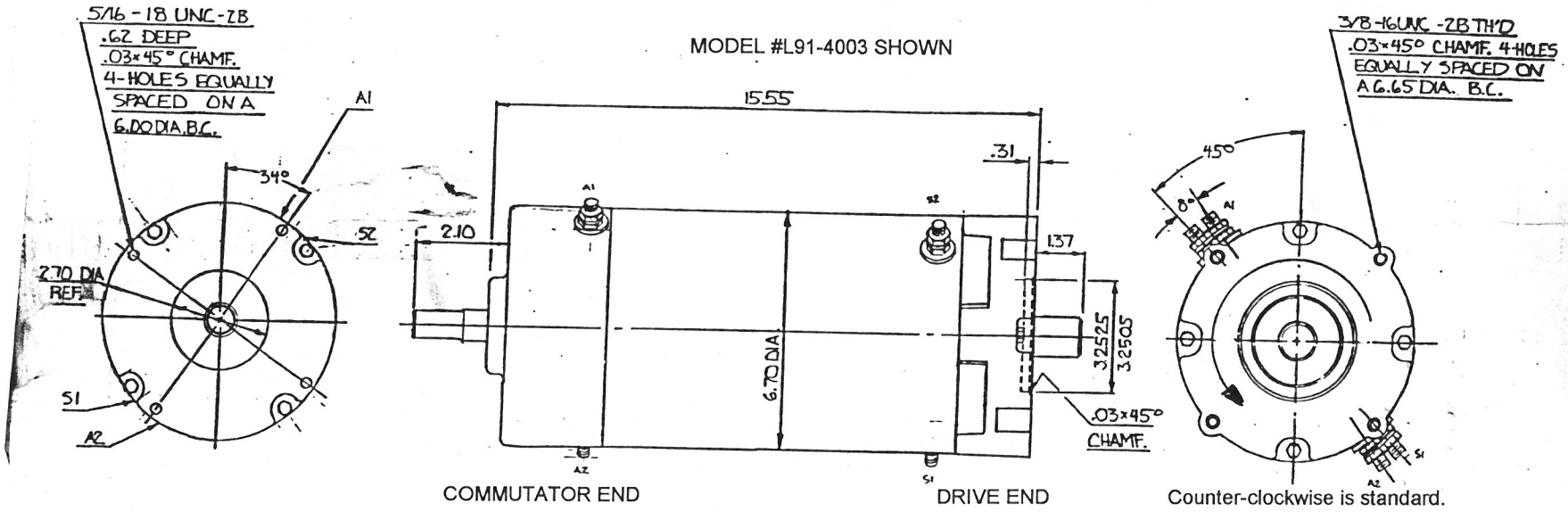

(1) At the COMMUTATOR END of the motor, remove the brush band and set it aside. Locate the springs that hold the 8 brushes into place. One-at-a-time, grasp the loose end of a brush spring between opposing index fingers. Pull the spring up away from the brush and park it behind its holding bar so that its loose end is pointing up into the air. In like fashion, park the other 7 brush springs away from the brushes.

(2) Remove the 4 bolts that attach the COMMUTATOR END assembly of the motor to the motor body.

(3) Pry loose and carefully remove the COMMUTATOR END assembly, being careful not to disturb or damage any part contained therein.

(4) At the COMMUTATOR END of the motor, locate the 8 threaded holes in the end of the motor body. 4 of these threaded holes will be empty, and the other 4 will have setscrews installed in them. With an allen wrench, remove the 4 setscrews and reinstall them into the empty threaded holes.

(5) Replace the COMMUTATOR END assembly onto the motor, being careful to align the bolt holes with the newly-emptied threaded holes in the end of the motor body. Reinstall the 4 bolts removed in step (2). Tighten them firmly.

(6) Restore all 8 brush springs from their parked positions to their original positions on the brushes. Reinstall the brush band. With a marking pen, write "C.W. DIR." on the motor nameplate.

DRAWN 1/2 SCALE

ADVANCED DC MOTORS MODEL FB1-4001

High Performance Curves for 96-144 VDC

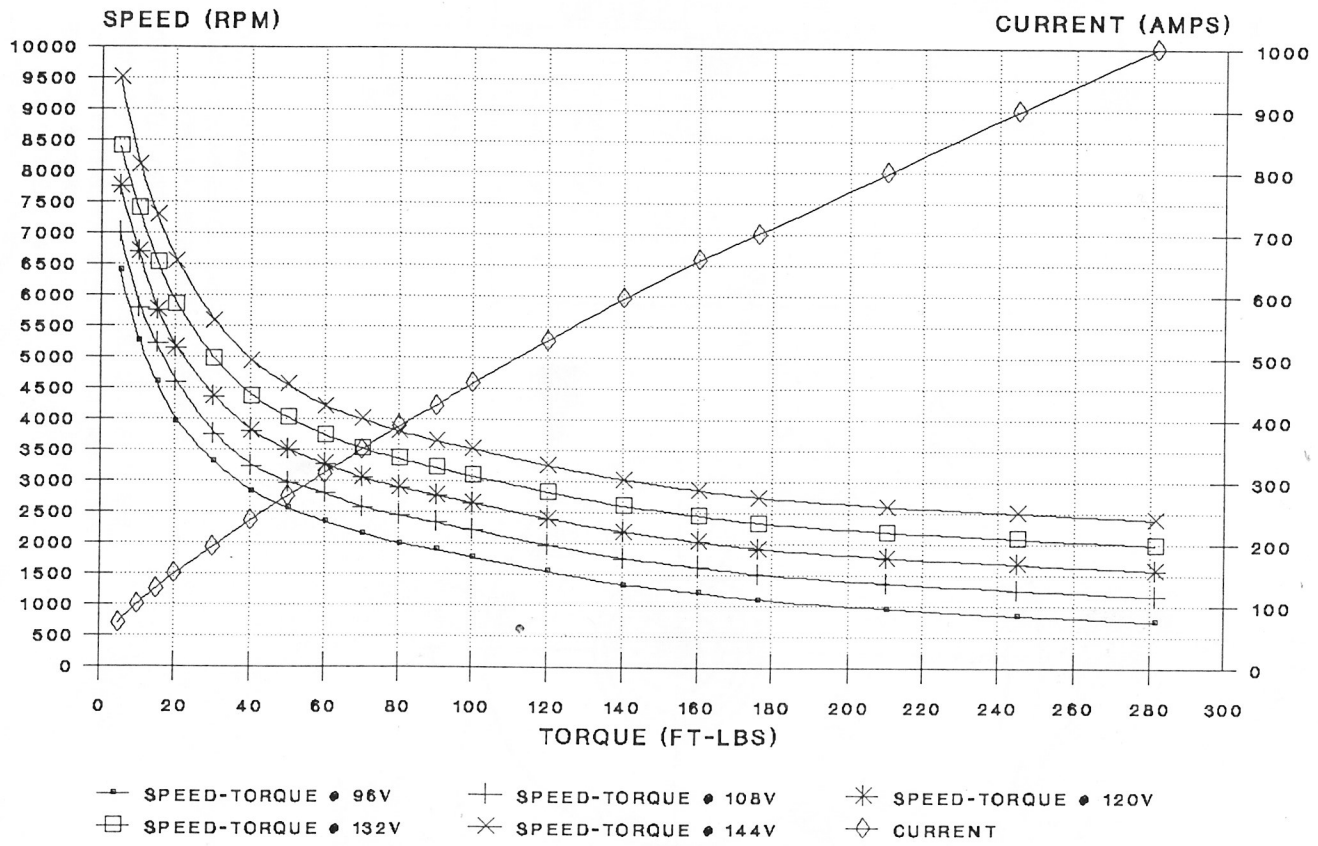

E	F	G	H

OUTLINE DIMENSIONS ARE NOMINAL UNLESS TOLERANCES ARE SPECIFIED

NO.	QUANT	PART NO.	DESCRIPTION

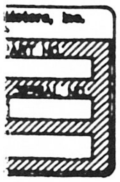

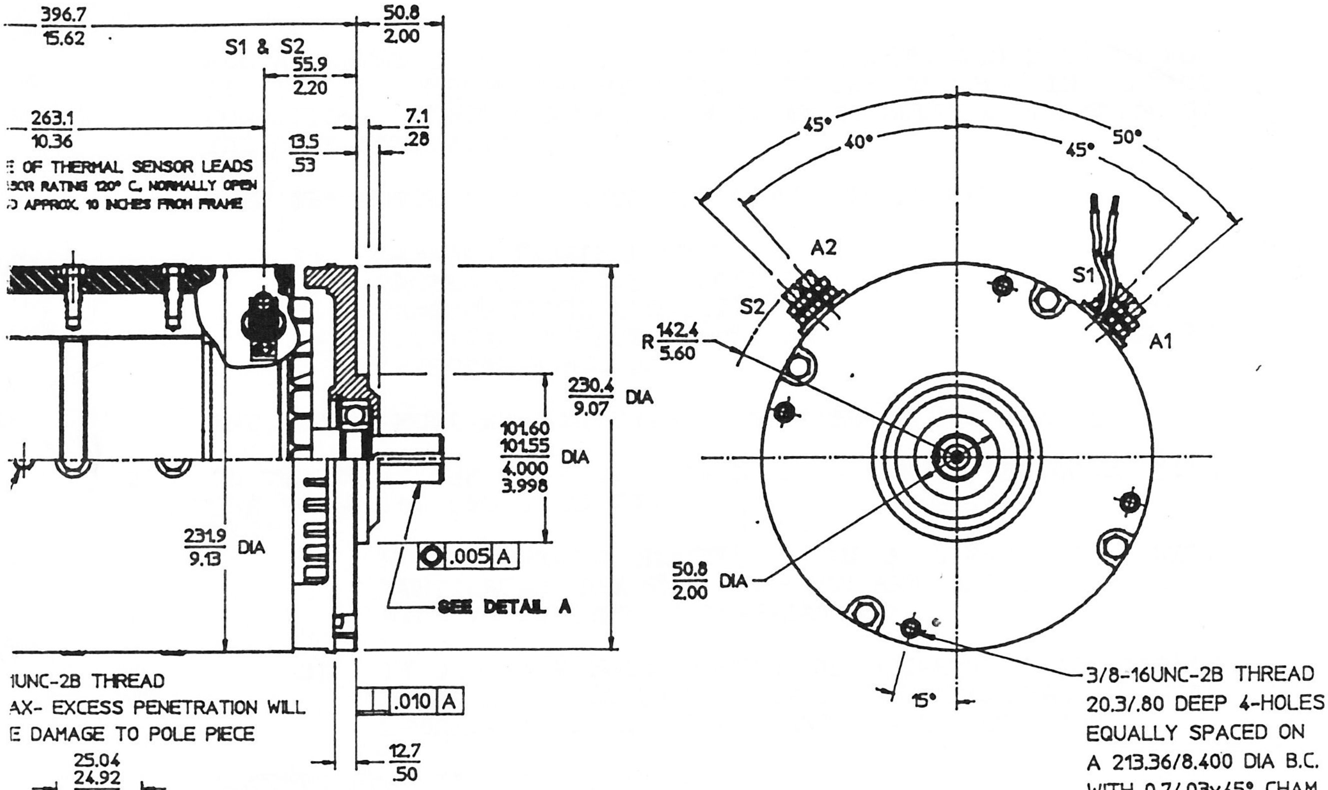

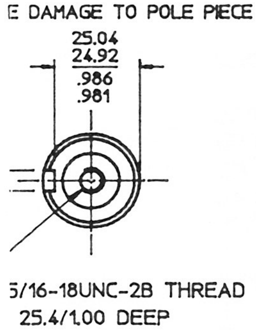

- -CLASS "H" INSULATION
- -FINISH: FRAME-BLACK PAINT
  END HEADS-NATURAL ALUMINUM
- -VENTILATED MOTOR WITH FAN
- -DESIGNED WITH INTENT TO MEET U.L. SPEC# 583 LATEST EDITION FOR TYPE "E" & "EE" INDUSTRIAL ELECTRIC MOTORS
- -TEST TO CURVE: C-59
- -MOTOR WEIGHT: 143 lbs.
- -DESIGNED TO OPERATE IN C.C.W. ROTATION FORWARD VEHICLE OPERATION

72/120 VOLT

TTERY TERMINAL

BATTERY TERMINAL

TTERY TERMINAL

BATTERY TERMINAL

MILLIMETER / INCHES OR MILLIMETER / INCHES

PROJECTION — THIRD ANGLE

ZONE	REV	WAS	BY	DATE
	B	CHG TO CONFORM TO DETAIL	PCR#916	02-13-95
	A	WAS 25.4/1.00 DP.	PCR#495	04-07-95
		REDRAWN IN CAD LAST REV U	TMC	09-16-92

MATERIAL

REF

This print is the property of Advanced D.C. Motors, Inc. and supersedes all prints previous to last revision. Do not scale -work to dimensions. Tolerances unless otherwise specified

[redacted]

Advanced D.C. Motors, Inc.
Syracuse N.Y.

NAME: TRACTION MOTOR OUTLINE

SIZE	SCALE	DRAWN	DATE
D	1/2	MM	04-19-91

PART NO. **FB1-4001A**

Advanced D.C. Motors, Inc.

, Syracuse, New York 13206
(315) 434-9303 Fax (315) 432-9290

Typical FB1 Type 9" Motor Performance
144 Volt -.03I CCW Drive End Rotation

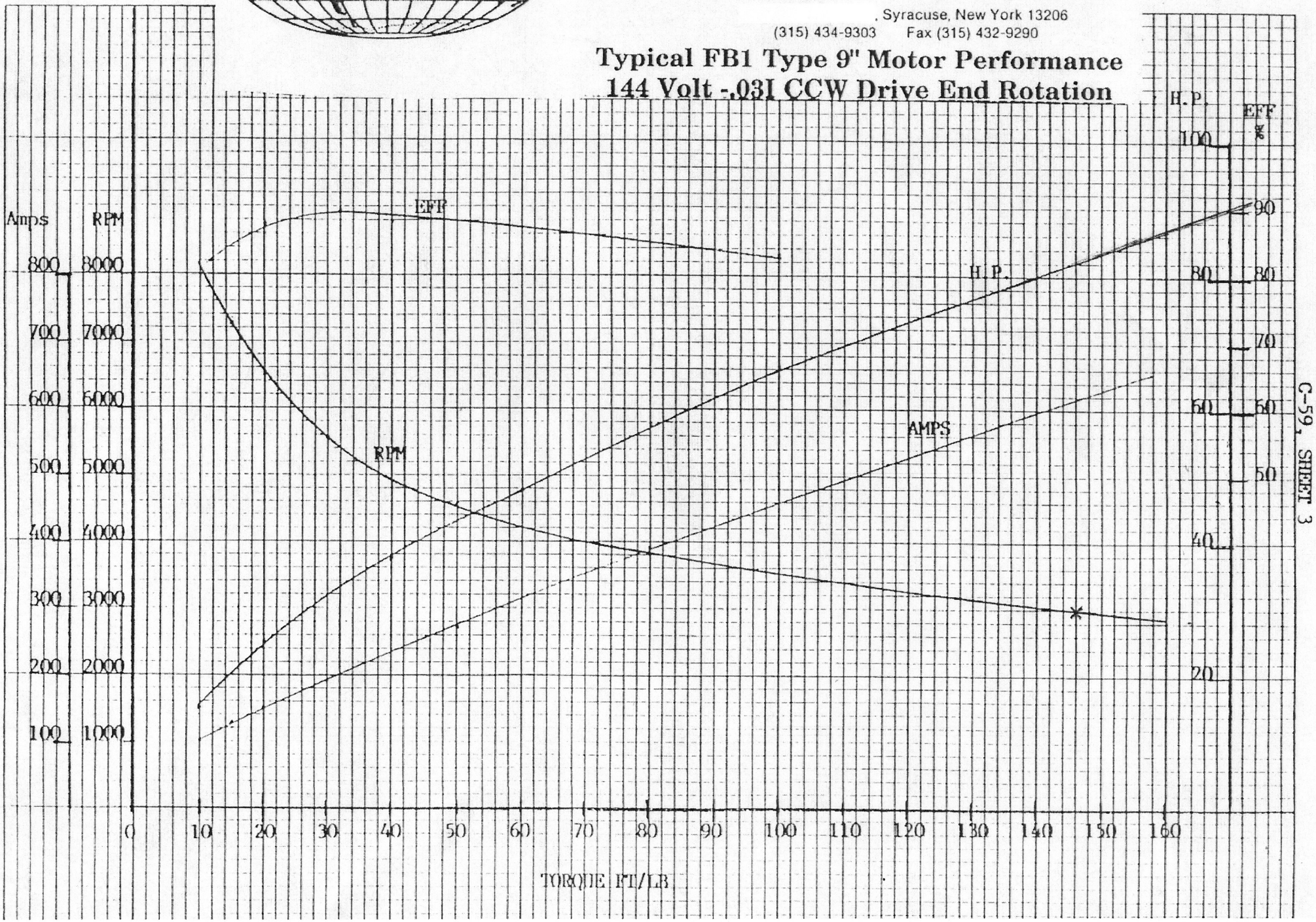

C-59, SHEET 3

-NAMELABEL STAMPED WITH ADVANCED PART NO. CUSTOMER PART NO. AND 72/120 VOLT
-NAMELABEL STAMPED WITH U.L. ID. NO. AU2500 & CURRENT DATE IN RATING BOX
-CODE DATE STAMPED ON FRAME NEAR NAMELABEL

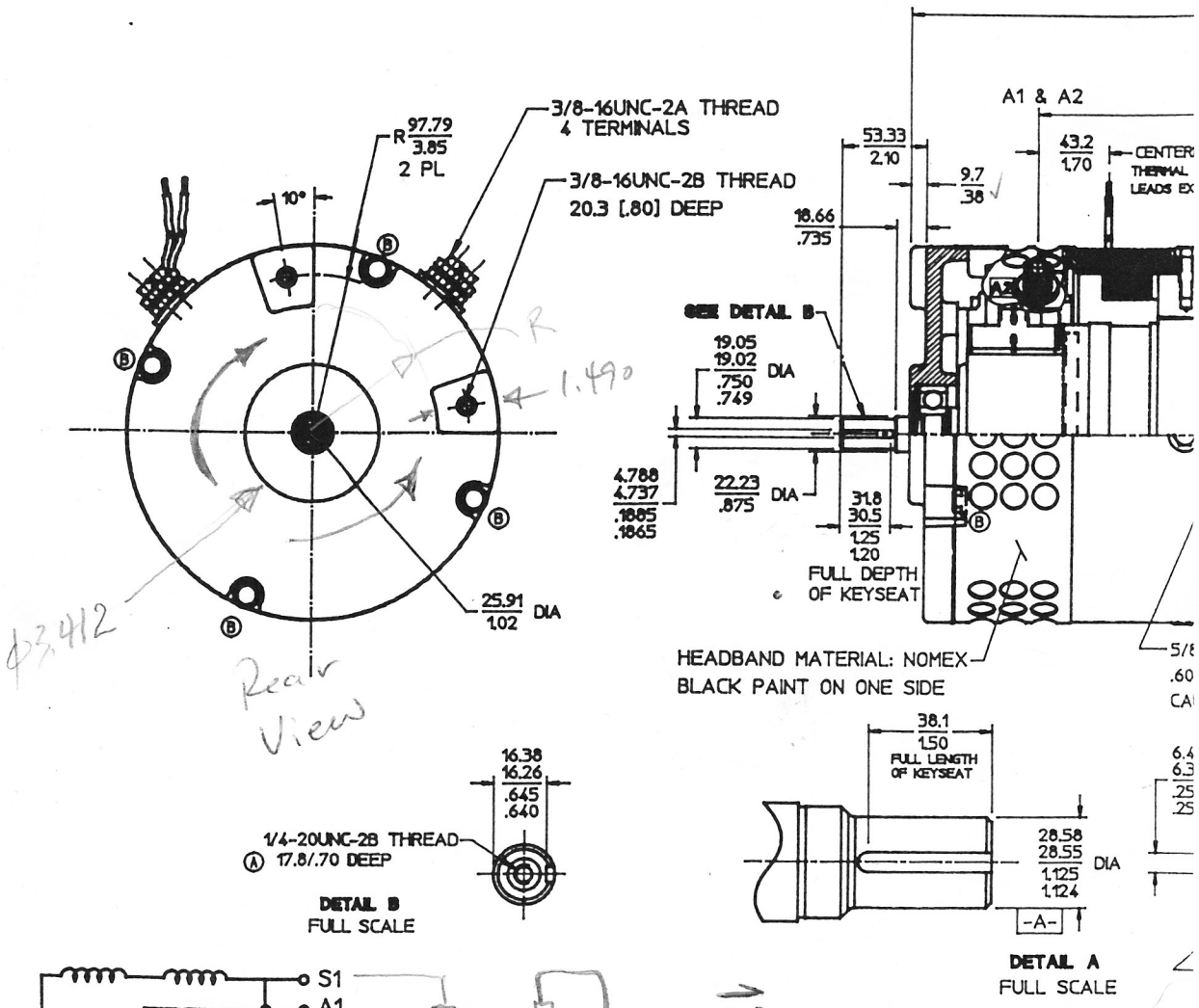

DETAIL B
FULL SCALE

DETAIL A
FULL SCALE

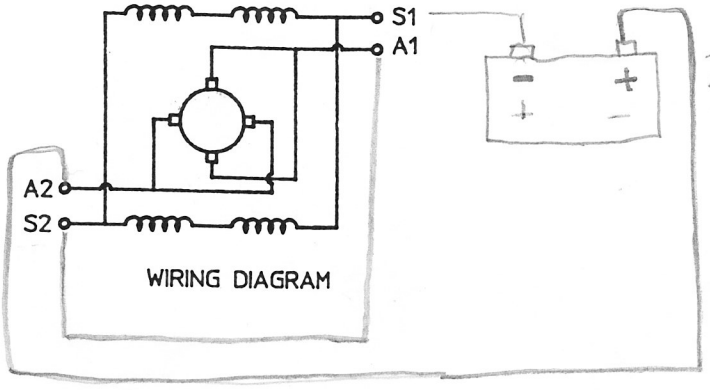

$\vec{\omega}$ points out Rear
Either polarity gives same rotation

ROTATION - REVERSIBLE
C.W.D.E.
CONNECT S-1 TO ONE E
CONNECT S-2 TO A-1
CONNECT A-2 TO OTHE
C.C.W.D.E.
CONNECT S-1 TO ONE E
CONNECT S-2 TO A-2
CONNECT A-1 TO OTHE

$S_2 - A_2$ $\vec{\omega}$ + Points out front
S_1 – GND
A_1 – ⊕

LO-60

Café Electric llc

Home of the Zilla

Owner's Manual
for the
Zilla Motor Controller Package
with
Hairball 2 Interface

Z1K

Z2K

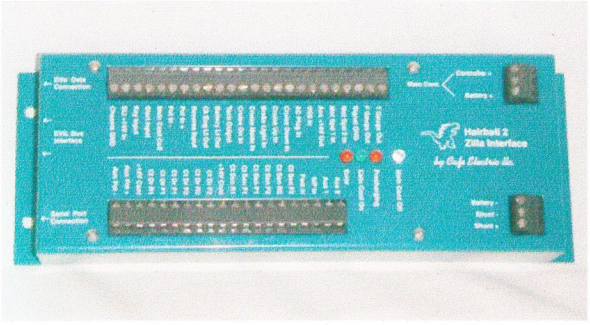

Hairball 2

Please read this manual before you ask questions.
Questions not answered in the manual
or the FAQ at the end will gladly be answered by email.

Latest revision 12.2.04 V2.02

Welcome

Thank you for purchasing a Zilla motor controller and Hairball interface.

We at Cafe Electric have worked many years to insure that the product you have in front of you is the best DC motor controller for electric vehicles on the market. We hope that you will enjoy many years of trouble free service from this device.

What is it?
A motor controllers' purpose is to regulate the power that flows from the batteries to the motor. It does this in response to commands from the accelerator pedal. It is very similar to a common dimmer switch in a home, except tha it can control much more power.

The Zilla line of controllers includes six models with current ratings of 1000 and 2000 amps with maximum nominal voltage ratings of 156, 300 and 348 Volts. All models will function with as little as 36V on the input, but we do not recommend using them in systems below 72V.

Zilla Controller Matrix

Model	Maximum Motor Amps	Nominal Battery Voltage
Z1K-LV	1000	72 to 156
Z1K-HV	1000	72 to 300
Z1K-EHV	1000	72 to 348
Z2K-LV	2000	72 to 156
Z2K-HV	2000	72 to 300
Z2K-EHV	2000	72 to 348

Dimensions

Dimensions of the Zilla Z2K 2000 Amp Controller:
7.00" Wide, 4.63" High, 14.75" Long, Weight 29.5 lb.
Dimensions of the Zilla Z1K 1000 Amp Controller:
7.00" Wide, 4.63" High, 9.00" Long, Weight 15.5 lb.

Dimensions of the Hairball:
3.5" Wide, 1.75" High, 10" Long

Shipping weight of Z2K Package is 37 lb. Z1K is 21 lb.

Zilla Specifications

- Maximum nominal input voltage range for Lead Acid batteries: 72 to 348 Volts. (-EHV Models)
- Absolute maximum fully loaded input voltage range: 36 to 400 Volts (-EHV Models)
- Maximum motor current at 50°C heatsink temperature:
  2000 Amps for Z2K /1000 Amps for Z1K
- Maximum Battery Current at 200V: 1900 Amps for Z2K, 950 Amps for Z1K
- Maximum Battery Current at 300V: 1770 Amps for Z2K, 885 Amps for Z1K
- Maximum Battery Current at 400V: 1600 Amps for Z2K, 800 Amps for Z1K
- Continuous motor current @ 50°C coolant temp & 100% Duty Cycle:
  over 700 Amps for Z2K, over 350 Amps for Z1K
- Peak Power: 640,000 Watts for Z2K, 320,000 Watts for Z1K
- PWM frequency: 15.7 kHz
- Power devices: IGBT
- On state Voltage Drop: < 1.9 Volts at maximum current.

Some Features of the Zilla controllers:

- Simply, the most powerful controller in the industry, by far.
- Backed by over ten years of experience making the worlds quickest controllers.
- Water cooling for sustained high power operation.
- 2000 motor Amps available with proper cooling for Z2K, 1000 Amps for Z1K.
- Multiple Microprocessors which cross check for security and safety.
- Full motor current limit control with smooth temperature cutback.
- Silent high frequency operation.
- Compact size.
- One year factory warranty.

Hairball Interface

The Hairball interface is required to run the Zilla controller.
It enables many new driving and safety features, some of which are listed here:

- Control connections to the Hairball are low voltage and referenced to the vehicle 12V ground for safety.
- Controller precharge circuit is included with self resetting fuse and arc-less main contactor control.
- Uses standard 5 K ohm potentiometer for accelerator pedal input. (not supplied in package)
- Can be built to accept non contact dual redundant hall effect pedal input. (HEPI) aka: Option -P
- Unique "accelerator to amps" transfer function for smooth starts, even in high voltage systems.
- Standard RS-232 serial port for customer adjustment of controller parameters.
- Programmable motor voltage and current limits.
- Programmable battery voltage and current limits.
- Adjustable low battery voltage protection.
- Additional battery voltage indicator set point for operating a dash warning light.
- Two motor speed inputs for overspeed limiting of one or two motors.
- Separate voltage, current and speed limit adjustment for reverse.
- Valet mode to allow yet another set of settings on the fly with the flip of a switch.
- More than forty status and error codes insure easy diagnostics in case of faults.
- No special tools are required to read and clear status and error codes.
- Main contactor voltage drop and stuck contactor monitoring.
- Pulse output for driving a standard 4 or 6 cylinder tachometer.
- Two dash light outputs for driving a check engine light and low battery indicator.
- Stalled rotor protection to reduce the possibility of damaged commutators. (requires motor speed sensor, not included)
- Optionally (Hairball Option -A) , up to six high side contactor drivers allow arc-less control of electric reversing and series parallel switching of dual motor systems.
- Autoshift automatically shifts dual motors from series to parallel and back again at the optimum time for more power and efficiency. (Requires Option -A)
- Hairball code with new features can be downloaded as it is developed by means of the bootloader and flash memory, using a standard home computer.

ALBRIGHT

SW200 SERIES OF D.C. CONTACTORS

UNIQUE RANGE

The SW200 series of contactors has been designed for direct current loads, particularly motors as used on larger electric vehicles such as industrial trucks, airport tractors, etc.

They have double breaking main contacts with silver alloy contact tips, which are weld resistant, hard wearing and have excellent conductivity.

The range comprises: Single Pole, on/off types (SW200), Single Pole normally closed types (SW210), paired version of these for motor reversing (SW202) and derivatives of these types to give various combinations and configurations.

COMPACT SIZE

The contactors are compact in size and are fully serviceable, with a full range of spare parts available.

EASY INSTALLATION

Mounting is by means of 5mm tapped holes in the switch frame together with a range of mounting brackets complete with screws and washers.

Coil connections are by means of 6mm spades of which two are supplied per terminal.

Contactor types SW202, SW204, SW205, SW208, SW213 and SW214 are supplied as an assembly which includes a mounting bracket as a standard feature.

Mounting attitudes are detailed in the drawings on the following pages.

OPERATING COILS

Coil voltages ranging from 6 to 240 are available and these are wound for D.C. operation.

However coils can be fitted with a bridge rectifier for use from A.C. supplies.

Coils are normally wound for intermittent duty (up to 70% "on" time) but continuous duty version (100%) are also available.

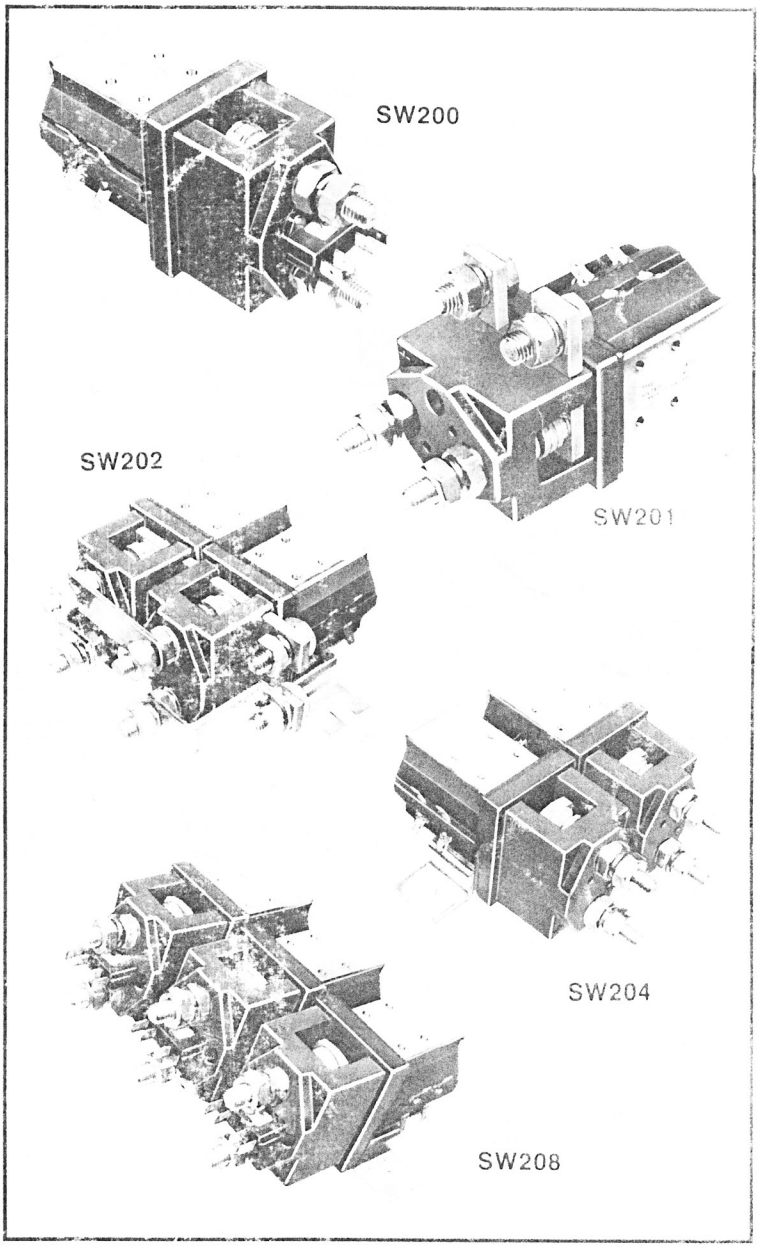

SW200	SINGLE POLE SINGLE THROW	SW205	2xSW201 ON DOUBLE BRACKET
SW201	SINGLE POLE DOUBLE THROW	SW208	3xSW200 ON TRIPLE BRACKET
SW202	PAIRED SINGLE POLE DOUBLE THROW ON DOUBLE BRACKET (for motor reversing)	SW210	SINGLE POLE SINGLE THROW (normally closed)
		SW213	3xSW210 ON TRIPLE BRACKET
SW204	2xSW200 ON DOUBLE BRACKET	SW214	2xSW210 ON DOUBLE BRACKET

PERFORMANCE DATA

Thermal current rating (100%)	250 Amperes
Intermittent current rating	
30% duty	450 Amperes
40% duty	390 Amperes
50% duty	360 Amperes
60% duty	320 Amperes
70% duty	300 Amperes
Typical fault currents which can be ruptured (5ms time constant)	
SW200N and SW210N	1500 Amperes at 48V D.C.
SW200 and SW210	1500 Amperes at 96V D.C.
SW201N * and SW202N *	600 Amperes at 48V D.C.
SW201 * and SW202 *	1500 Amperes at 96V D.C.
Maximum recommended contact voltages	
SW200N and SW210N	48V D.C.
SW200 and SW210	96V D.C.
SW201N and SW202N	48V D.C.
SW201 and SW202	96V D.C.
Typical voltage drop across contacts per 100 Amperes	
SW200 and SW210	40mV
SW201 and SW202 (normally open contacts)	40mV
SW201 and SW202 (normally closed contacts)	40mV
Mechanical life	$> 5 \times 10^6$
Coil power dissipation	
Intermittently rated types	30-60 Watts
Continuously rated types	13-21 Watts
Maximum pull-in voltage (coil at 20°C)	
Intermittently rated types	60%V
Continuously rated types	66%V
Typical drop-out voltage	10-20%V
Typical pull-in time (n/o contacts to close)	40ms
Typical drop-out time (n/o contacts to open)	
Without suppression	10ms
With diode suppression	100ms
With diode and resistor (depending on value)	30ms
Typical main contact changeover time (SW201 and SW202)	
Normally closed to normally open	14ms
Normally open to normally closed	8ms
Typical contact bounce period	3ms
Auxiliary contact thermal current rating	5 Amperes
Auxiliary contact switching capacities (resistive load)	5A at 24V D.C. 2A at 48V D.C. 0.5A at 240V D.C.

* *Normally open contacts, not normally closed contacts.*

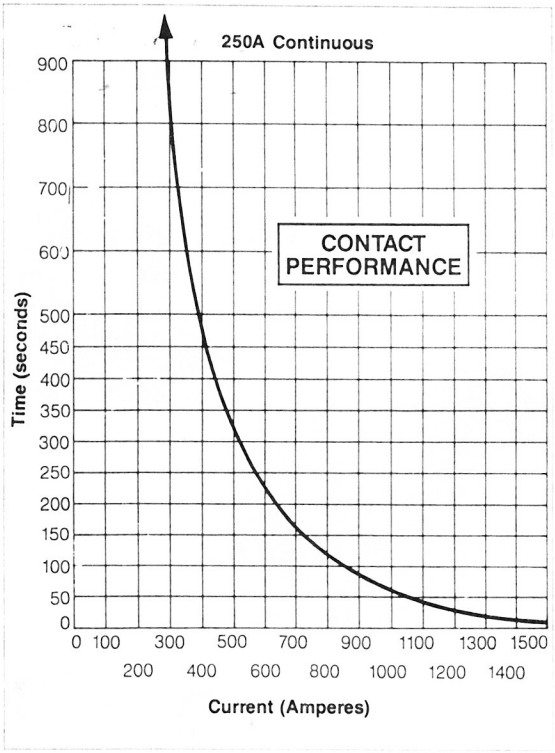

All the above figures should be used as a guide only. Some derating may be necessary according to type and application.

Appendix II

ONLY ADDITIONS OR ALTERATIONS TO THE EXISTING PLATE ARE DIMENSIONED

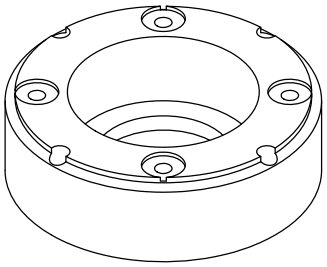

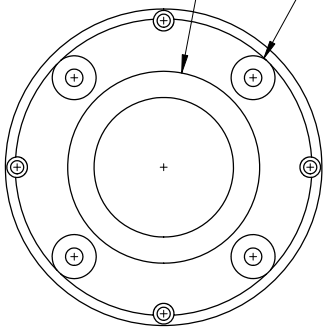

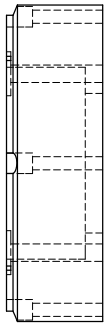

NOTES
UNLESS OTHERWISE SPECIFIED:
1. ALL DIMS. IN INCHES
2. TOLERANCES:
   X.XX = ±0.10
   ANGLES = ±1°
3. INSIDE TOOL RADIUS 0.5 MAX
4. BREAK SHARP EDGES 0.5 MAX

Mechanical Engineering CAL POLY
E-PORSCHE

Material: ALUMINUM	Part Name: Aluminum Motor Interface	
Scale: 1:4	Date: Monday, May 26, 2014	Drawn By: Quinton Petty

NOTES
UNLESS OTHERWISE SPECIFIED:
1. ALL DIMS. IN INCHES
2. TOLERANCES:
   X.XX = ±0.10
   ANGLES = ±1°
3. INSIDE TOOL RADIUS 0.5 MAX
4. BREAK SHARP EDGES 0.5 MAX

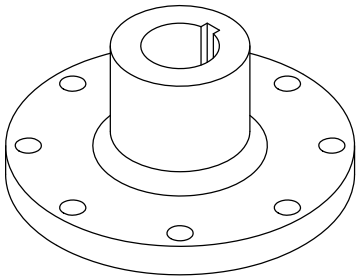

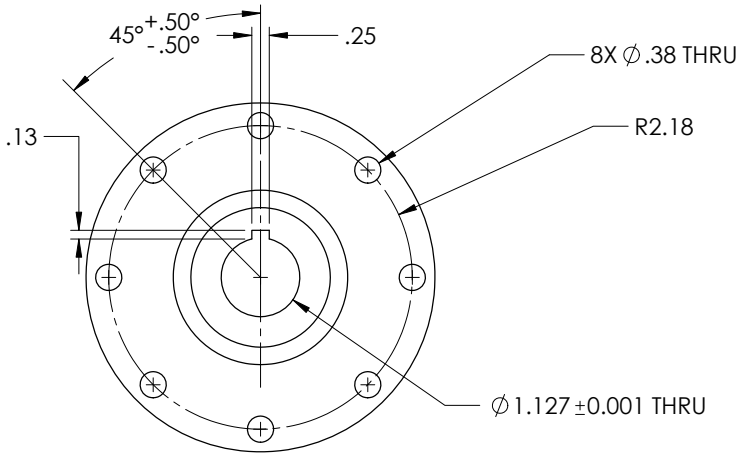

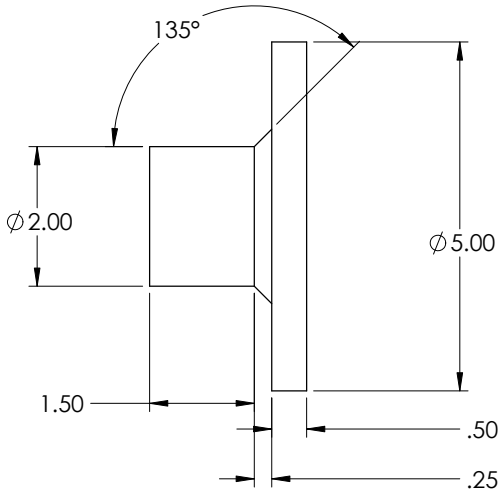

Mechanical Engineering CAL POLY
E-PORSCHE

Material: 1018 STEEL	Part Name: Motor Shaft Collar	
Scale: 1:2	Date: Monday, May 26, 2014	Drawn By: Quinton Petty

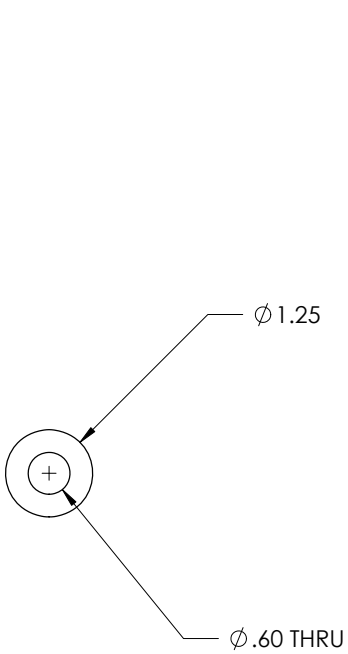

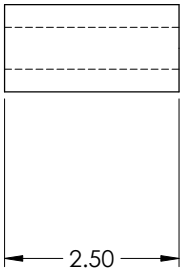

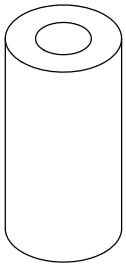

NOTES
UNLESS OTHERWISE SPECIFIED:
1. ALL DIMS. IN INCHES
2. TOLERANCES:
   X.XX = ±0.10
   ANGLES = ±1°
3. INSIDE TOOL RADIUS 0.5 MAX
4. BREAK SHARP EDGES 0.5 MAX

Mechanical Engineering CAL POLY
E-PORSCHE

Material: 6061-T6 ALUMINUM	Part Name: Motor-Differential Spacer	
Scale: 1:2	Date: Tuesday, May 27, 2014	Drawn By: Quinton Petty

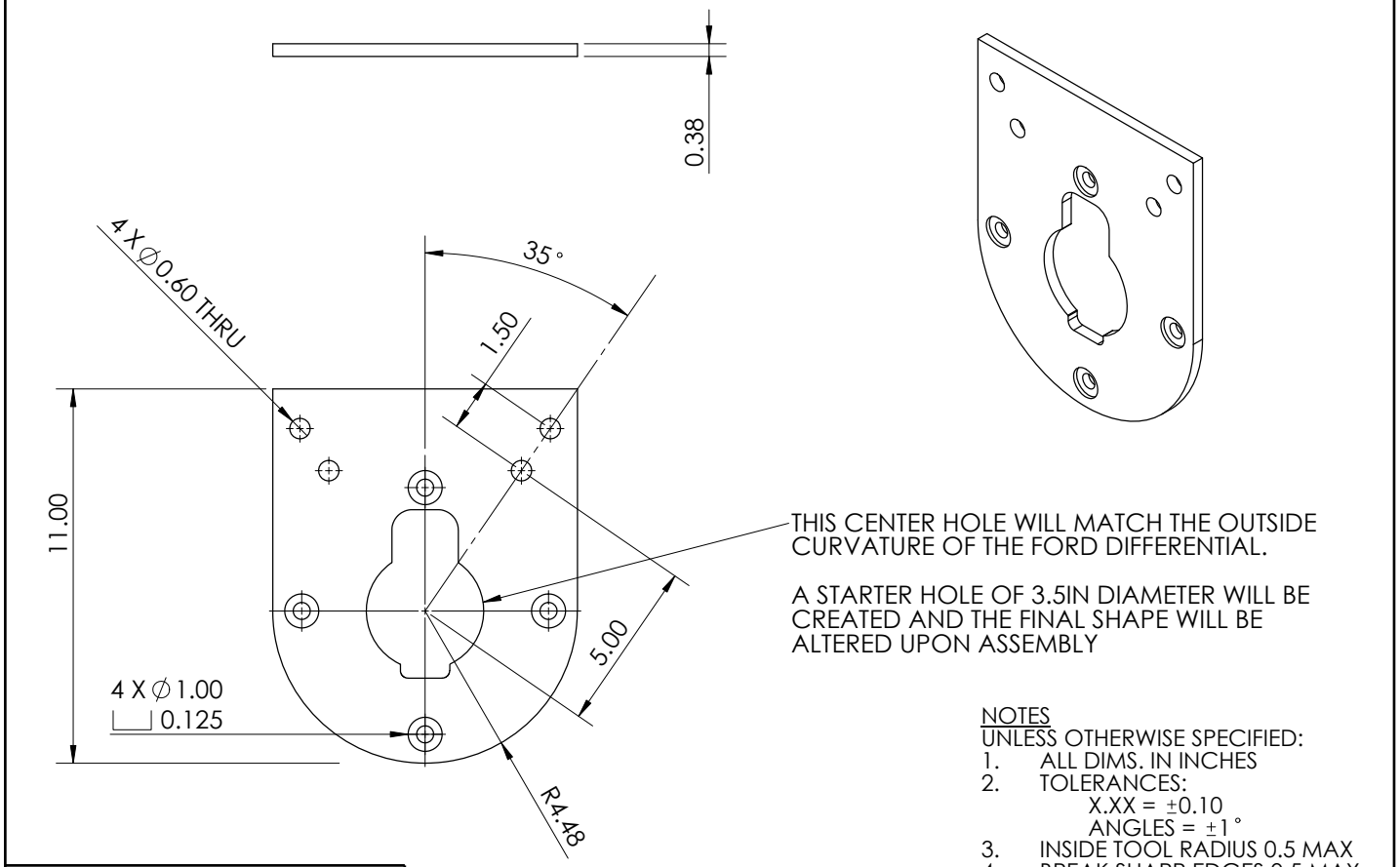

THIS CENTER HOLE WILL MATCH THE OUTSIDE CURVATURE OF THE FORD DIFFERENTIAL.

A STARTER HOLE OF 3.5IN DIAMETER WILL BE CREATED AND THE FINAL SHAPE WILL BE ALTERED UPON ASSEMBLY

NOTES
UNLESS OTHERWISE SPECIFIED:
1. ALL DIMS. IN INCHES
2. TOLERANCES:
   X.XX = ±0.10
   ANGLES = ±1°
3. INSIDE TOOL RADIUS 0.5 MAX
4. BREAK SHARP EDGES 0.5 MAX

Mechanical Engineering CAL POLY
E-PORSCHE

Material: A36 STEEL	Part Name: Front Drivetrain Mount	
Scale: 1:4	Date: Tuesday, May 27, 2014	Drawn By: Quinton Petty

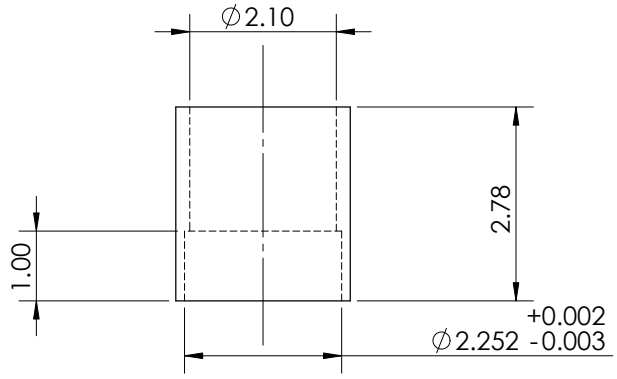

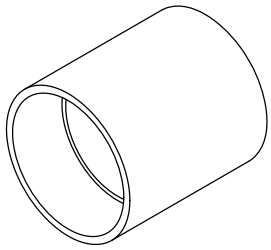

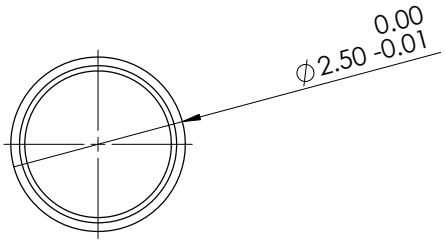

NOTES
UNLESS OTHERWISE SPECIFIED:
1. ALL DIMS. IN INCHES
2. TOLERANCES:
   X.XX = ±0.10
   ANGLES = ±1°
3. INSIDE TOOL RADIUS 0.5 MAX
4. BREAK SHARP EDGES 0.5 MAX

Mechanical Engineering CAL POLY
E-PORSCHE

Material: 6061-T6 ALUMINUM	Part Name: Left Bearing Spacer	
Scale: 1:2	Date: Monday, May 26, 2014	Drawn By: Quinton Petty

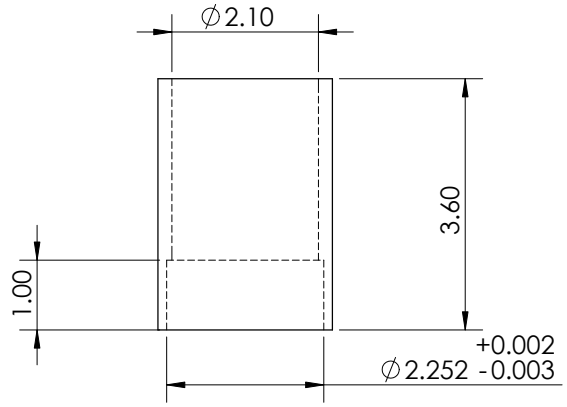

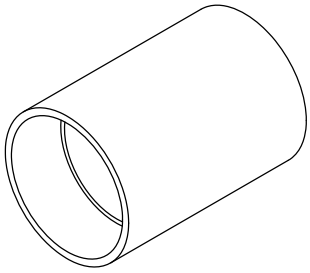

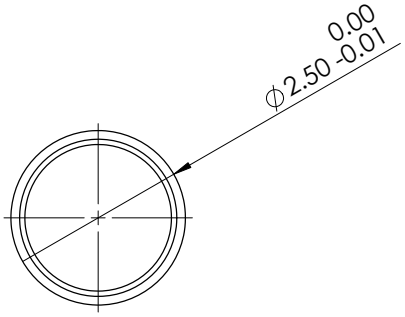

NOTES
UNLESS OTHERWISE SPECIFIED:
1. ALL DIMS. IN INCHES
2. TOLERANCES:
   X.XX = ±0.10
   ANGLES = ±1°
3. INSIDE TOOL RADIUS 0.5 MAX
4. BREAK SHARP EDGES 0.5 MAX

Mechanical Engineering CAL POLY
E-PORSCHE

Material: 6061-T6 ALUMINUM	Part Name: Right Bearing Spacer	
Scale: 1:2	Date: Monday, May 26, 2014	Drawn By: Quinton Petty

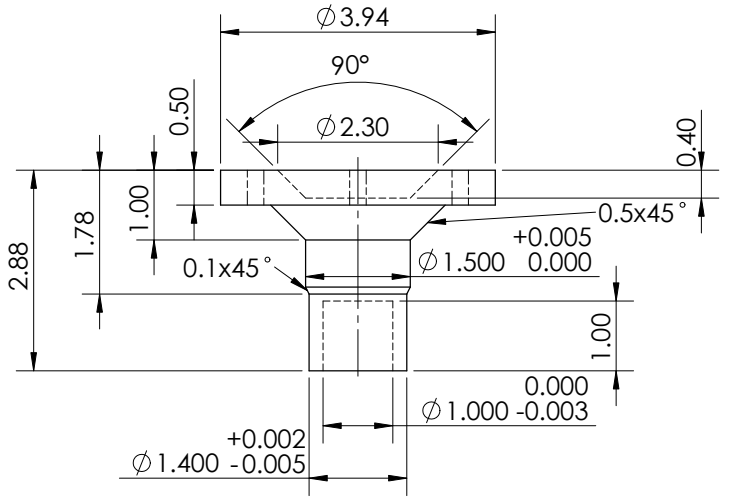

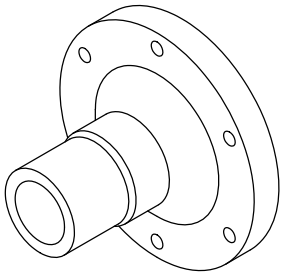

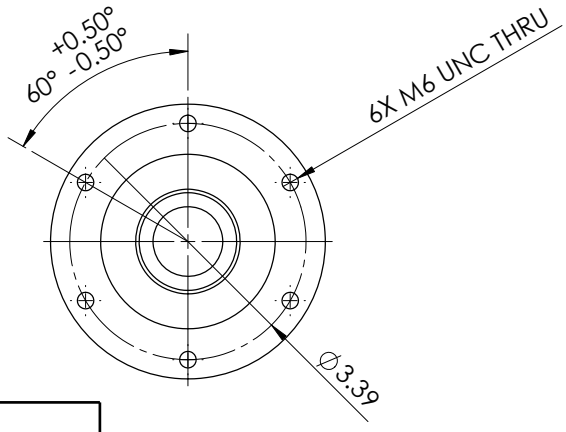

NOTES
UNLESS OTHERWISE SPECIFIED:
1. ALL DIMS. IN INCHES
2. TOLERANCES:
   X.XX = ±0.10
   ANGLES = ±1°
3. INSIDE TOOL RADIUS 0.5 MAX
4. BREAK SHARP EDGES 0.5 MAX

Mechanical Engineering CAL POLY
E-PORSCHE

Material: 1018 STEEL	Part Name: CV Joint Half Shaft Interface	
Scale: 1:2	Date: Tuesday, May 27, 2014	Drawn By: Quinton Petty

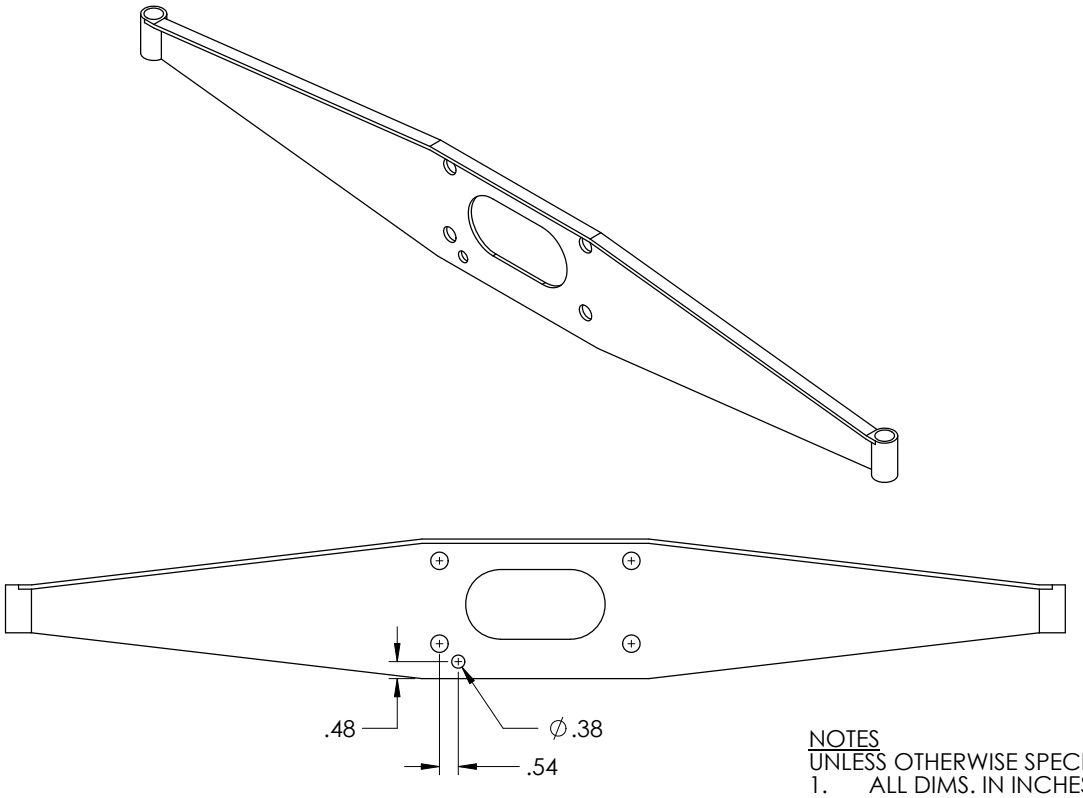

NOTES
UNLESS OTHERWISE SPECIFIED:
1. ALL DIMS. IN INCHES
2. TOLERANCES:
   X.XX = ±0.10
   ANGLES = ±1°
3. INSIDE TOOL RADIUS 0.5 MAX
4. BREAK SHARP EDGES 0.5 MAX

Mechanical Engineering CAL POLY
E-PORSCHE

Material: STEEL	Part Name: Rear Motor Mounting Bar	
Scale: 1:4	Date: Tuesday, May 27, 2014	Drawn By: Quinton Petty

ONLY ADDITIONS OR ALTERATIONS TO THE EXISTING PLATE ARE DIMENSIONED

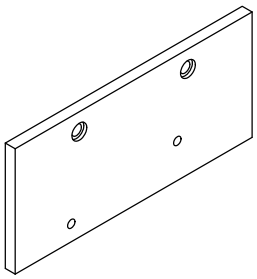

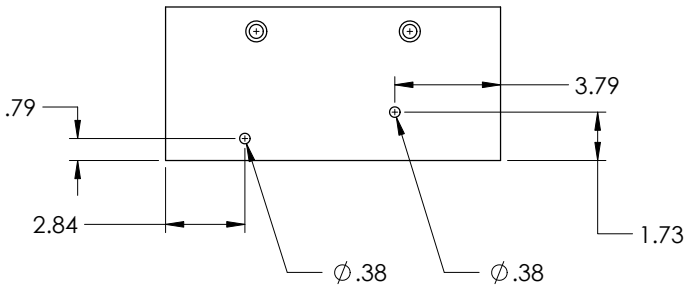

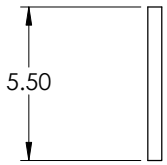

NOTES
UNLESS OTHERWISE SPECIFIED:
1. ALL DIMS. IN INCHES
2. TOLERANCES:
   X.XX = ±0.10
   ANGLES = ±1°
3. INSIDE TOOL RADIUS 0.5 MAX
4. BREAK SHARP EDGES 0.5 MAX

Mechanical Engineering CAL POLY
E-PORSCHE

Material: ALUMINUM	Part Name: Rear Drivetrain Mounting Plate	
Scale: 1:5	Date: Tuesday, May 27, 2014	Drawn By: Quinton Petty

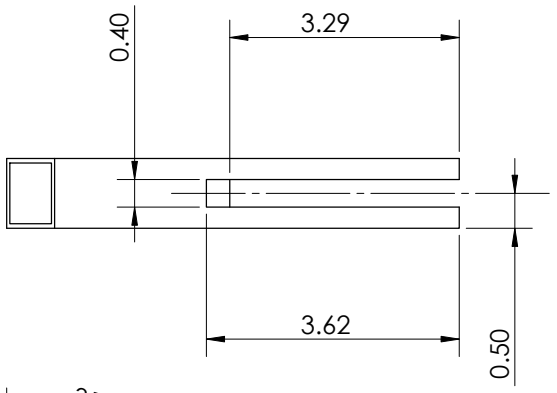

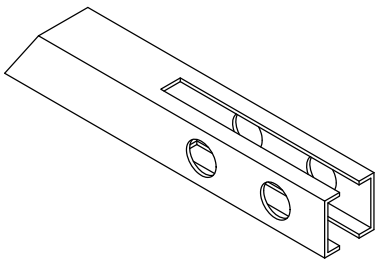

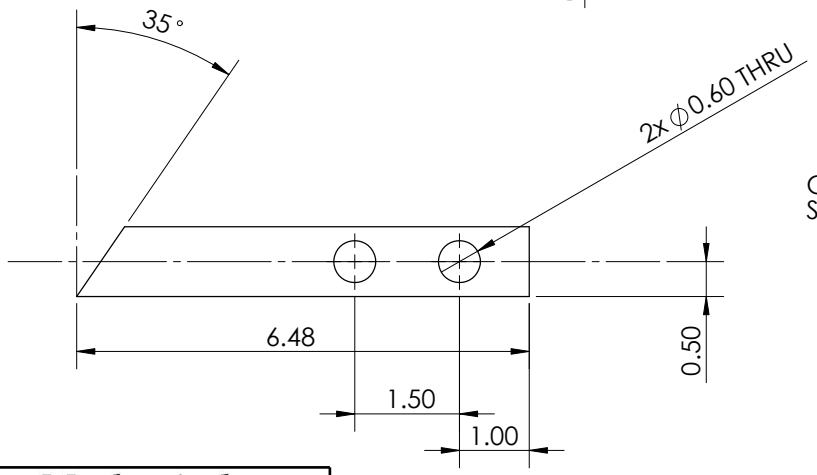

CUT FROM: 1 INCH X 1 INCH X 16GAUGE STEEL STRUCTURAL SQUARE TUBE

NOTES
UNLESS OTHERWISE SPECIFIED:
1. ALL DIMS. IN INCHES
2. TOLERANCES:
   X.XX = ±0.10
   ANGLES = ±1°
3. INSIDE TOOL RADIUS 0.5 MAX
4. BREAK SHARP EDGES 0.5 MAX

Mechanical Engineering CAL POLY
E-PORSCHE

Material: A513 STEEL	Part Name: Left Vertical Bar	
Scale: 1:2	Date: Tuesday, May 27, 2014	Drawn By: Quinton Petty

ITEM NO.	PART NUMBER	MATERIAL	QTY.
1	Advanced DC Motor	-----	1
2	Differential	-----	1
3	Rear Drivetrain Mounting Plate	ALUMINUM	1
4	Aluminum Motor Interface	ALUMINUM	1
5	Front Drivetrain Mount	A36 STEEL	1
6	Motor Shaft Collar	1018 STEEL	1
7	Horizontal Suspenion Bar	A513 STEEL	1
8	Vertical Support Bar	A513 STEEL	2
9	Left Bearing Spacer	6061-T6 ALUMINUM	1
10	Right Bearing Spacer	6061-T6 ALUMINUM	1
11	CV Joint Half Shaft Interface	1018 STEEL	2
12	Axle Shaft Oil Seal	STEEL & PTFE	2
13	Left Axle Shaft	STEEL	1
14	Right Axle Shaft	STEEL	1
15	Motor-Differential Spacer	6061-T6 ALUMINUM	4
16	0.5" Threaded Rod	ZINC PLATED STEEL	4
17	Polyurethane Bushing	POLYURETHANE	4
18	Rear Motor Mounting Bar	STEEL	1
19	Hex Bolts 18-8, 3/8"-16 x 2"	STAINLESS STEEL	4
20	Hex Bolts 1/2"-13 x 1-1/4"	STEEL	8
21	Existing Motor Bolts	STEEL	4
22	Flat Washers 3/8"	STAINLESS STEEL	4
23	Hex Nuts 18-8, 3/8"-16	STAINLESS STEEL	4
24	Lock Washers 1/2"	STEEL	4

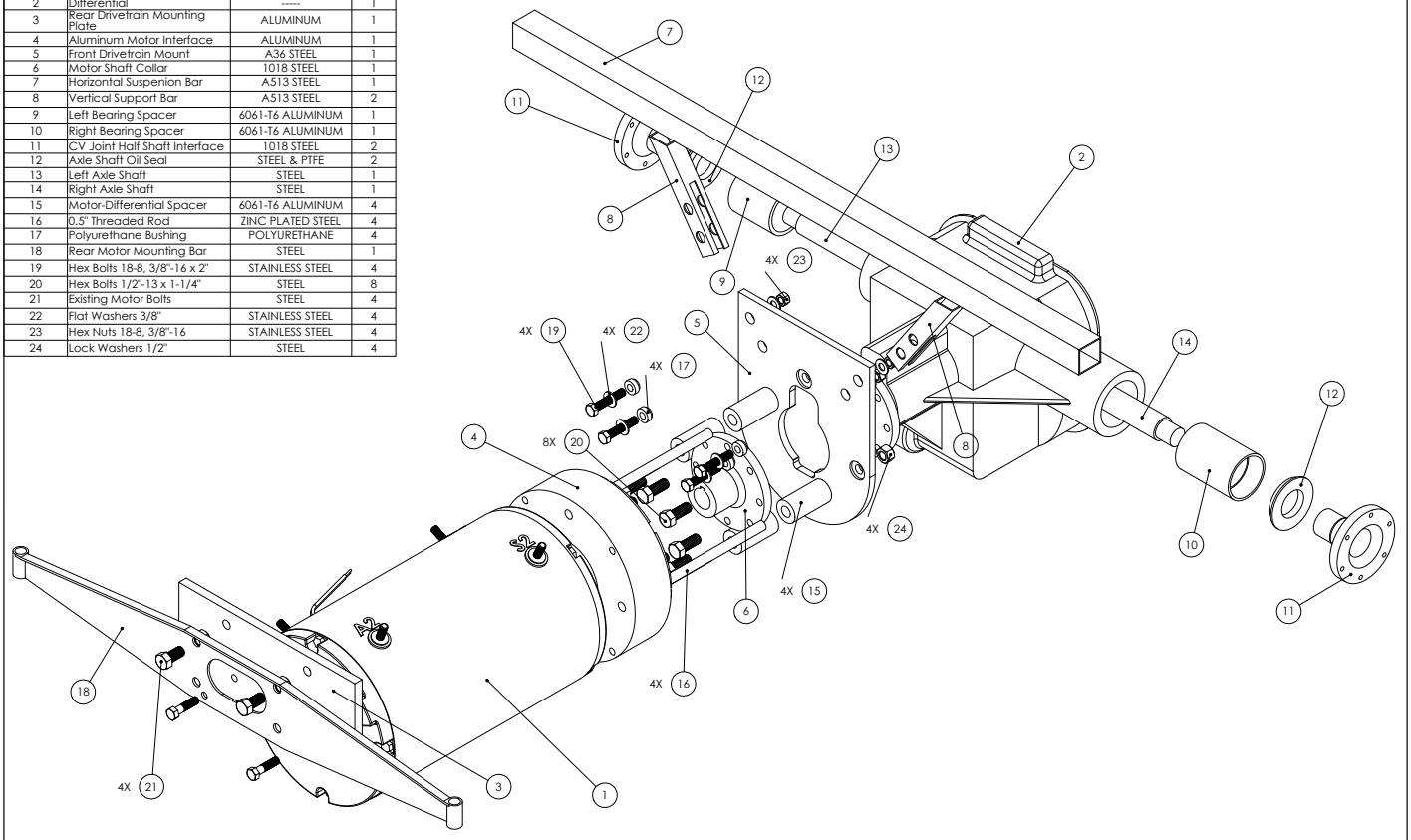

Drawn By: Spencer Treffry, Taylor Carlson & Quinton Petty

Scale: 1:3 | Date: Tuesday, May 27, 2014

Mechanical Engineering CAL POLY

E-PORSCHE

Appendix III

GEAR RATIO CALCULATIONS

* SPONSORS REQUESTED THE MOTOR OPERATE AT PEAK EFFICIENCY BETWEEN 60 AND 80 MPH

SYSTEM PARAMETERS:

WHEEL RADIUS $r = 12.5 in$
MOTOR SPEED @ MAX EFF. $N_M = 3750 \text{ rpm} = 392.7 \text{ rad/s}$

80 MPH OPERATING SPEED:

$$V_{op} = 80 \text{ MPH} \cdot \frac{1.4667 \text{ ft/s}}{1 \text{ MPH}} = 117.3 \text{ ft/s}$$

REAR AXLE SPEED (N_{RA}):

$$N_{RA} = \frac{V_{OP}}{r} = \frac{117.3 \text{ ft/s}}{12.5 \text{ in} \left(\frac{1 \text{ ft}}{12 \text{ in}}\right)} = 112.6 \text{ rad/s}$$

GEAR RATIO:

$$G.R. = \frac{N_M}{N_{RA}} = \frac{392.7 \text{ rad/s}}{112.6 \text{ rad/s}} = 3.49$$

@ 80 MPH
G.R. = 3.49

60 MPH OPERATING SPEED:

* SAME PROCESS AS OUTLINED ABOVE TO FIND OPTIMUM RATIO

@ 60 MPH
G.R. = 4.65

- RATIO DESIRED WITHIN THIS RANGE

$$3.49:1 < G.R. < 4.65:1$$

CV-HALF SHAFT INTERFACE DEFLECTION

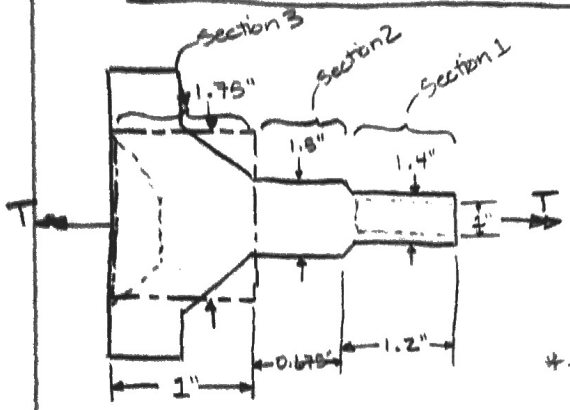

$T = 1107\ ft\text{-}lbf$

$G_{1018\ Steel} = 20.3 \times 10^6\ psi$

Deflection Equation:

$$\theta\,[deg] = \frac{583.6\,T\,[in\text{-}lbf]\,L\,[in]}{G\,[psi]\,(d^4_{outer}\,[in] - d^4_{inner}\,[in])}$$

* The part was broken into 3 sections to be analyzed. Section 3 was modeled as a solid shaft with a conservative 1.75" diameter

Section 1:

$$\theta_1 = \frac{583.6(1107\ ft\text{-}lbf)(12\ in/ft)(1.2in)}{(20.3\times10^6\ psi)((1.4in)^4 - (1in)^4)}$$

$$\theta_1 = 0.16°$$

Section 2:

$$\theta_2 = \frac{583.6(1107\ ft\text{-}lbf)(12\ in/ft)(0.675in)}{(20.3\times10^6\ psi)((1.5in)^4 - (0)^4)}$$

$$\theta_2 = 0.051°$$

Section 3:

$$\theta_3 = \frac{583.6(1107\ ft\text{-}lbf)(12\ in/ft)(1in)}{(20.3\times10^6\ psi)((1.75in)^4 - (0)^4)}$$

$$\theta_3 = 0.041°$$

Total Deflection:

$$\theta_{tot} = \theta_1 + \theta_2 + \theta_3$$

$$\theta_{tot} = 0.16° + 0.051° + 0.041°$$

$$\boxed{\theta_{tot} = 0.25°}$$

MOTOR DIFFERENTIAL INTERFACE DEFLECTION

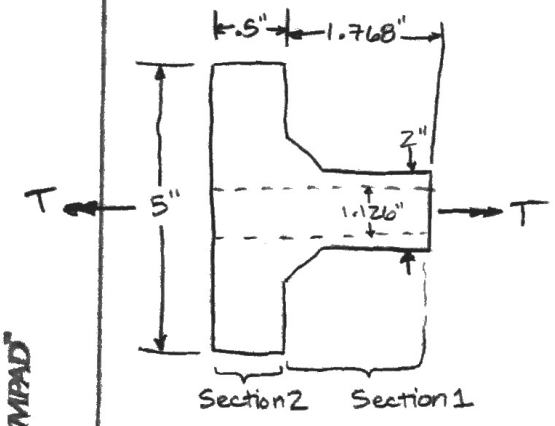

$T = 270\ ft\text{-}lb_f$

$G_{10B5t} = 20.3 \times 10^6\ psi$

Deflection Equation:

$$\theta\,[deg] = \frac{583.6\ T\,[in\text{-}lbf]\ \ell\,[in]}{G\,[psi]\left(d_{OUTER}^{[IN]^4} - d_{INNER}^{[IN]^4}\right)}$$

* The part was broken into 2 sections to be analyzed

Section 1:

$$\theta_1 = \frac{583.6(270\,ft\text{-}lb_f)(12\,in/ft)(1.768\,in)}{(20.3\times10^6\,psi)((2\,in)^4 - (1.126\,in)^4)}$$

$$\theta_1 = 0.0129°$$

Section 2:

$$\theta_2 = \frac{583.6\,(270\,ft\text{-}lb_f)(12\,in/ft)(0.5\,in)}{(20.3\times10^6\,psi)((5\,in)^2 - (1.126\,in)^2)}$$

$$\theta_2 = 0.000075°$$

Total Deflection:

$$\theta_{tot} = \theta_1 + \theta_2$$

$$\theta_{tot} = 0.0129° + 0.000075°$$

$$\boxed{\theta_{tot} = 0.013°}$$

SHAFT KEY CALCULATIONS

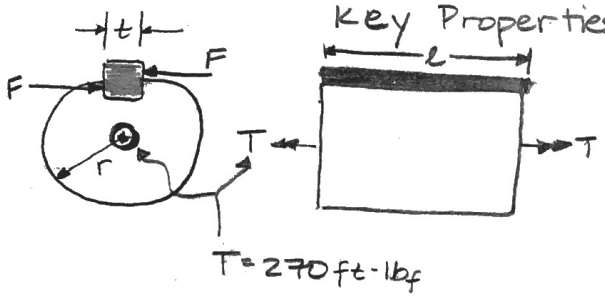

Key Properties: $S_y = 65000$ psi

$S_{sy} = 37510$ psi (DE theory)

$t = 0.25$ in

length $= l = 1.5$ in

$r = 0.56$ in

Force on shaft:

$$F = \frac{T}{r} = \frac{(270\ \text{ft-lbf})\left(\frac{12\ \text{in}}{1\ \text{ft}}\right)}{0.56\ \text{in}}$$

$$F = 5760\ \text{lbf}$$

Key shear factor of safety:

$$n = \frac{S_{sy}\, t\, l}{F} = \frac{(37510\ \text{psi})(0.25\ \text{in})(1.5\ \text{in})}{5760\ \text{lbf}}$$

$$\boxed{n = 2.44}$$

Key crushing factor of safety:

$$n = \frac{S_y\, t\, l}{2F} = \frac{(65000\ \text{psi})(0.25\ \text{in})(1.5\ \text{in})}{2(5760\ \text{lbf})}$$

$$\boxed{n = 2.12}$$

BOLT PRELOAD EXAMPLE CALCULATION

ASTM 612.9 BOLT Properties: $S_p = 140{,}600$ psi

$A_t = 0.026\ in^2$

$K = 0.3$ (Nonplated, black finish)

$d = 0.236$ in

Proofload:

$$F_p = S_p A_t = (140{,}600\ psi)(0.026\ in^2)$$

$$F_p = 3655.6\ lb_f$$

Preload:

$$F_{Pre} = 0.75 F_p = 0.75(3655.6\ lb_f)$$

$$F_{Pre} = 2741.7\ lb_f$$

Required Torque for Preload:

$$T = K F_{Pre} d = (0.3)(2741.7\ lb_f)(0.236\ in)\left(\frac{1\ ft}{12\ in}\right)$$

$$\boxed{T = 16.2\ ft\text{-}lb_f}$$

PRESS FIT CALCULATIONS

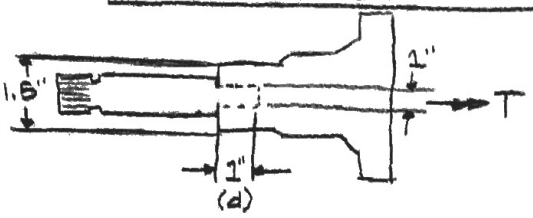

$E_{1018 St} = 29.7 \times 10^6$ psi $d = 1$ in

$\nu_{steel} = 0.29$ $R = 0.5$ in

$T = 270$ ft-lbf $r_{out} = 0.75$ in

Pressure needed to withstand T:

$$P = \frac{F}{A} = \frac{\frac{T}{R}}{2\pi R d} = \frac{\frac{270 \text{ ft·lbf}(12 \text{ in/ft})}{0.5 \text{ in}}}{2\pi(0.5 \text{ in})(1 \text{ in})}$$

$P = 24751.8$ psi

Radial Interference that will produce P:

$$\delta = \frac{P(2R^3)}{E}\left(\frac{r_o^2}{(r_o^2 - R^2)(R^2)}\right) = \frac{(24751.8 \text{ psi})(2(0.5 \text{ in})^3)}{29.7 \times 10^6 \text{ psi}}\left(\frac{0.75 \text{ in}}{(0.75 \text{ in}^2 - 0.5 \text{ in}^2)(0.5}\right.$$

$\boxed{\delta = 0.0015 \text{ in}}$ Radial interference

EXAMPLE BOLT CALCULATION — DIFF.-CV INTERFACE

- Assume:-preload is lost
  - all bolts are active

SIDE VIEW

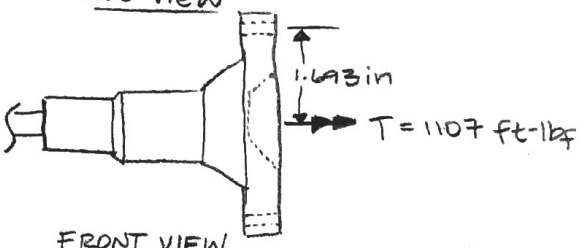

FRONT VIEW

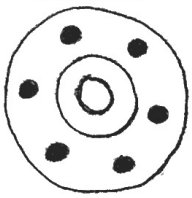

ASTM Grade 12.9 Bolt Properties

$S_p = 140600$ psi

$S_{UT} = 176900$ psi

Force per bolt:

$$F_b = \frac{T}{n \cdot r} = \frac{(1107\ \text{ft-lbf})(12\ \text{in/ft})}{(6\ \text{bolts})(1.693\ \text{in})}$$

$$F_b = 1307.7\ \text{lbf/bolt}$$

Bolt Shear Factor of Safety:

$$n = \frac{0.577 S_{UT}}{\left(\frac{F_b}{A_r}\right)} = \frac{0.577(176900\ \text{psi})}{\left(\frac{1307.7\ \text{lbf}}{0.0211\ \text{in}^2}\right)}$$

where A_r = minor diameter area

$$n = 1.64$$

DIFFERENTIAL MOUNTING PLATE WELD CALCULATIONS

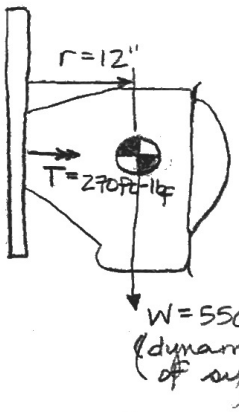

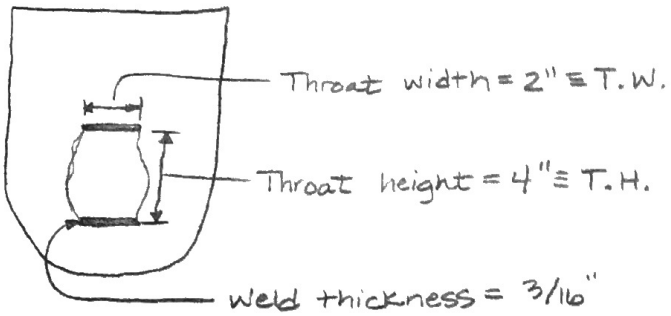

Primary Shear on Weld:

$$\tau' = \frac{T\left(\frac{2}{T.H.}\right) + W}{1.414(T.W. \times T.H.)} = \frac{270\,ft\text{-}lbf\,(12\,in)\left(\frac{2}{4\,in}\right) + 550\,lbf}{1.414\,(2in)(4in)}$$

$$\tau' = 191.8\ psi$$

Secondary Shear:

$$\tau'' = \frac{(r \times W)\left(\frac{T.H.}{2}\right)}{I} = \frac{(12in)(550lbf)\left(\frac{4in}{2}\right)}{0.707\left(\frac{3}{16}"\right)\left(\frac{2"\,(4")^2}{2}\right)}$$

$$\tau'' = 6223.5\ psi$$

Total Shear:

$$\tau = \sqrt{(\tau')^2 + (\tau'')^2} = \sqrt{(191.8psi)^2 + (6223.5psi)^2}$$

$$\tau = 6226.4\ psi$$

Weld Shear Factor of Safety:

$$n = \frac{S_p}{\tau} = \frac{18000\ psi}{6226.4\ psi}$$

$S_p = 18000\ psi$ → permissible bending stress of E60 electrode

$$\boxed{n = 2.89}$$

DIFFERENTIAL MOUNTING PLATE WELD FATIGUE

Fatigue Strength:

$$S_{se} = K_a K_b K_c K_d K_e K_f (0.5 S_{UT}) \quad ; \quad S_{UT} = 58000 \text{ psi}$$

Where: $K_b = K_d = K_f = 1$

$$K_a = 14.4 \left(S_{UT[ksi]}\right)^{-0.718} = 0.78$$

$K_c = 0.59$ (torsional loading)

$K_e = 0.753$ (99.9% reliability)

$$S_{se} = (0.78)(1)(0.59)(1)(0.753)(1)(0.5)(58000 \text{ psi})$$

$$S_{se} = 10052.3 \text{ psi}$$

Goodman Fatigue Factor of Safety:

$$n_f = \frac{1}{\frac{\tau'}{S_{se}} + \frac{\tau''}{S_{UT}}} = \frac{1}{\frac{191.8 \text{ psi}}{10052 \text{ psi}} + \frac{6226.4 \text{ psi}}{0.3(58000 \text{ psi})}}$$

$$\boxed{n_f = 2.65}$$

HALF SHAFT SLEEVE WELD CALCULATIONS

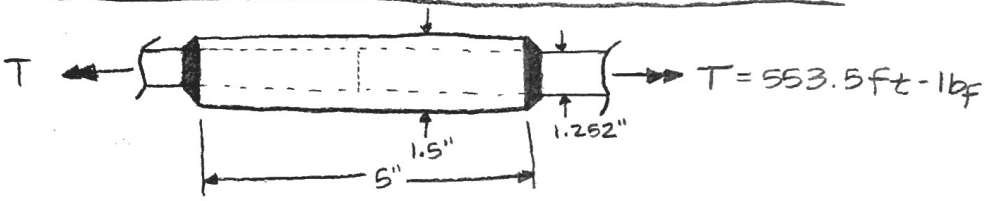

Primary Shear:

$$\tau' = \frac{Tr}{J} = \frac{(553.5\,ft\text{-}lbf)(12\,in)(0.626in)}{\frac{\pi}{32}\left((1.5")^4-(1.252")^4\right)}$$

$$\tau' = 12161.7\,psi$$

E60 Electrode: Permissible bending stress $S_p = 18000\,psi$

Weld Shear Factor of Safety:

$$n = \frac{S_p}{\tau'} = \frac{18000\,psi}{12161.7\,psi}$$

$$\boxed{n = 1.48}$$

SLEEVE DEFLECTION CALCULATION

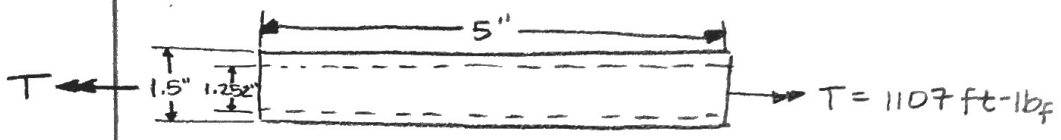

$G_{10B5t} = 20.3 \times 10^6$ psi

$d_{OUTER} = 1.5"$

$d_{INNER} = 1.252"$

$$\theta_{max} = \frac{583.6\,T\,l}{G(d_{out}^4 - d_{in}^4)}$$

$$= \frac{583.6(1107\,lb_f \cdot \cancel{ft})(12\,\cancel{in}/\cancel{ft})(5\,in)}{(20.3\times10^6\,psi)(1.5^4\,in - 1.252^4\,in^4)}$$

$$\boxed{\theta_{max} = 0.73^\circ}$$

Rear Mounting Bolts

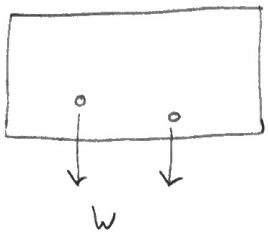

Maximum Dynamic Force of System Downward

$$F_o = 2(W)(F.S) = 2(200\ lbs)(4) = 1600\ lbs$$

Minimum Diameter on a single bolt if all load was on one bolt.

$$\tau = \frac{V}{A} \Rightarrow A = \frac{V}{\tau} = \frac{\pi}{4} D^2 \qquad \tau = 29 * 10^6 \frac{lb}{in^2} \text{ for Steel}$$

$$D = \sqrt{\frac{4V}{\pi \tau}} = \sqrt{\frac{4(1600\ lbs)}{\pi\left(29 \times 10^6 \frac{lbs}{in^2}\right)}} = \boxed{0.008\ in}$$

Bending of Front Horizontal Drivetrain Support Bar

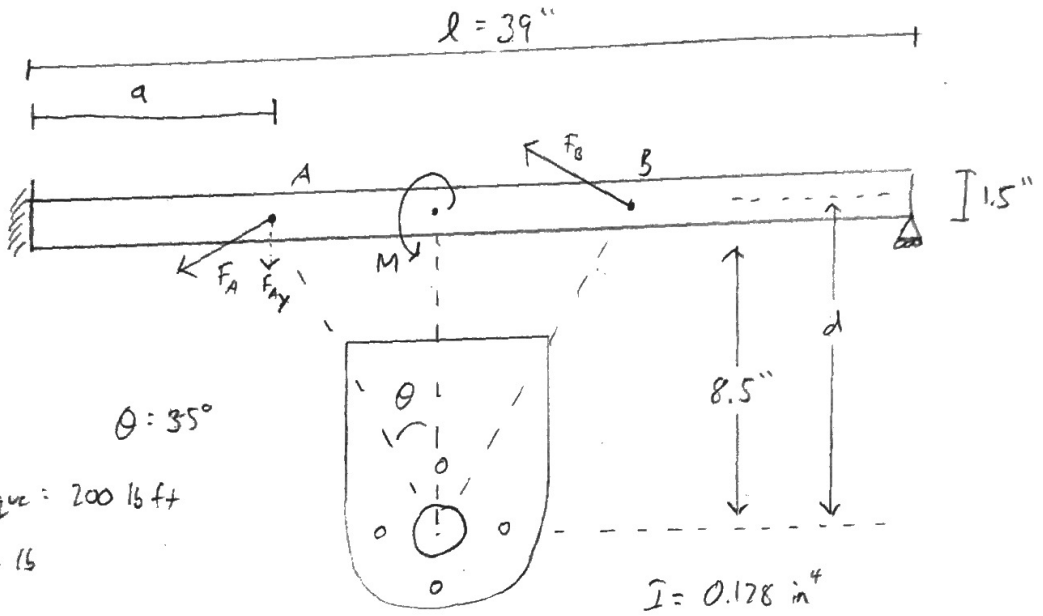

Max Torque = 200 lb ft

W = 200 lb

$I = 0.178\ in^4$

$$d = 8.5" + \left(\frac{1.5"}{2}\right) = 9.25"$$

$$a = \left(\frac{l}{2}\right) - (d \tan\theta) = \left(\frac{39"}{2}\right) - \left((9.25")\tan(35°)\right) = 13.02"$$

$$F_{Ay} = (\text{Max Torque})\left(\frac{\cos\theta}{d}\right)\cdot\sin\theta = (200\ lb\,ft)\left(\frac{\cos(35°)}{9.25\ in}\right)\cdot\sin(35°)\left(\frac{12\ in}{1\ ft}\right) = 121.9\ lb$$

$$M = 2\left(F_{Ay} + \frac{W}{2}\right)(d\tan\theta) = 2\left(121.9\ lb + \frac{200\ lb}{2}\right)(9.25\ in\ \tan 35°) = 2874.8\ in\cdot lb$$

$$y_{\substack{max\\bending\\torsion}} = \frac{M}{6EI}\left(\frac{x^3}{l} - \frac{x\,l}{4}\right) \quad @\ x = \sqrt{\frac{l^2}{12}}$$

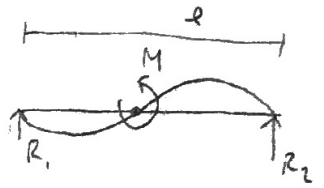

$$x = \sqrt{\frac{(39\ in)^2}{12}} = 11.26\ in$$

$$y_{\substack{max\\bending\\torsion}} = \frac{2874.8\ in\cdot lb}{6\left(29\times10^6\ \frac{lb}{in^2}\right)(0.178\ in^4)}\left(\frac{(11.26\ in)^3}{39\ in} - \frac{(11.26\ in)(39\ in)}{4}\right) = \boxed{-0.009\ in}$$

Scripts for calculations can be found at: https://github.com/qpetty/me_coursework/tree/master/senior_project

$$y_{\substack{\text{bending} \\ @x \\ \text{weight}}} = \frac{F \cdot x}{6EI}\left(x^2 + 3a^2 - 3la\right)$$

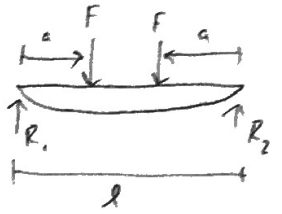

$F = \frac{W}{2}$ $\quad x = 11.26\text{ in}$ $\quad a = 13.02\text{ in}$

$$y_{\substack{\text{bending} \\ @x \\ \text{weight}}} = \frac{\left(\frac{200\text{ lb}}{2}\right)(11.26\text{ in})}{6\left(29\times10^6\ \frac{\text{lb}}{\text{in}^2}\right)(0.128\text{ in}^4)}\left((11.26\text{ in})^2 + 3(13.02\text{ in})^2 - 3(39\text{ in})(13.02\text{ in})\right) = \boxed{-0.045\text{ in}}$$

$$y_{\substack{\text{max} \\ @x}} = y_{\substack{\text{max} \\ \text{bending} \\ \text{torsion}}} + y_{\substack{\text{bending} \\ @x \\ \text{weight}}} = -0.009\text{ in} + (-0.045\text{ in}) = \boxed{0.054\text{ in}}$$

$$y_{\substack{\text{max} \\ \text{bending} \\ \text{weight}}} = \frac{F \cdot a}{24EI}\left(4a^2 - 3l^2\right)$$

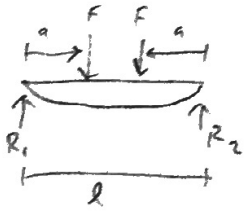

$$y_{\substack{\text{max} \\ \text{bending} \\ \text{weight}}} = \frac{\left(\frac{200\text{ lb}}{2}\right)(13.02\text{ in})}{24\left(29\times10^6\ \frac{\text{lb}}{\text{in}^2}\right)(0.128\text{ in}^4)}\left(4(13.02\text{ in})^2 - 3(39\text{ in})^2\right) = \boxed{-0.057\text{ in}}$$

$\boxed{y_{max} = -0.057\text{ in}}$

Max horizontal axial force created by moment on bar

$$F_H = 2\left(\text{Max Torque}\right)\left(\frac{\cos\theta}{d}\right)\cos\theta$$

$$F_H = 2\left(200\text{ lb ft}\right)\left(\frac{\cos(35°)}{9.25\text{ in}}\right)\cos(35°)\left(\frac{12\text{ in}}{1\text{ ft}}\right) = \boxed{348\text{ lbs}}$$

Max vertical force created by moment on bar

$$F_V = M\left(\frac{1}{l}\right) = (2874.5\text{ in}\cdot\text{lb})\left(\frac{1}{39\text{ in}}\right) = \boxed{147\text{ lbs}}$$

Vertical Strut Bar Displacements

Dynamic Force felt on end of vertical bar during average 10G crash

$F_D = 2 * \text{mass} * \text{deceleration}$

$$F_D = 2\left(200\ lb_f\right)\left(\frac{1.0\ slug}{32.2\ lbf}\right)\left(10\ \frac{ft}{s^2}\right) = 4000\ lbf$$

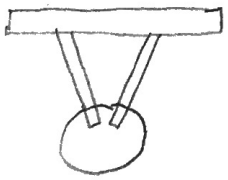

Maximum Displacement of vertical bars seen as cantilevered beams

$$X_{max} = \frac{F_D \ell^3}{3EI} = \frac{(4000\ lbf)(1.8\ in)^3}{3\left(29\times10^6\ \frac{lb}{in^2}\right)(0.0355\ in^4)} = 0.007\ \text{inches}$$

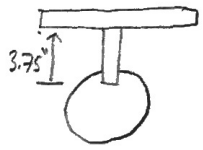

Maximum Torsion felt at welds

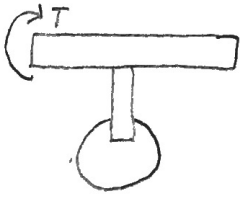

$$T = F \cdot d = (4000\ lb)(1.8\ in) = 7{,}200\ in\ lb$$

Stress per inch at welds on horizontal bar ($\frac{3}{16}$ inch weld)

$$I_b = \frac{c^2}{6}(3b + c) = \frac{(1.5in)^2}{6}\left(3(2.5in) + (1.5in)\right)\left(\tfrac{3}{16}in\right) = .707$$
$$= 0.447\ in^4$$

$$\sigma = \frac{T(Y_2)}{I_b} = \left(7{,}200\ in\ lb\right)\left(\frac{1.5in}{2\left(0.447in^4\right)}\right)$$
$$= 12070\ lb$$

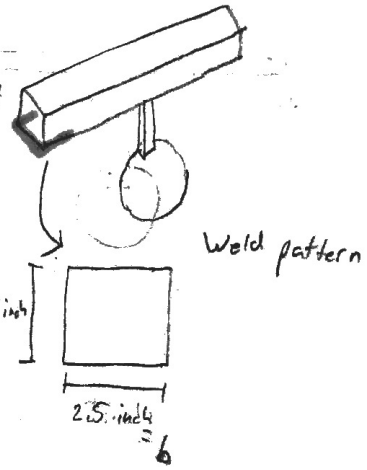

$$\frac{\sigma}{in} = \frac{12070\ psi}{4(2.5\ in)} = 1207\ \frac{psi}{in} = 1.207\ \frac{kpsi}{in}$$

Stress per linear in of $\frac{3}{16}$" weld & E60 electrode = $2.39\ \frac{kpsi}{in}$

Factor of Safety: $\frac{(2.39 - 1.207) + 2.39}{2.39} = \boxed{1.49}$

CV HALF SHAFT YIELD AND FATIGUE CALCS

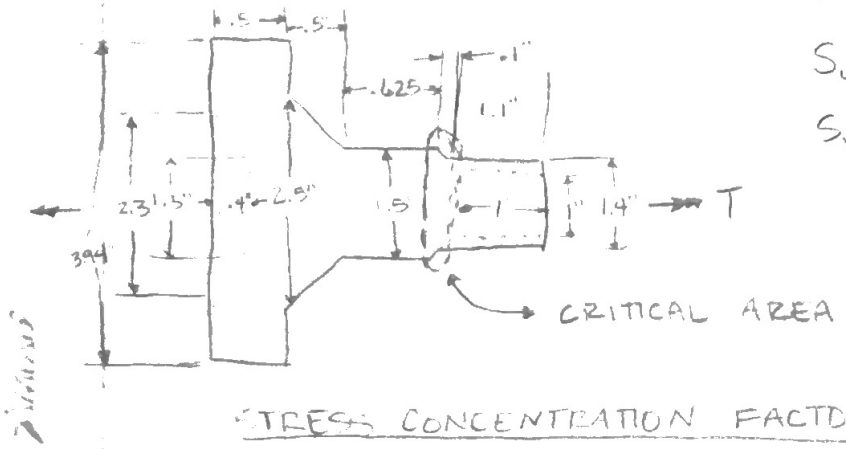

$T = 270\ ft \cdot lb_f$

$S_{ut} = 63800\ psi$

$S_y = 53700\ psi$

STRESS CONCENTRATION FACTOR @ CRITICAL AREA

$K_{fs} = 1 + q(K_{ts} - 1)$

From Table A-15: $K_{ts} = 1.3$

Fig. 6-20: $q = 0.8$

$K_{fs} = 1 + 0.8(1.3 - 1)$

$K_{fs} = 2.84$

STRESS AT CRITICAL AREA

$$\tau_{max} = \frac{Tr}{J} = \frac{(270\ ft\ lbf)(12\ in/ft)(0.7\ in)}{\frac{\pi (0.7\ in)^4}{2}}$$

$\tau_{max} = 6013.6\ psi$

$\tau_{min} = 0\ psi$

$$\sigma_m = \frac{\sigma_{max} + \sigma_{min}}{2} = \frac{6013.6\ psi + 0\ psi}{2}$$

$\sigma_m = 3006.8\ psi$

$$\sigma_a = \frac{|\sigma_{max} - \sigma_{min}|}{2} = \frac{6013.6\ psi + 0\ psi}{2}$$

$\sigma_a = 3006.8\ psi$

CV HALF SHAFT YIELD AND FATIGUE CALCS CONT'D

CHECK FOR YIELDING

$$n = \frac{S_y}{K_{fs}(\sigma_m + \sigma_a)} = \frac{53,700 \text{ psi}}{2.84(3006.8 \text{ psi} + 3006.8 \text{ psi})}$$

$\boxed{n_1 = 1.81}$ SAFETY FACTOR FOR YIELDING

EQUIVALENT REVERSED STRESS (mod-Goodman)

$$\sigma_{rev} = \frac{\sigma_a}{1 - \left(\frac{\sigma_m}{S_{ut}}\right)} = \frac{3006.8 \text{ psi}}{1 - \left(\frac{3006.8 \text{ psi}}{63800 \text{ psi}}\right)}$$

$\boxed{\sigma_{rev} = 3155.5 \text{ psi}}$

ENDURANCE STRENGTH

$$S_e = K_a K_b K_c K_d K_e K_f (0.5 S_{ut})$$

where $K_a = a S_{ut}^{\ b}$ for Cold-Drawn Steel $a = 2.7$; $b = -0.265$

$K_a = 2.7(63.8)^{-0.265}$

$\boxed{K_a = 0.897}$

$K_b = 0.897\, d^{-0.107}$

$K_b = 0.897(1.41)^{-0.107}$

$\boxed{K_b = 0.865}$

$\boxed{K_c = 0.59}$ for Torsion loading

$\boxed{K_d = 1}$ for moderate temperatures

$\boxed{K_e = 0.897}$ for 90% reliability

$\boxed{K_f = 1}$ no misc. considerations

$$S_e = (0.897)(0.865)(0.59)(1)(0.897)(1)(0.5)(63,800 \text{ psi})$$

$\boxed{S_e = 13112.3 \text{ psi}}$

CV HALF SHAFT YIELD AND FATIGUE CALCS CONT'D

DETERMINING LIFE CYCLES (N)

From Fig 6-18: fatigue strength fraction $f = 0.9$

$$a = \frac{(f S_{ut})^2}{S_e / K_{fs}} = \frac{(0.9(63800\,psi))^2}{\frac{13112.3\,psi}{2.84}}$$

$$a = 714112.4$$

$$b = -\frac{1}{3}\log\left(\frac{f S_{ut}}{S_e / K_{fs}}\right) = -\frac{1}{3}\log\left(\frac{0.9(63800\,psi)}{\frac{13112.3\,psi}{2.84}}\right)$$

$$b = -0.365$$

$$N = \left(\frac{\sigma_{rev}}{a}\right)^{1/b} = \left(\frac{3155.5\,psi}{714112.4}\right)^{\frac{1}{-0.365}}$$

$$N = 2.8 \times 10^6 \text{ cycles}$$

Appendix IV

Bill of Materials

Sub-Assembly	Material/Operation	Labor ($)	Qty.	Total Cost ($)
Differential				
	2000 Ford Ranger Differential Housing		1	216.00
	Powertrax Limited Slip Carrier		1	402.61
	6061 Aluminum Tube - 2.5" OD, 2" ID, 1 ft		1	15.66
	Timken Shaft Oil Seal		2	16.98
Motor-Differential Interface				
	Steel Plate - 3/8" thick, 1x1 ft		1	39.30
	Welding	15/hour	3	45.00
	Aluminum Round - 1.25", 1 ft		1	8.64
	1018 Steel Round - 5", 1 ft		1	166.90
Differential-CV Interface				
	*1018 Steel Round - 5", 1 ft		-	-
	Welding	15/hour	2	30.00
Half Shaft Sleeves				
	1018 Steel Round - 1.5", 1 ft		1	14.70
	Welding	15/hour	2	30.00
Mounts				
	A513 Steel Square Tube - 1.5" x 1.5", 16 GA, 4 ft		1	13.28
	A513 Steel Square Tube - 1" x 1", 16 GA, 2 ft		1	3.98
Hardware				
	Prothane Bushing - 19-921		2	17.98
	Hex Bolts - Stainless Steel 18-8, 0.375"-16 x 2"		4	2.16
	Hex Nuts - Stainless Steel 18-8, 0.375"-16		4	0.60
	Flat Washers - Stainless Steel 18-8, 0.375"		8	0.64
	Welding Electrodes - E6013		1	17.66
	Threaded Rod - 0.5" x 3 ft		1	9.36
	Hex Bolts - Zinc Plated Steel, 0.5"-13 x 1.25"		8	2.40
	Lock Washer - Zinc Plated Steel, 0.25		8	0.48
		Metalsdepot Shipping		40.70
		Boltdepot Shipping		9.56
		MSC Direct Shipping		22.66
		Fastenal Shipping		10.59
		Andy's Auto Sport Shipping		36.94
		Total ($)		**1174.78**

* Material already purchased for earlier part

Appendix V

Potential
Failure Mode and Effect Analysis
(Design FMEA)

Differential System
___ Subsystem
___ Component

FMEA Number: 1

Design Responsibility: QTS

Page 1 of 1

Model Year: 1977

Key Date:

Prepared By: E-Porsche

Core Team: Quinton Petty, Spencer Treffry, and Taylor Carlson

FMEA Date (Orig.) 3/13/14 (Rev.) 5/19/14

Item / Function	Potential Failure Mode	Potential Effect(s) of Failure	Sev	Potential Cause(s) / Mechanism(s) of Failure	Occur	Crit	Recommended Action(s)	Responsibility & Target Completion Date	Action Results: Actions Taken	Sev	Occur	Crit
				Weld shear failure	7	49	Design sufficient factor of safety for weld and hire experienced welder	Taylor (4/25/14)	No action necessary			
Frame mounting	Material yield	No power transmission	7	Insufficient mounting point strength	4	28	Increase factors of safety	Quinton (4/15/14)	No action necessary			
				Insufficient load in fasteners	3	21	Measure pre-load on bolts	Quinton (4/15/14)	No action necessary			
Frame	Material yield	Catastrophic structural failure	10	Removed structural members for installation of differential	3	30	Design structural reinforcement	Quinton (4/15/14)	No action necessary			
				Joint stress concentrations	3	30	Reinforce joints	Quinton (4/15/14)	No action necessary			

Potential
Failure Mode and Effect Analysis
(Design FMEA)

Differential System
___ Subsystem
___ Component

Design Responsibility: QTS

Model Year: 1977

Key Date:

Core Team: Quinton Petty, Spencer Treffry, and Taylor Carlson

FMEA Number: 1

Page 1 of 1

Prepared By: E-Porsche

FMEA Date (Orig.) 3/13/14 (Rev.) 5/19/14

Item / Function	Potential Failure Mode	Potential Effect(s) of Failure	Sev	Potential Cause(s) / Mechanism(s) of Failure	Occur	Crit	Recommended Action(s)	Responsibility & Target Completion Date	Action Results			
									Actions Taken	Sev	Occur	Crit

Potential
Failure Mode and Effect Analysis
(Design FMEA)

Differential System
___ Subsystem
___ Component

Design Responsibility: QTS

Model Year: 1977

Key Date:

Core Team: Quinton Petty, Spencer Treffry, and Taylor Carlson

FMEA Number: 1

Page 1 of 1

Prepared By: E-Porsche

FMEA Date (Orig.) 3/13/14 (Rev.) 5/19/14

Item / Function	Potential Failure Mode	Potential Effect(s) of Failure	Sev	Potential Cause(s) / Mechanism(s) of Failure	Occur	Crit	Recommended Action(s)	Responsibility & Target Completion Date	Action Results			
									Actions Taken	Sev	Occur	Crit

Appendix VI

DVP

Report Date: 12-11-2014		Sponsor: Cal Poly Motorcar Association			Component/Assembly: Single Speed Differentail Reduction							REPORTING ENGINEER: QTS
TEST PLAN									**TEST REPORT**			
Item No	Specification or Clause Reference	Test Description	Acceptance Criteria	Test Responsibility	Test Stage	SAMPLES TESTED		TIMING		TEST RESULTS			NOTES
						Quantity	Type	Start date	Finish date	Test Result	Quantity Pass	Quantity Fail	
Engineering Specifications													
1	Power losses	Known interia will be accelerated from one speed to another to determine power of the system. A baseline will be measured with the current transmission and will be compared with the same test when the prototype is complete.	Power losses calculated less than the baseline	Quinton	DV	3 Speeds	B	10/20/14	11/7/14	Diff exhibited less losses for high V test	Trans. Passed all tests with more mechanical losses	Diff failed low voltage tests while exhibiting less mechanical losses	
2	Torque Capacity	Prototype will be tested with an input torque of greater than 270 ft-lbs	Gears and shafts do not yield	Spencer	DV	Minimum of 5 runs	B	10/13/14	10/20/14	N/A			
3	Cost	Prototype is created within budget given by Sponsor	Less than $2,200	Quinton	CV	1	C	2/3/14	11/20/14	N/A			
4	Volume	Measure the total volume required to install the prototype in the car	Less than the volume currently taken up by the transmission and differential	Spencer	DV	3 measurements	B	10/27/14	11/10/14	N/A			
5	Weight	Measure weight of all newly created and installed parts into the car.	Less than weight of current transmission and differential	Spencer	DV	2	B	10/20/14	11/10/14	N/A			
6	Required maintenance	Installation and access to most likely failed parts can be tested through a few installations by the group	Parts installed with only student labor	Quinton	PV	3	C	10/6/14	11/8/14	Completed	Porsche is prepared for future installations		
Motor Interface													
7	Material Deformation	A smaller electric motor will be attached and run at a slower speed and lower torque eventiually leading up to the currently installed motor.	No material deformation	Taylor	DV	5 increments	B	10/13/14	10/20/14	Completed	No visible mat'l deformation with 3 hp electric motor		
Gear Teeth													
8	Material Deformation	A smaller electric motor will be attached and run at a slower speed and lower torque eventiually leading up to the currently installed motor.	No material deformation	Taylor	DV	5 increments	B	10/13/14	10/20/14	N/A			
9	Partial tooth material loss	A smaller electric motor will be attached and run at a slower speed and lower torque eventiually leading up to the currently installed motor. Case and lubrication will be inspected for metal fragments	No visible loss of material on gear teeth	Taylor	DV	5 increments	B	10/20/14	11/2/14	N/A			
Shaft													
10	Material Deformation	A smaller electric motor will be attached and run at a slower speed and lower torque eventiually leading up to the currently installed motor.	No material deformation	Quinton	DV	5 increments	B	10/13/14	10/20/14	N/A			
Frame													
11	Material Yield	Strain Gauges will be attached to the frame and measure the strain in areas that will experience the highest strains based on frame geometry	Less than baseline testing	Spencer	DV	8 readings	B	10/20/14	11/10/14	N/A			
12													
13													
14													
15													
16													
17													
18													
19													
20													
21													
22													
23													
24													
25													
26													
27													
28													

Appendix VII

ID	Task Name	Start	Finish	Predecessors	Duration
1	Intro Letter to Sponsor	Tue 1/14/14	Tue 1/14/14		1 day
2	Background Research	Wed 1/15/14	Wed 2/12/14		21 days
3	Meet with Sponsor	Thu 1/16/14	Thu 1/16/14		1 day
4	Identify Sponsor Requirements	Fri 1/17/14	Tue 1/21/14	1,3	3 days
5	Examine Current Car Configuration	Thu 1/16/14	Thu 1/16/14		1 day
6	Team Contract	Thu 1/16/14	Fri 1/17/14		2 days
7	Problem Statement	Wed 1/22/14	Thu 1/23/14	4,2SS,5SS	2 days
8	Contact Potential Outside Sponsors	Fri 1/17/14	Wed 2/5/14	3	14 days
9	QFD House of Quality	Fri 1/24/14	Tue 1/28/14	7	3 days
10	Project Proposal	Wed 1/29/14	Tue 2/4/14	9	5 days
11	Meet with Outside Sponsors	Fri 1/17/14	Wed 2/5/14	8SS	14 days
12	Ideation	Wed 2/5/14	Mon 2/24/14	10	14 days
13	Pugh Matrix	Tue 2/25/14	Tue 2/25/14	12	1 day
14	Weighted Decision Matrix	Wed 2/26/14	Wed 2/26/14	13	1 day
15	Concept Modeling	Wed 2/26/14	Thu 2/27/14	14SS	2 days
16	Gantt Chart	Wed 2/26/14	Wed 2/26/14		1 day
17	Choose Leading Concept	Sat 2/15/14	Sat 2/15/14		1 day
18	Preliminary Engineering Analysis	Mon 2/17/14	Tue 2/25/14	17	7 days
19	Preliminary CAD Model	Fri 2/28/14	Mon 4/7/14	15	27 days
20	Preliminary Design Report	Fri 2/28/14	Thu 3/6/14	17,18SS,19SS	5 days
21	Preliminary Design Presentation	Fri 3/7/14	Fri 3/7/14	20	1 day
22	Disassemble Current Transmission	Thu 2/6/14	Fri 2/14/14	5,11	7 days
23	Design Testing Procedure	Mon 2/17/14	Thu 2/27/14	5,17	9 days
24	Test Transmission	Fri 2/28/14	Mon 3/10/14	23	7 days
25	Contact Manufacturing Sponsors	Fri 3/7/14	Wed 3/26/14	20	14 days
26	Manufacturing Design	Fri 3/7/14	Mon 3/17/14	25SS	7 days
27	Assembly Design	Fri 3/7/14	Mon 3/17/14	20	7 days
28	Detailed CAD Modeling	Fri 3/7/14	Mon 3/17/14	20,27SS,26SS	7 days
29	Compile BOM	Tue 3/18/14	Thu 3/20/14	27	3 days
30	Critical Design Report	Thu 4/17/14	Tue 5/27/14	28,29	29 days
31	Critical Design Presentation	Tue 4/1/14	Thu 5/15/14	30	33 days
32	Order Parts	Thu 5/29/14	Fri 5/30/14	29	2 days
33	Receive Parts	Fri 6/6/14	Fri 6/13/14	32	6 days
34	Prototype Construction	Mon 6/16/14	Tue 9/30/14	33	77 days
35	Prototype Installation	Tue 9/30/14	Fri 10/3/14	34	4 days
36	Prototype Testing	Mon 10/6/14	Fri 11/7/14	35	25 days
37	Prototype Demo	Mon 11/3/14	Mon 11/3/14	34SS	1 day
38	Senior Design Expo Preparation	Fri 10/31/14	Wed 11/19/14	37	14 days
39	Senior Design Expo	Thu 11/20/14	Thu 11/20/14	38	1 day
40	Final Project Report	Thu 10/30/14	Tue 11/18/14	37	14 days

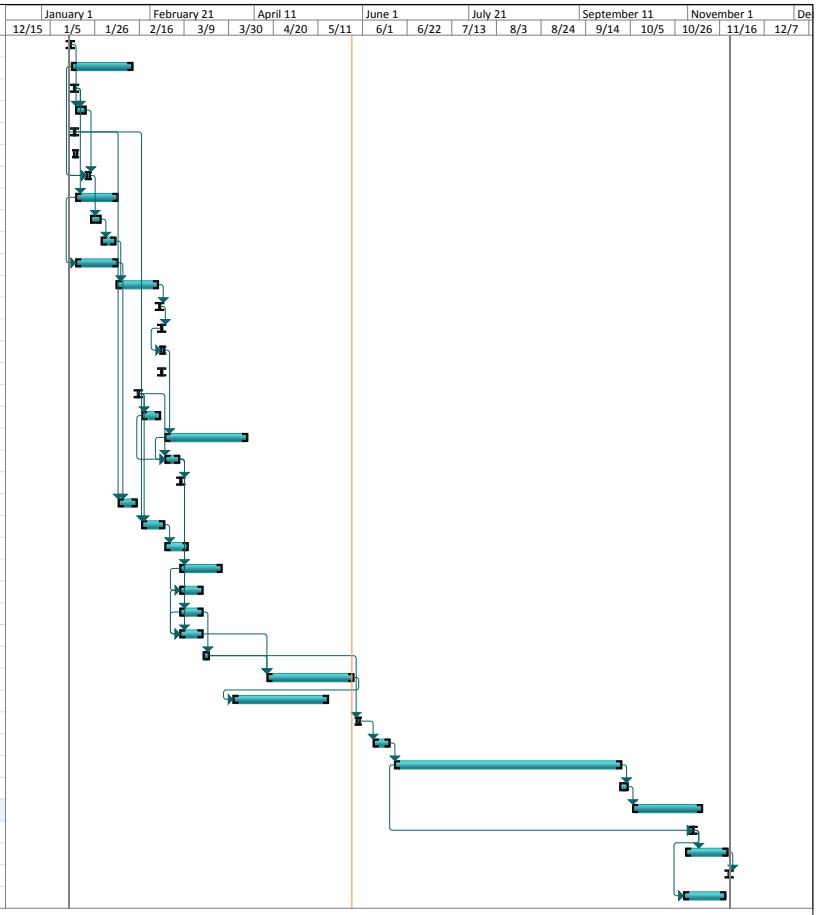

Project: Gantt Chart
Date: Tue 5/27/14

Task	Project Summary	Inactive Milestone	Manual Summary Rollup	Deadline			
Split	External Tasks	Inactive Summary	Manual Summary	Progress			
Milestone	External Milestone	Manual Task	Start-only				
Summary	Inactive Task	Duration-only	Finish-only				

Appendix VIII

		One motor						Two Motors				
		Single speed redux	Belt drive	Chain drive	Electromechanical CVT	Electronic Differential	Current Drivetrain	Hub Motors	2 controllers & microprocessor	Independent gear redux	Independent CVT's	AWD
												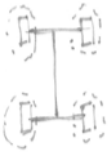
safe to drive	1	0	-	-	0	0	D	0	0	0	0	0
match factory performance	2	+	-	0	+	+	D	+	+	+	+	+
increased range	3	+	0	0	-	-	D	-	-	-	-	-
efficiency	4	+	+	+	-	-	D	+	+	-	-	-
adaptability	5	+	+	+	-	-	D	+	+	+	-	+
ease of maintenance	6	+	+	+	-	-	D	0	+	0	-	0
fun to drive	7	+	0	0	+	+	D	+	+	+	+	+
aesthetics	8	0	-	-	0	0	D	0	0	0	0	0
cost	9	+	+	+	-	-	D	-	-	-	-	-
manufacturability	10	+	+	+	-	-	D	0	+	0	-	0
simplicity	11	+	+	+	-	-	D	-	+	0	-	-
	Σ+	9	6	6	2	2	0	4	7	3	2	3
	Σ-	0	3	2	7	7	0	3	2	3	7	4
	Σs	9	3	4	-5	-5	0	1	5	0	-5	-1

Example Pugh Matrix completed by Spencer Treffry

	A	B	C	D	E	F	G	H	I
1									
2		Match factory driving specification	Efficiency	Adapability	Ease of Maintenance	Aesthetics	Minimal Cost	Manufacturability	Overall Satisfaction
3	Weight	0.20	0.10	0.06	0.09	0.05	0.40	0.10	
4	Fixed Gear Reduction Differential	70.00	60.00	70.00	80.00	65.00	80.00	70.00	
5	Two direct drive motors	80.00	60.00	50.00	95.00	80.00	40.00	90.00	
6									
7	Fixed Gear Reduction Differential	14.00	6.00	4.20	7.20	3.25	32.00	7.00	73.65
8	Two direct drive motors	16.00	6.00	3.00	8.55	4.00	16.00	9.00	62.55

Weighted Decision Matrix

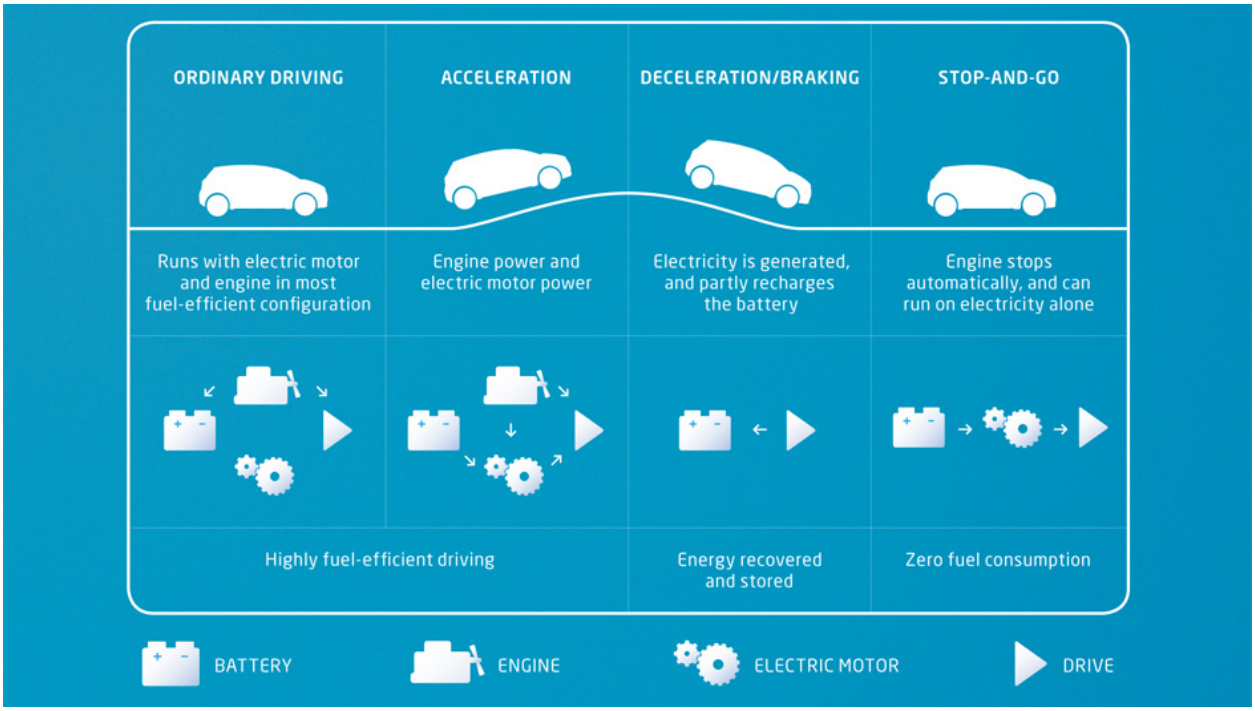

Different Driving Modes of Toyota's Hybrid Synergy Drive

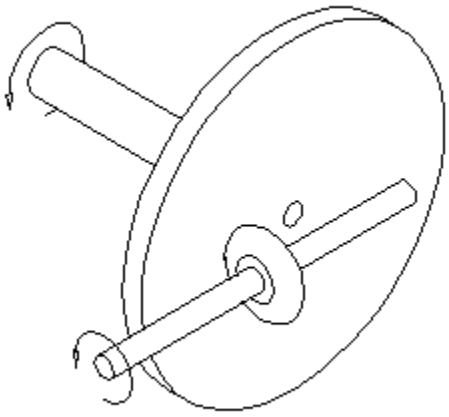

Wheel and Disc CVT Concept

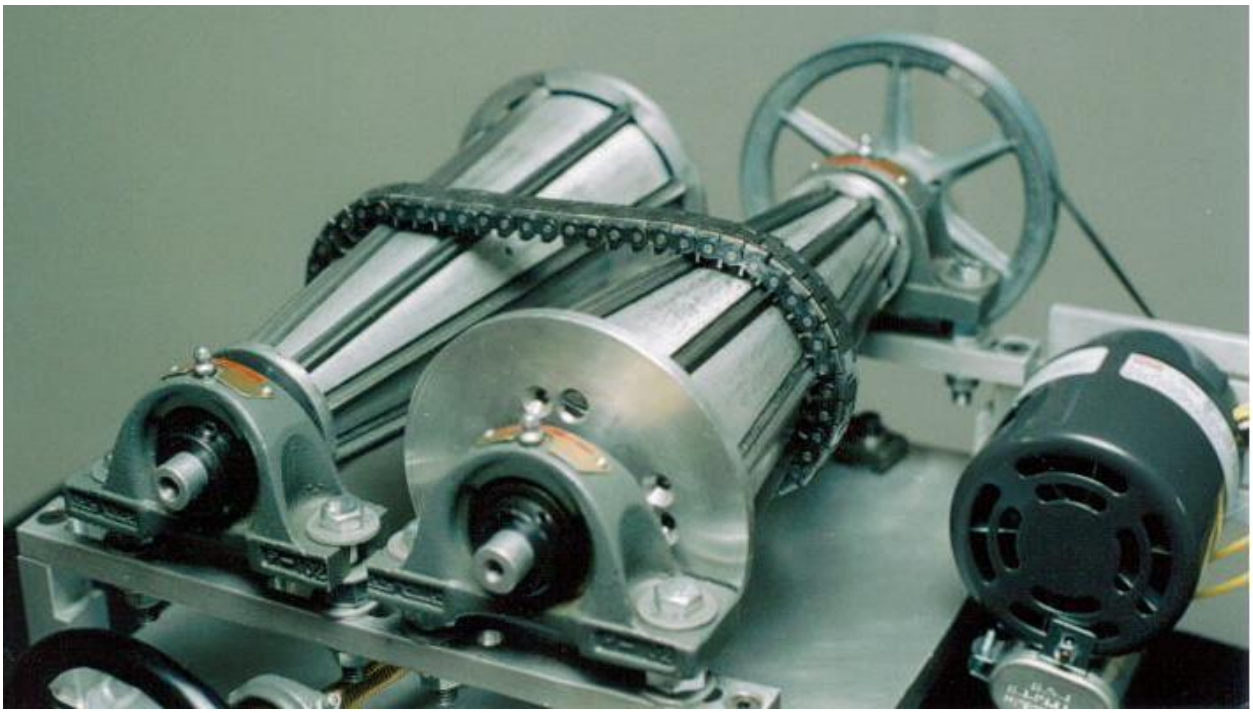

Example of a Cone CVT

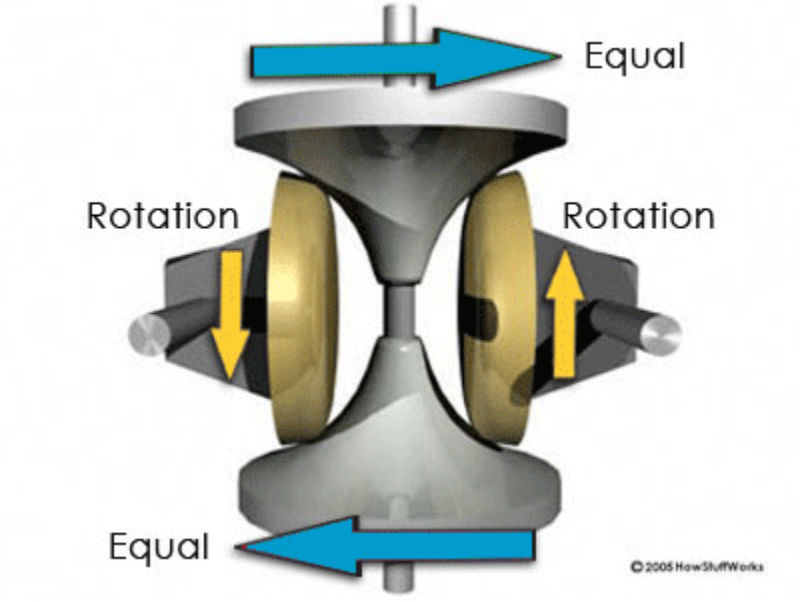

Toroidal CVT Concept

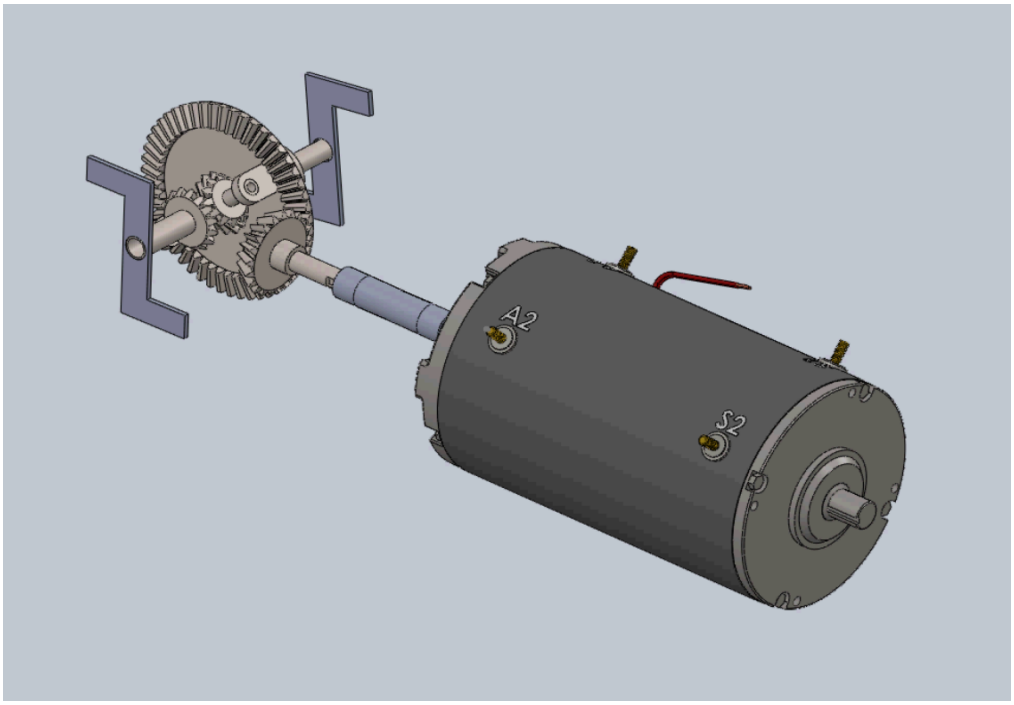

Layout of our single gear reduction design

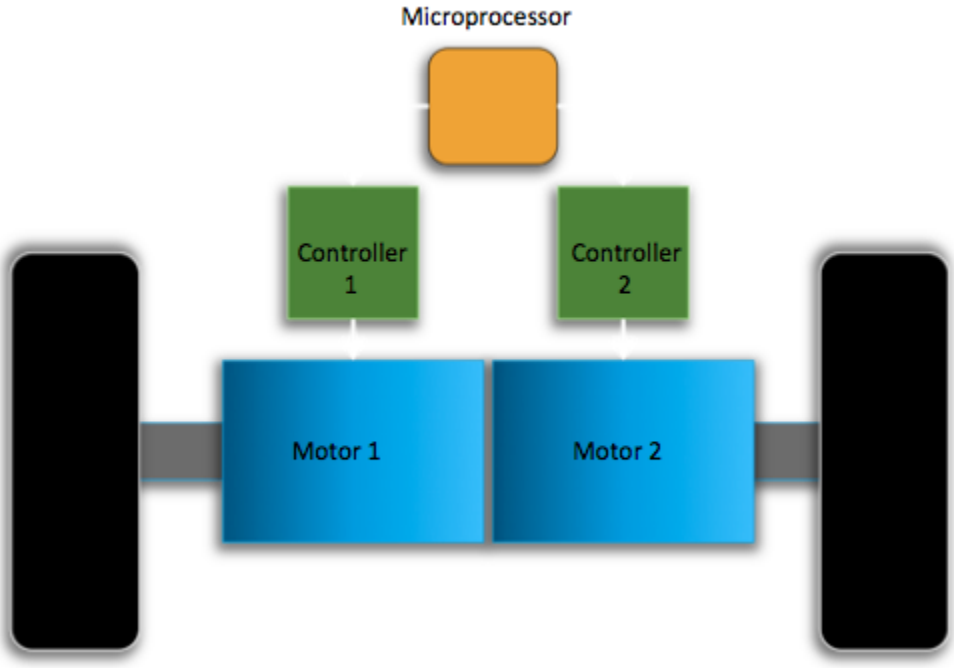

Layout of our two motor design. The blue boxes represent the motors directly attached to the wheels, the green boxes represent the motor controllers, and the yellow box represents the microprocessor.